Singularity Formation in Three-Dimensional Vortex Sheets

A Thesis by

Gang Hu

In Partial Fulfillment of the Requirements

for the Degree of

Doctor of Philosophy

California Institute of Technology

Pasadena, California

2001

(Submitted August 2, 2000)

DEDICATION

To My Grandmother

Acknowledgements

I am deeply indebted to Professor Thomas Y. Hou, my thesis advisor, who suggested this work and guided me through many difficulties and obstacles. What I learned from him is not only about scientific research, but more importantly, about the attitude towards life and career. I feel extremely fortunate to be able to work closely with him in the past five years. I would like to thank him both professionally and personally. I would also like to express my appreciation to Professor Oscar Bruno, Professor Pingwen Zhang, Dr. Hector D. Ceniceros, Dr. Helen Si, Dr. Patrick Guidotti, and Dr. John Pelesko for valuable discussions and suggestions. I thank many professors and instructors at Caltech who led me through my journey in Applied Mathematics.

My study in America is made possible by the Graduate Research and Teaching Assistantship from the California Institute of Technology. I greatly appreciate its generosity.

Next I would like to extend my thanks to a more personal level. I would like to thank my grandparents for bringing me up in those difficult years, my parents for all the sacrifice they have made for me. Especially I would like to dedicate this thesis to my grandmother, who will always live in my heart.

I would also like to thank all my friends at Caltech who have made this journey an enjoyable one, in particular, Mayya Tokman, as my closest friend and officemate; Patrick Guidotti, Danny Patrasek, Chad Schmutzer, Yalchin R. Efendiev, Randy Paffenroth, and Dave Amundsen, the AMA gang; Sue Zhang, Vivian Guo, Jin Yu, Hongyu Ran, John Li, Guangyang Wang, and Qianli Liu, the Caltech Cer's and card game gang.

Finally, special thanks go to my wife, Jingying, for all her love and support.

Abstract

In this thesis, we investigate both theoretically and numerically the singularity formation and long time existence of three-dimensional vortex sheets.

For the theoretical work, we divide it into two parts. In the first part, we study the early time singularity formation and the local form of the vortex sheet in the neighborhood of a singularity near the singularity time. We show that under a special set of coordinates, the three-dimensional vortex sheet can be viewed as a two-dimensional vortex sheet along certain space curves. As a result, the study of singularity formation of a three-dimensional vortex sheet can be related to that of the corresponding two-dimensional vortex sheet. And the singular behavior of these two problems is very similar. Moreover, by performing a transformation in the interface variables and deriving leading order asymptotic approximations for the evolution of these transformed variables, we show that the Kelvin-Helmholtz instability is a result of the coupling of two of these three variables to the leading order. This observation simplifies significantly our singularity analysis for three-dimensional vortex sheets and allows us to reveal clearly the nature of the curvature singularity in the three-dimensional vortex sheet equation. In the second part of our theoretical work, we prove the long time existence of the three-dimensional vortex sheet problem for analytic initial conditions near equilibrium. Moreover, the existence time is almost optimal if the initial perturbation over the equilibrium is sufficiently small.

We have performed careful numerical study to validate our theoretical results. Well-resolved numerical study of the full three-dimensional vortex sheet equation is difficult

due to the complexity in evaluating the interface velocity. To alleviate this difficulty, we introduce two model equations. An important feature of these models equations is that they can be expressed in terms of convolution operators and consequently they can be computed efficiently by Fast Fourier Transform. Moreover, we show by asymptotic analysis that these model equations preserve the singularity type of the full equations. Our analysis also suggests that the model equations generate the same local form of curvature singularity near the physical singularity time as that of the full equations. Our detailed numerical computations on the two-dimensional problem show that the model equation captures all the essential singularity behavior of the full vortex sheet equation. Our calculations based on the three-dimensional model equation provide convincing evidences that a curvature singularity develops in finite time in the three-dimensional vortex sheet. And the type of the singularity is of order $-1/2$ in the mean curvature.

Contents

List of Figures

Chapter 1 Introduction and Background

One of the generic features of shear flows at high Reynolds numbers is Kelvin-Helmholtz (K-H) instability. It has been suggested that K-H instability plays a role in maintaining turbulent flow by causing the break-up of shear layers [21]. One of the well-known examples where K-H waves develop is the instability of the vortex sheet centered on the dividing streamline of a separated flow. It is an asymptotic model of a parallel shear flow in which the thickness of the transition region between the two streams is small compared with a typical stream-wise length-scale.

The singularity formation in two-dimensional vortex sheets has been thoroughly studied in the last two decades. Among the early contributions, Moore [23] studied the nonlinear evolution of a vortex sheet with a small sinusoidal initial disturbance of amplitude ε. He predicted that close to the singularity, the curvature of the sheet is proportional to $|\Gamma - \Gamma_s|^{-\frac{1}{2}}$, where Γ is the circulation in the sheet measured from a fixed reference particle and Γ_s is the position of the singularity. Although Moore's analysis was based on formal asymptotic analysis, his result was supported by Meiron, Baker & Orszag [22], who analyzed a power series solution in time using series extension techniques. Further, their results were confirmed numerically by Krasny [19] and Shelley [28], in which the roundoff error growth was controlled by spectral filtering. Moreover, as a rigorous validation of Moore's analysis, Caflisch & Orellana [9] proved the existence for a slightly perturbed vortex sheet up to $t = O(|\log(\varepsilon)|)$ for Moore's initial condition.

A recent article by Cowley, Baker & Tanveer [12] presented a complete study to the

two-dimensional problem. Among other results, they studied the early time singularity formation on the Birkhoff-Rott equation, and showed by complexifying the independent variable ξ, that early time complex singularities of power $\frac{3}{2}$ can be developed at $t = 0+$. Further, the singularity moves around the complex ξ-domain towards the real ξ-axis without changing its type. The first time at which a singularity intersects the real ξ-axis gives the time at which a singularity forms in the physical problem. Moreover, they obtained an asymptotic description of the sheet shape as the physical singularity forms, and explained certain results observed numerically for the larger initial condition studied by Shelley [28].

The three-dimensional vortex sheet equation has also been studied by a number of researchers recently. Among them, Ishihara & Kaneda [18] provided some evidence of the singularity formation in the three-dimensional problem. Brady & Pullin [7] presented analysis on three-dimensional vortex sheets which have cylindrical shape and normal mode initial data. They showed that in planes normal to the generator of the cylindrical sheet geometry, the nonlinear evolution of the sheet is the same as that of an equivalent two-dimensional vortex sheet motion. Consequently, singularity formation of this special three-dimensional vortex sheet problem is reduced exactly to that of the corresponding two-dimensional problem. Our study of singularity formation in three-dimensional vortex sheets is partially motivated by Brady & Pullin's result. Here we consider generic three-dimensional initial data and show that the evolution of three-dimensional vortex sheets can be reduced to that of two-dimensional vortex sheets to the leading order.

In this thesis, we study the singular behavior of three-dimensional vortex sheets. Our study is divided into four parts. In the first part, by performing asymptotic analysis on the three-dimensional vortex sheet equation, we study the formation of early time singularity and the local form of the vortex sheet in the neighborhood of the singularity near the

singularity time. In the second part, we provide a long time existence proof to the three-dimensional vortex sheet equation. The existence time is almost optimal for small initial perturbations. In the third part of this thesis, we introduce two model equations and study their singular behavior comparing to the full equations. An important feature of these model equations is that they capture the leading order singularity behavior of the full vortex sheet equation and can be computed efficiently. In the fourth part of this thesis, we perform a detailed numerical study which confirms some of the theoretical findings. Below, we summarize the main results that we obtain in this thesis.

1.1 Three-dimensional Vortex Sheets' Early Time Singularities Formation

In Chapter 3, we study the early time singularity formation of solutions to the three-dimensional vortex sheet equation. We show that along certain space curves on the three-dimensional vortex sheet interface, singularity formation is equivalent to that of a two-dimensional vortex sheet interface to the leading order. In fact, by choosing a special set of coordinates and complexifying one of the two independent variables, we show that branch point singularities of order 3/2 develop spontaneously at $t = 0+$ in the extended complex domain. Further, following the idea by Cowley, Baker & Tanveer, [12] we derive an asymptotic expansion which describes the local form of the three-dimensional vortex sheet at the physical singularity time.

As pointed out by a number of researchers (Moore in [23], [24], Caflisch & Semmes in [10], Cowley, Baker & Tanveer in [12]), the key in studying the early time singularity is to derive a local approximation from the vortex sheet equation. Previous studies relied on

complexifying the integral and applying the Residue Theorem. However, it is not trivial to extend this idea to the three-dimensional problem. Therefore, we take a different approach which is generalizable to the three-dimensional problem. By using the dipole representation and Bernoulli's equation, we are able to derive the same local terms from the velocity jump in the tangential direction across the sheet. As we will see later, this tangential velocity jump is the physical driving force of the singularity formation in two and three-dimensional vortex sheets.

The local terms derived from the three-dimensional vortex sheet equation suggest that under a set of special orthogonal coordinates (α_1, α_2), the three-dimensional problem develops the same type of the singularity along the space curves $\mathbf{z}(\alpha_1, \cdot, t)$ as that of the two-dimensional problem. The reason is that by taking α_1 as parameter, the three-dimensional problem has the same leading order terms as those of the two-dimensional problem. Furthermore, by complexifying α_2 and comparing the governing equation of the arc length functions of $\mathbf{z}(\alpha_1, \cdot, t)$ to the two-dimensional interface, we show formally that same type of the singularities form at the early time stage for both equations. From this asymptotic analysis, we conclude that the three-dimensional vortex sheet develops the same type of singularity on the α_2 direction in the complex α_2 domain as that of the two-dimensional vortex sheet.

To study the local form of the curvature singularity, we employ the asymptotic analysis performed by Hou & Zhang [17]. We present a description to the local vortex sheet interface in the neighborhood of singularity near the physical singularity time. From our analysis, we show that under the special orthogonal coordinates mentioned above, with special choices of three interface variables, the local form of the curvature singularity is only observed in two of the three components.

1.2 Existence Proof of the Three-dimensional Vortex Sheet Problem

In Chapter 4, we provide an existence proof for a three-dimensional vortex sheet that is slightly perturbed from a plane uniform vortex sheet. Our result shows that given a small analytic periodic initial perturbation, an analytic solution exists and remains small for a long time. The existence time interval depends on the amplitude of the perturbation ε and the dipole strength γ. Specifically, we assume that the initial perturbation can be analytically continued into a strip of width $\max(|Im(\alpha_1)|, |Im(\alpha_2)|) < \rho_0$, where (α_1, α_2) is the Lagrangian parameter. Under this assumption, our theorem ensures the existence of an analytic solution to the three-dimensional vortex sheet equation for $0 < t < \rho_0/(\frac{\gamma}{2} + \kappa)$, where κ is a constant, which can be chosen as any small positive number provided that the initial perturbation is sufficiently small. This is an optimal result if the initial perturbation is sufficiently small.

In the two-dimensional problem, Caflisch & Orellana [9] proved the long time existence of the solution to the Birkhoff-Rott equation. The key to their proof is to analytically continue the interface variables into the complex domain. In the extended complex domain, an elliptic system can be considered as a hyperbolic system with complex characteristic speed, and thus, an existence result can be established within a time interval which depends on the initial perturbation. Specifically, they first derived a system from the Birkhoff-Rott equation whose leading order terms are identical to Moore's equation [23], [24]. Furthermore, they split the solution into two parts, the first part satisfies Moore's equation with the full initial condition. The second part is the difference between the full solution and the first part of the solution. The existence of Moore's equation is proved using Lax's estimates for a 2×2

system of nonlinear conservation laws [20]. The existence of the second part of the solution is proved by using the extended abstract Cauchy-Kowalewski theorem [25, 9], which ensures that the remaining terms in their derived system are of smaller amplitude.

Our proof is close to that of Caflisch and Orellana [9]. The key to our proof is also to analytically continue the interface variables into the complex domain. In the first part of the proof, we derive a linear leading order system from the three-dimensional vortex sheet equation. Although a nonlinear leading order system (similar to Moore's system) can also be derived, we find that the linear leading order system gives a better structure for our analysis. As in [9], we split the solution into a leading order part and a lower order part. The existence of the leading order part of the solution can be obtained immediately from the linearity. To estimate the nonlinear nonlocal lower order part, we apply the extended abstract Cauchy-Kowalewski theorem which shows that the second part is indeed of lower order and smaller amplitude in a suitable norm. This proves the existence of the three-dimensional vortex sheet solution. Throughout the proof, in order to control the nonlinear growth of the vortex sheet solution, we complexify both of the two independent variables and apply the Lipschitz norm in the two-dimensional complex domain.

1.3 Some Theoretical Results on Model Equations

In Chapter 5, we introduce two model equations for two and three-dimensional vortex sheet equations for computational purposes.

From the study of singularity formation in three-dimensional vortex sheet problems, most of theoretical work is done by formal asymptotic analysis. It requires confirmation from numerical studies. However, from the nature of integro-differential equations, the computation of the three-dimensional vortex sheet equation takes $O(N^4)$ computational

complexity in every time step by direct double summation, where N is the number of particles used to discretize the surface in each dimension. It becomes prohibitively expensive even with N at the level of $O(100)$. On the other hand, although the Fast Multipole Methods (Greengard & Rokhlin [13], Berman & Greengard [5]) is able to reduce the operating account to cN^2, the constant c is still very large. Recently, Haroldsen & Meiron [14] applied this method on the numerical computation of several cases of three-dimensional water waves. They could just perform the computation up to $N = 64$ in their time-dependent calculations. To overcome this difficulty, we introduce our model equation for the three-dimensional vortex sheet problem.

The evolution equation of a three-dimensional vortex sheet interface S is:

$$\frac{\partial \mathbf{z}}{\partial t}(\mathbf{z}) = \int_{S'} |\nabla_\alpha \mu(\alpha')^T, \nabla_\alpha \mathbf{z}(\alpha')^T| \times \nabla_{\mathbf{z}'} G(\mathbf{z}(\alpha) - \mathbf{z}(\alpha'))\, d\alpha' \,, \tag{1.1}$$

where

$$\begin{aligned} G(\mathbf{z} - \mathbf{z}') &= -\frac{1}{4\pi|\mathbf{z} - \mathbf{z}'|} \,, \\ \nabla_{z'} G(\mathbf{z} - \mathbf{z}(\alpha')) &= -\frac{\mathbf{z} - \mathbf{z}}{4\pi|\mathbf{z} - \mathbf{z}'|^3} \,, \end{aligned}$$

and

$$|\nabla_\alpha \mu(\alpha')^T, \nabla_\alpha \mathbf{z}(\alpha')^T| = \frac{\partial \mu}{\partial \alpha_1} \mathbf{z}_{\alpha_2} - \frac{\partial \mu}{\partial \alpha_2} \mathbf{z}_{\alpha_1} \,,$$

where (α_1, α_2) is the Lagrangian parameter, $\mathbf{z}$ is the interface particle position written in a vector form, and μ is the dipole strength.

In the first part of Chapter 5, we introduce a model equation for the three-dimensional problem. The idea is to capture the leading order behavior of the singular integral on the right-hand side of equation (1.1) at small scales. This is achieved by using first order Taylor expansion

$$\mathbf{z}_{\alpha_1}(\alpha')(\alpha_1 - \alpha_1') + \mathbf{z}_{\alpha_2}(\alpha')(\alpha_2 - \alpha_2') \ ,$$

to approximate

$$\mathbf{z}(\alpha) - \mathbf{z}(\alpha') \ .$$

This leads to our three-dimensional model equation [16]:

$$\frac{\partial \mathbf{z}}{\partial t} = \frac{1}{4\pi} \int\int \frac{(\mu'_{\alpha_1}(\alpha_1 - \alpha_1') + \mu'_{\alpha_2}(\alpha_2 - \alpha_2'))|\mathbf{z}'_{\alpha_1} \times \mathbf{z}'_{\alpha_2}|\mathbf{N}(\alpha')}{|\mathbf{z}'_{\alpha_1}(\alpha_1 - \alpha_1') + \mathbf{z}'_{\alpha_2}(\alpha_2 - \alpha_2')|^3} d\alpha_1' d\alpha_2' \ , \qquad (1.2)$$

where

$$\mathbf{N} = \frac{\mathbf{z}_{\alpha_1} \times \mathbf{z}_{\alpha_2}}{|\mathbf{z}_{\alpha_1} \times \mathbf{z}_{\alpha_2}|} \ .$$

The goal of our theoretical work on the three-dimensional model equation is to show its connection to the full three-dimensional vortex sheet equation. In particular, we show that our model equation forms the same tangential velocity jump condition as that of the full equation. Therefore, by applying the same analysis developed for the full equation in Chapter 3, we can show that our model equation captures the singularity type of the full equation. Furthermore, we show that the local singularity structure of our model equation

has the same form as that of the full equation near the physical singularity time.

To further illustrate our idea of the model equations, we introduce a model equation for the two-dimensional vortex sheet equation in the second part Chapter 5.

The evolution of a two-dimensional vortex sheet is described by the Birkhoff-Rott integro-differential equation [6]

$$\overline{\frac{\partial z}{\partial t}}(\xi,t) = \frac{1}{2\pi i}\int_{-\infty}^{\infty} \frac{\Gamma_\xi(\xi')d\xi'}{z(\xi)-z(\xi')}\ , \tag{1.3}$$

where the over-bar denotes the complex conjugate, t is time, $z(\xi,t) = x(\xi,t) + iy(\xi,t)$ is the complex interface position parametrized by a Lagrangian variable ξ, and $\Gamma(\xi)$ is the circulation in the sheet measured between the point with coordinate z and a reference particle. By Kelvin's circulation theorem, Γ is independent of time, which makes it possible to re-write the Birkhoff-Rott equation so that Γ is the independent variable in the case that $\Gamma_\xi > 0$.

To study the singular behavior of this integro-differential equation, several model equations have been derived by previous researchers in this field. Moore [23] was the first one who derived an approximate differential equation for the evolution of the vortex sheet. Subsequently, Caflisch & Orellana [9], Caflisch & Semmes [10] presented a system of four first-order differential equations, which generalized Moore's approximation. Recently, Cowley, Baker, & Tanveer [12] further extended Caflisch's model equation and provided a more extensive study of the singularity. Although their derivations are formal, numerical computations did confirm that their models capture the essence of the singularity.

Our two-dimensional model equation further generalizes the model derived by Caflisch & Semmes [10]. Similar to our three-dimensional model equation, the idea is using the first

order Taylor expansion

$$z_{xi}(\xi')(\xi - \xi') \ ,$$

to approximate

$$z(\xi) - z(\xi')$$

in equation (1.3). This leads to our two-dimensional model equation [16]

$$\overline{\frac{\partial z}{\partial t}}(\xi, t) = \frac{1}{2\pi i} \int_{-\infty}^{\infty} \frac{\Gamma_{\xi}(\xi') d\xi'}{z_{\xi}(\xi', t)(\xi - \xi')} \ . \tag{1.4}$$

By applying the analysis conducted by Cowley, Baker & Tanveer [12], we can show that our model equation captures the singularity type for a vast class of initial conditions (all initial conditions studied in [12] in fact). Furthermore, our model equation can be used to derive an asymptotic approximation to the interface shape in neighborhood of singularities when physical singularities appear. We show that the model equation has the same form of singularities as that of the full equation. Another important feature of our model equation is that it is expressed in terms of the Hilbert transform, which can be evaluated by means of the Fast Fourier Transform (FFT). This allows us to perform computations with an operating count $O(N \log N)$ per time step. It offers a tremendous saving over the full equation which requires $O(N^2)$ operations per time step by direct sum methods.

1.4 Numerical Study on the Model Equations

In Chapter 6, we confirm our theoretical analysis of Chapter 5 by performing numerical computation on both two-dimensional and three-dimensional vortex sheet problems.

In the two-dimensional problem, we apply the modified point vortex approximation used by Shelley [28] and the spectral filtering technique of Krasny [19] in our numerical study. Further, to provide convincing evidence on the singularity type and the propagating trajectory, we form-fit the Fourier coefficients of the interface following [26, 28]. Our form-fitting result shows that when we evolve the vortex sheet from the initial condition used in the analysis of Meiron, Baker & Orszag [22] (subsequently referred to as MBO), our two-dimensional model equation generates the same type of singularities as the full equation. But the speed of which the singularity propagates is different from the full equation. This is because the lower order terms we changed in defining our model equation also contribute to this quantity. Our results also show that at the time of physical singularity, our model equation preserves the singularity structure in the neighborhood of singularity.

In three-dimensional problems, the application of our model equation is less straightforward, since the model equation is in general not of convolution type. By choosing the coordinates (α_1, α_2) which satisfy

$$\mathbf{z}_{\alpha_1} \cdot \mathbf{z}_{\alpha_2} = C_1 \mathbf{z}_{\alpha_2} \cdot \mathbf{z}_{\alpha_2} , \tag{1.5}$$

$$\mathbf{z}_{\alpha_1} \cdot \mathbf{z}_{\alpha_1} = C_2 \mathbf{z}_{\alpha_2} \cdot \mathbf{z}_{\alpha_2} , \tag{1.6}$$

with C_1, C_2 independent of (α_1, α_2), Hou & Zhang [16] derived a model equation in convolution form. To ensure that the conditions in (1.5) and (1.6) are satisfied in time, they introduced two tangential velocities at every time step [16]. With this special coordinate,

the integral operators in the model equations become Riesz transforms, which can be evaluated by the Fast Fourier Transform with $O(N^2 \log(N))$ complexity at every time step, where N is the number of particles used to discretize the surface in each dimension.

Further, with the three-dimensional computational results, we form-fitted its singularity time and the singularity power. Combining our numerical calculation with our theoretical derivation, we claim that for the full three-dimensional vortex sheet equation, curvature singularity appears in finite time. Moreover, the type of singularity is of order 3/2 which is the same as the two-dimensional vortex sheet problem.

The rest of the thesis is organized as follows. In Chapter 2, we provide general formulations for vortex sheet equations. In Chapter 3, we study the early time singularity formation and the local singularity form in the three-dimensional vortex sheet problem. In Chapter 4, we present a proof for the long time existence of the three-dimensional vortex sheet equation. Our model equations are introduced and analyzed by asymptotic analysis in Chapter 5. We devote Chapter 6 to present the numerical computations.

Chapter 2 General Formulation

In this chapter, we introduce the general formulation used in this thesis. We divide this chapter into two sections. In the first section, the three-dimensional vortex sheet equation is derived from the dipole representation and the Bernoulli's equation. In the second section, we present a brief derivation to the model equations proposed to simulate the full vortex sheet equations.

2.1 Vortex Sheet Equation

We consider an interface S separating two infinite layers of incompressible, inviscid, irrotational and identical fluids in the absence of surface tension. Using the Lagrangian frame, the interface location at any instant t is given by:

$$\mathbf{z}(\alpha_1, \alpha_2, t) = (x(\alpha_1, \alpha_2, t)\ , y(\alpha_1, \alpha_2, t), z(\alpha_1, \alpha_2, t))^T\ , \tag{2.1}$$

where (α_1, α_2) is the Lagrangian surface parameter. Thus, the normalized tangential vectors of the surface T_1 and T_2 are defined by

$$\mathrm{T}_1 = \frac{\mathbf{z}_{\alpha_1}}{|\mathbf{z}_{\alpha_1}|}\ , \qquad \mathrm{T}_2 = \frac{\mathbf{z}_{\alpha_2}}{|\mathbf{z}_{\alpha_2}|}\ , \tag{2.2}$$

and the normal vector to the surface $\mathbf{N}$ is defined by

$$\mathbf{N} = \frac{\mathbf{z}_{\alpha_1} \times \mathbf{z}_{\alpha_2}}{|\mathbf{z}_{\alpha_1} \times \mathbf{z}_{\alpha_2}|}\ . \tag{2.3}$$

We label the region below the interface as region 1 and the region above the interface as region 2. Therefore, the velocity field $\mathbf{u}_1$ ($\mathbf{u}_2$) is the velocity below (above) the interface. We define $\mathbf{u}_+$ to be the limit of $\mathbf{u}_2$ approaching the interface from Region 2 and $\mathbf{u}_-$ to be the limit of $\mathbf{u}_1$ approaching the interface from Region 1.

Since the flow in each region is irrotational, we can introduce the velocity potentials ϕ_1 and ϕ_2 so that

$$\mathbf{u}_1 = \nabla\phi_1 \ , \qquad \mathbf{u}_2 = \nabla\phi_2 \ . \tag{2.4}$$

Furthermore, since the flows are incompressible, the velocity potentials satisfy the Laplace equation:

$$\nabla^2\phi_1 = 0 \quad \text{and} \quad \nabla^2\phi_2 = 0 \ . \tag{2.5}$$

Therefore, the potentials in the fluid domain can be written in the following dipole representation:

$$\phi(\mathbf{z}) = \int_{S'} \mu(\alpha')(\mathbf{z}_{\alpha_1} \times \mathbf{z}_{\alpha_2})(\alpha') \cdot \nabla_{z'} G(\mathbf{z} - \mathbf{z}(\alpha'))d\alpha' \ , \tag{2.6}$$

where

$$\begin{aligned} G(\mathbf{z} - \mathbf{z}') &= -\frac{1}{4\pi|\mathbf{z} - \mathbf{z}'|} \ , \\ \nabla_{z'} G(\mathbf{z} - \mathbf{z}(\alpha')) &= -\frac{\mathbf{z} - \mathbf{z}}{4\pi|\mathbf{z} - \mathbf{z}'|^3} \ , \end{aligned}$$

and $\mu(\alpha) = \phi_- - \phi_+$.

By differentiating equation (2.6) with respect to $\mathbf{z}$ and then integrating by parts, we obtain

$$\nabla\phi(\mathbf{z}) = \int_{S'} |\nabla_\alpha \mu(\alpha')^T, \nabla_\alpha \mathbf{z}(\alpha')^T| \times \nabla_{\mathbf{z}'} G(\mathbf{z}(\alpha) - \mathbf{z}(\alpha'))\, d\alpha' \ , \tag{2.7}$$

where we have used the notation

$$|\nabla_\alpha \mu(\alpha')^T, \nabla_\alpha \mathbf{z}(\alpha')^T| = \frac{\partial \mu}{\partial \alpha_1}\mathbf{z}_{\alpha_2} - \frac{\partial \mu}{\partial \alpha_2}\mathbf{z}_{\alpha_1} \ .$$

The motion of the interface is governed by

$$\frac{\partial \mathbf{z}}{\partial t} = \mathbf{u} \ ,$$

where $\mathbf{u} = (u, v, w)$ is the velocity of fluid particles on the interface. The kinematic condition that ensures the interface moving with the fluid, requires that the normal component of velocity be continuous at the interface. However, the tangential velocity at the interface is arbitrary and can be chosen at our convenience.

For the vortex sheet problems, by combining equation (2.6), equation (2.7) and the Bernoulli equation for both layers of fluid and using the continuity of normal stress, it can be shown that when choose $\mathbf{u} = \frac{1}{2}(\mathbf{u}_+ + \mathbf{u}_-)$,

$$\frac{\partial \mu}{\partial t} = 0 \tag{2.8}$$

holds ([4]). (2.8) says that the circulation stays constant along the trajectories whose motion are determined by the average fluid velocity, a well-known result in Fluid Mechanics.

With this particular choice of tangential velocity, the velocity of the vortex sheet interface has the form of (2.7). The equation of the surface particle motion can be written down as:

$$\frac{\partial \mathbf{z}}{\partial t}(\mathbf{z}) = \int_{S'} |\nabla_\alpha \mu(\alpha')^T, \nabla_\alpha \mathbf{z}(\alpha')^T| \times \nabla_{\mathbf{z}'} G(\mathbf{z}(\alpha) - \mathbf{z}(\alpha'))\, d\alpha' \ , \tag{2.9}$$

where $\mathbf{z} \in S$ and the integral takes Cauchy principle value.

From the three-dimensional vortex sheet equation, it is quite straightforward to derive the Birkhoff-Rott equation for the two-dimensional vortex sheet evolution from it.

In fact, a two-dimensional vortex sheet is a special case of three-dimensional vortex sheets with

$$\mathbf{z}(\alpha_1, \alpha_2, t) = \begin{pmatrix} x(\alpha_1, t) \\ \alpha_2 \\ y(\alpha_1, t) \end{pmatrix} \ , \qquad \mu = \mu(\alpha_1) \ . \tag{2.10}$$

Then, it follows from substituting (2.10) into (2.9) and integrating out α_2 that

$$\frac{\partial \mathbf{z}}{\partial t}(\mathbf{z}) = \int_{-\infty}^{\infty} \frac{\mu_{\alpha_1}(\alpha_1')}{(x - x(\alpha_1'))^2 + (y - y(\alpha_1'))^2} \begin{pmatrix} y - y(\alpha_1') \\ 0 \\ -x + x(\alpha_1') \end{pmatrix} d\alpha_1' \ . \tag{2.11}$$

Further, by combining x and y into one complex function as $z = x + iy$, (2.11) can be re-written as

$$\overline{\frac{\partial z}{\partial t}}(\alpha, t) = \frac{1}{2\pi i} \int_{-\infty}^{\infty} \frac{\mu_\alpha(\alpha') d\alpha'}{z(\alpha) - z(\alpha')} \ , \tag{2.12}$$

which is the Birkhoff-Rott equation [6].

Chapter 3 Formation of Early Time Singularities in 3-D Vortex Sheets

In this chapter, we study early time singularity formations in three-dimensional vortex sheets with a wide range of initial conditions.

The sections in this chapter are arranged as follows. A different derivation of two-dimensional leading order approximation is presented in Section 1. In Section 2, we extend the analysis and derive a leading order local system for the three-dimensional vortex sheet equation. In Section 3, we present the main result of this chapter, where we identify the singularity type in the three-dimensional vortex sheet evolution. In the final section, we derive the local form of the vortex sheet at the time close to the formation of a physical singularity in the neighborhood of the singularity.

3.1 Alternative Approach for Analyzing the Two-dimensional Problem

In this section, we provide an alternative derivation to the leading order approximation to the two-dimensional Problem derived by Cowley, Baker & Tanveer [12].

In fact, the system we want to derive in this section has been derived and studied by many researchers in this field. In most of the previous articles, the system was derived by means of complex analysis. A special feature of the two-dimensional vortex sheet problem is that one can combine x and y to form a complex variable $z(\alpha) = x(\alpha) + iy(\alpha)$, and further complexify α to model z as an analytic function. This idea has no obvious extension to the

three-dimensional problem.

However, physically, the tangential velocity difference is always the driving force of the instability. This is the common feature between the two and the three-dimensional problem. We want to use this physical property to re-derive the ill-posed system from the two-dimensional equation. In the next section, we extend the idea to the three-dimensional case.

In the first half of this section, we briefly review the derivation by Cowley, Baker & Tanveer [12] which used complex analysis and the Residue Theorem. In the second half of this section, we provide an alternative derivation using the dipole representation and Bernoulli equation.

We consider a free interface, parameterized by $(x(\alpha,t), y(\alpha,t))$, between two layers of identical fluids in absence of surface tension. By combining x and y into a complex number $z = x + iy$, the motion of the interface is determined by the well-known Birkhoff-Rott equation [6].

$$\overline{\frac{\partial z(\alpha,t)}{\partial t}} = \frac{1}{2\pi i}\int_{-\infty}^{\infty} \frac{\Gamma_\alpha(\alpha')d\alpha'}{z(\alpha)-z(\alpha')} , \tag{3.1}$$

where α is a Lagrangian marker variable, t is the time and the over-bar denotes the complex conjugate. The integral takes Cauchy principal value.

Cowley, Baker & Tanveer [12] studied the case in which the interface is a periodic disturbance of the equilibrium state, $z = \alpha$. Without loss of generality, they assumed that

$$z(\alpha + 2\pi, t) = 2\pi + z(\alpha, t) ,$$

and

$$\Gamma(\alpha + 2\pi) = 2\pi + \Gamma(\alpha) \ .$$

Under these assumptions, (3.1) can be rewritten as [12]

$$\overline{\frac{\partial z}{\partial t}}(\alpha, t) = \frac{1}{4\pi i} \int_{-\pi}^{\pi} \Gamma_\alpha(\alpha') \cot(\frac{1}{2}(z(\alpha, t) - z(\alpha', t)))d\alpha' \tag{3.2}$$

Furthermore, by analytically continuing z into the complex α' domain, they were able to write the Cauchy principle value integral as a contour integral:

$$\begin{aligned} &\int_{-\pi}^{\pi} \Gamma_\alpha(\alpha') \cot(\frac{1}{2}(z(\alpha, t) - z(\alpha', t)))d\alpha' = \\ &\qquad \int_{\mathcal{C}} \Gamma_\alpha(\alpha') \cot(\frac{1}{2}(z(\alpha, t) - z(\alpha', t)))d\alpha' + \frac{2\pi i \Gamma_\alpha(\alpha)}{z_\alpha(\alpha, t)} \ , \end{aligned} \tag{3.3}$$

where the contour $\mathcal{C}$ runs from $\alpha' = -\pi$ to $\alpha' = \pi$, and is assumed to be deformed beneath a simple pole at $\alpha' = \alpha$.

Moreover, with the periodicity properties of $z(\alpha, t)$ and $\Gamma(\alpha)$, it is convenient to write

$$z(\alpha, t) = \alpha + s(\alpha, t), \qquad \Gamma(\alpha) = \alpha + \sigma(\alpha) \ , \tag{3.4}$$

so that s and σ are identified as the 2π-periodic part of z and Γ respectively. Following Caflisch & Orellana [9], Cowley, Baker & Tanveer introduced the analytic extension of $\overline{s}(\alpha, t)$ by the following $*$ operator:

$$s^*(\alpha, t) = \overline{s(\overline{\alpha}, t)} \tag{3.5}$$

which has the following properties.

1. s^* is an analytic function if, and only if, s is an analytic function.

2. if s and s^* are known in the upper half plane, s is known in the whole complex plane.

3. if s is real when α is real, then $s^* = s$ for all complex α.

4. when α is real, $s^*(\alpha, t) = \overline{s(\alpha, t)}$.

Using the last property and the Residue Theorem, one can analytically continue equation (3.2) into the upper half complex α-plane as

$$\frac{\partial s^*(\alpha,t)}{\partial t} = \frac{1}{4\pi i}\int_{\mathcal{C}} \frac{1+\sigma_\alpha(\alpha')}{1+s_\alpha(\alpha',t)} \cot(\frac{1}{2}W(\alpha,\alpha',t))d\alpha' + \frac{1+\sigma_\alpha(\alpha)}{2(1+s_\alpha(\alpha,t))} , \tag{3.6}$$

where

$$W(\alpha,\alpha',t) = \alpha - \alpha' + s(\alpha,t) - s(\alpha',t) . \tag{3.7}$$

Furthermore, equation (3.6) can be re-written as

$$\frac{\partial s^*(\alpha,t)}{\partial t} = \frac{\sigma_\alpha(\alpha) - s_\alpha(\alpha,t)}{2(1+s_\alpha(\alpha,t))} + J(\alpha,t) , \tag{3.8}$$

where

$$J(\alpha,t) = \frac{1}{4\pi i}\int_{\mathcal{C}} \frac{1+\sigma_\alpha(\alpha')}{1+s_\alpha(\alpha',t)} \left(i + \cot\left(\frac{1}{2}W(\alpha,\alpha',t)\right)\right) d\alpha' . \tag{3.9}$$

For simplicity, Cowley, Baker & Tanveer [12] assumed that the contour $\mathcal{C}$ can be deformed so that it runs from $\alpha' = -\pi$ to $\alpha' = \pi$ along the real α'-axis. This assumption was

confirmed by their subsequent analysis and numerical calculations.

To obtain another equation for the leading order system, they took the complex conjugate of equation (3.2) so that

$$\frac{\partial z}{\partial t}(\alpha,t) = -\frac{1}{4\pi i}\int_{-\pi}^{\pi} \Gamma_\alpha(\alpha')\cot(\frac{1}{2}(\overline{z}(\alpha,t)-\overline{z}(\alpha',t)))d\alpha' \ . \tag{3.10}$$

By using the Residue Theorem similar to (3.3) before analytically continuing the functions into the upper complex α domain, they obtained:

$$\frac{\partial s(\alpha,t)}{\partial t} = -\frac{\sigma_\alpha(\alpha)-s^*_\alpha(\alpha,t)}{2(1+s^*_\alpha(\alpha,t))} + K(\alpha,t) \ , \tag{3.11}$$

where

$$K(\alpha,t) = -\frac{1}{4\pi i}\int_C \frac{1+\sigma_\alpha(\alpha')}{1+s_\alpha(\alpha',t)}\left(i+\cot\left(\frac{1}{2}W^*(\alpha,\alpha',t)\right)\right)d\alpha' \ . \tag{3.12}$$

Equation (3.8) and (3.11) constitute the ill-posed system derived from the Birkhoff-Rott equation. There is one important aspect of equation (3.11) which was not addressed explicitly in [12]. During the derivation, the complex conjugate of (3.2) is analytically continued into the upper half complex α-plane with respect to s^*. This is equivalent to analytically continuing the equation into the lower half of the complex α-plane with respect to s because of the definition of $s^*(\alpha,t) = \overline{s(\overline{\alpha},t)}$. Therefore, the directions towards which the analytically continuations take place are in fact opposite for (3.8) and (3.11). As a result, it provides the coupling from s on the upper half complex α-domain to s on the lower half complex α-domain by introducing s^*. More importantly, it is the coupling itself that generates the Kelvin Helmholtz instability. In the rest of this section, we present an

alternative derivation to (3.8) and (3.11) without complexifying α' and without using the Residue Theorem. Instead, we use the dipole representation and Bernoulli equation to derive the leading order system.

We consider an interface separating two layers of identical, incompressible, and irrotational fluid in the absence of surface tension. We assume that the fluids move with velocities (u_1, v_1) and (u_2, v_2) respectively, where the subscripts 1 and 2 refer to quantities associated with the lower and upper fluids. There is a tangential velocity jump along the interface when approached from lower or upper fluid. The jump of velocity potential is Γ. Since we use Γ as the independent variable in equation (3.2), the jump is also equal to the complex variable α.

Since it is a two-dimensional problem, it is convenient to use the notation

$$z(\alpha, t) = x(\alpha, t) + iy(\alpha, t)$$

to describe the fluid particle position and

$$q(\alpha, t) = u(\alpha, t) + iv(\alpha, t)$$

to describe the fluid particle velocity.

By applying the dipole representation and Bernoulli equation to the fluid on both sides of the interface, one can show that (Baker [2])

$$q^*(\alpha) = q_1^*(\alpha) - \frac{1}{2z_\alpha(\alpha)} , \tag{3.13}$$

$$q^*(\alpha) = q_2^*(\alpha) + \frac{1}{2z_\alpha(\alpha)} , \tag{3.14}$$

where $*$ stands for the complex conjugate, and

$$q_i^*(\alpha) = u_i(\alpha) - iv_i(\alpha)$$

are the limiting velocities of the interface particle approach from upper or lower layers of fluid. Although equation (3.13) and equation (3.14) are still written in the complex form, they are essentially real functions with complex expressions since α is a real variable. Without complexifying α, (3.13) and (3.14) specify the velocity jump across the interface, which is $1/z_\alpha$. On the other hand, it is interesting to notice that the velocity jump specified from (3.13) and (3.14) coincides with the local terms in (3.8) and (3.11). From the analysis by Cowley, Baker & Tanveer in [12], the local terms are the leading order terms that generate the singularity; this suggests that the velocity jump is the driving force for singularity formation.

To derive the ill-posed system (3.8) and (3.11), we use the interface equation

$$q^*(\alpha,t) = \frac{\partial z}{\partial t}(\alpha,t) \ , \tag{3.15}$$

and the extended velocity expression

$$q(z) = \frac{1}{4\pi i}\int_{-\pi}^{\pi} \cot[\frac{1}{2}(z - z(\alpha'))]d\alpha' \ , \tag{3.16}$$

which describes the velocity in the upper or lower layer of fluid.

By substituting (3.15) and (3.16) into (3.14), we get

$$\frac{\partial \overline{z}}{\partial t} = \frac{1}{2z_\alpha(\alpha)} + \lim_{\substack{(x+iy)\to z(\alpha) \\ y>Im(z(\alpha))}} \frac{1}{4\pi i}\int_{-\pi}^{\pi} \cot[\frac{1}{2}(x+iy-z(\alpha'))]d\alpha' \tag{3.17}$$

Following the derivation by Cowley, Baker & Tanveer, we continue α into the upper complex domain and let $z(\alpha) = \alpha + s(\alpha)$, $s^*(\alpha,t) = \overline{s(\overline{\alpha},t)}$.

When $\alpha \notin \Re$, there is no singular point in the integral any more. Therefore, we can remove the "limit" on the right-hand side and get:

$$\begin{aligned} \frac{\partial s^*}{\partial t} &= \frac{1}{2(1+s_\alpha(\alpha))} + \frac{1}{4\pi i}\int_{-\pi}^{\pi} \cot[\frac{1}{2}(\alpha-\alpha'+s(\alpha)-s(\alpha'))]d\alpha' \\ &= -\frac{s_\alpha(\alpha)}{2(1+s_\alpha(\alpha))} + \frac{1}{4\pi i}\int_{-\pi}^{\pi} i + \cot[\frac{1}{2}(\alpha-\alpha'+s(\alpha)-s(\alpha'))]d\alpha' \end{aligned} \tag{3.18}$$

To derive equation (3.11), we substitute (3.15) and (3.16) into the complex conjugate of (3.13) and get

$$\frac{\partial z}{\partial t} = \frac{1}{2\overline{z}_\alpha(\alpha)} + \lim_{\substack{(x-iy)\to \overline{z}(\alpha) \\ y>Im(z(\alpha))}} \frac{1}{4\pi i}\int_{-\pi}^{\pi} \cot[\frac{1}{2}(x-iy-\overline{z}(\alpha'))]d\alpha' \ . \tag{3.19}$$

Then, we analytically continue α into the upper complex domain to get

$$\frac{\partial s}{\partial t} = \frac{s^*_\alpha(\alpha)}{2(1+s^*_\alpha(\alpha))} - \frac{1}{4\pi i}\int_{-\pi}^{\pi} i + \cot[\frac{1}{2}(\alpha-\alpha'+s^*(\alpha)-s^*(\alpha'))]d\alpha' \ . \tag{3.20}$$

In the analysis performed by Cowley, Baker & Tanveer [12], they focused on the singular behavior of $s(\alpha,t)$ and $s^*(\alpha,t)$ around the points α_d where either one or both of the

conditions

$$1 + s_\alpha(\alpha_d) = 0 \ , \quad \text{and} \quad 1 + s_\alpha(\alpha_d) = 0$$

hold. In particular, they expanded the solution of (3.8) and (3.11) at $t = 0+$ in powers of t and assumed that around α_d, the integrals only contribute to the $O(t)$ terms. In this way, they showed that the integral terms in (3.8) and (3.11) have little effect on the early time singularity formation.

Remarks: The fundamental difference between our derivation and the derivation by Cowley, Baker & Tanveer is how the local terms are derived. In [12], Cowley, Baker & Tanveer complexified α' before the jump condition was derived. In fact, they derived the jump condition from the complexification and the residue theory, which can be seen from equation (3.10) and equation (3.11). Our analysis does not complexify α' in the Birkhoff-Rott equation. We develop the jump condition essentially from real α'. Further, as we can see from (3.19), we do not take the complex conjugate on the Birkhoff equation until the jump condition is derived. This makes it easier for us to extend our methodology into the three-dimensional problem.

3.2 Extension to the Three-dimensional Problem

We now extend the idea to the three-dimensional problem. We assume that the system at time t is specified by the interface position $\mathbf{z}(\alpha, t)$ and the velocity potential $\phi(\alpha, t)$ on the interface, where $\alpha = (\alpha_1, \alpha_2)$. We begin with a double layer or dipole representation for the potential in terms of the dipole strength $\mu(\alpha)$. In the case of vortex sheet problems, since the velocity on the interface is defined as the average of the limiting velocities approaching

from the upper and lower fluids, it is well-known [4] that $\mu(\alpha)$ stays fixed over time along the Lagrangian trajectory, i.e. ,

$$\frac{\partial \mu}{\partial t} = 0 \ . \tag{3.21}$$

We write the potential in the fluid domain as:

$$\begin{aligned} \phi(\mathbf{z}) &= \int \mu(\alpha')(\mathbf{z}_{\alpha_1} \times \mathbf{z}_{\alpha_2})(\alpha') \cdot \nabla_{\mathbf{z}'} G(\mathbf{z} - \mathbf{z}') d\alpha' \\ &\triangleq K\mu \ , \end{aligned} \tag{3.22}$$

where

$$G(\mathbf{z} - \mathbf{z}') = -\frac{1}{4\pi|\mathbf{z} - \mathbf{z}'|} \ ,$$

$$\nabla_{\mathbf{z}'} G(\mathbf{z} - \mathbf{z}') = -\frac{\mathbf{z} - \mathbf{z}'}{4\pi|\mathbf{z} - \mathbf{z}'|^3} \ .$$

Using the limit of the double layer potential, we find that the value of ϕ on the interface is given by

$$\phi(\mathbf{z}(\alpha)) = -\frac{1}{2}\mu(\alpha) + \lim_{\substack{\mathbf{z} \to \mathbf{z}(\alpha) \\ \textit{from lower layer.}}} \phi(\mathbf{z}) \ . \tag{3.23}$$

By differentiating (3.22) with respect to $\mathbf{z}$ and integrating by parts, we obtain:

$$\nabla\phi(\mathbf{z}) = \int |\nabla_\alpha \mu(\alpha')^T, \nabla_\alpha \mathbf{z}(\alpha')^T| \times \nabla_{z'} G(\mathbf{z} - \mathbf{z}(\alpha')) d\alpha' \ , \tag{3.24}$$

where we have used the notation

$$|\nabla_\alpha \mu(\alpha')^T, \nabla_\alpha \mathbf{z}(\alpha')^T| = \frac{\partial \mu}{\partial \alpha_1}\mathbf{z}_{\alpha_2} - \frac{\partial \mu}{\partial \alpha_2}\mathbf{z}_{\alpha_1} \ .$$

By combining the dipole formulation with the vorticity formulation, Haroldsen and Meiron [14] have derived the velocity on the interface. It is given by:

$$\omega(\alpha) = \nabla\phi(\mathbf{z}(\alpha)) = \omega_{loc}(\alpha) + \omega_1(\alpha) \ , \tag{3.25}$$

where ω stands for the velocity on the interface, and

$$\omega_1(\alpha) = \lim_{\substack{\mathbf{z}\to\mathbf{z}(\alpha) \\ from\ lower\ layer.}} \int |\nabla_\alpha \mu(\alpha')^T, \nabla_\alpha \mathbf{z}(\alpha')^T| \times \nabla_{z'} G(\mathbf{z} - \mathbf{z}(\alpha'))d\alpha' \ , \tag{3.26}$$

$$\omega_{loc}(\alpha) = \frac{1}{2}|\nabla_\alpha \mu(\alpha')^T, \nabla_\alpha \mathbf{z}(\alpha')^T| \times \frac{\mathbf{z}_{\alpha_1} \times \mathbf{z}_{\alpha_2}}{|\mathbf{z}_{\alpha_1} \times \mathbf{z}_{\alpha_2}|^2} \ . \tag{3.27}$$

Similarly, using the equation related to the upper layer fluid, we get:

$$\omega(\alpha) = \nabla\phi(\mathbf{z}(\alpha)) = -\omega_{loc}(\alpha) + \omega_2(\alpha) \ , \tag{3.28}$$

where

$$\omega_2(\alpha) = \lim_{\substack{\mathbf{z}\to\mathbf{z}(\alpha) \\ from\ upper\ layer.}} \int |\nabla_\alpha \mu(\alpha')^T, \nabla_\alpha \mathbf{z}(\alpha')^T| \times \nabla_{z'} G(\mathbf{z} - \mathbf{z}(\alpha'))d\alpha' \ . \tag{3.29}$$

Assume further that there exists orthogonal coordinates (α_1, α_2), such that, at time

$t = 0$, the coordinates satisfy:

$$\mathbf{z}_{\alpha_1} \cdot \mathbf{z}_{\alpha_2} = 0 \ , \tag{3.30}$$

$$\frac{\partial \mu}{\partial \alpha_1} = 0 \ , \qquad \frac{\partial \mu}{\partial \alpha_2} = 1 \ . \tag{3.31}$$

Above assumptions can be relaxed to a much more general class of μ-functions. In fact, we can prove that starting from any orthogonal coordinates, given that μ is a small perturbation of $\gamma_1\alpha_1 + \gamma_2\alpha_2$ with γ_1 and γ_2 being constants, we can always find a set of coordinates that satisfy (3.30) and (3.31). We defer the proof to the end of next section.

Using the properties (3.30) and (3.31), we can simplify the local term to

$$\begin{aligned} \omega_{loc}(\alpha) &= \frac{1}{2}|\nabla_\alpha \mu(\alpha')^T, \nabla_\alpha \mathbf{z}(\alpha')^T| \times \frac{\mathbf{z}_{\alpha_1} \times \mathbf{z}_{\alpha_2}}{|\mathbf{z}_{\alpha_1} \times \mathbf{z}_{\alpha_2}|^2} \\ &= \frac{1}{2}\mathbf{z}_{\alpha_1} \times \frac{\mathbf{z}_{\alpha_1} \times \mathbf{z}_{\alpha_2}}{|\mathbf{z}_{\alpha_1} \times \mathbf{z}_{\alpha_2}|^2} \\ &= -\frac{\mathbf{z}_{\alpha_2}}{2|\mathbf{z}_{\alpha_2}|^2} \ . \end{aligned} \tag{3.32}$$

By substituting (3.32) into equation (3.25) and (3.28), we get

$$\omega(\alpha) = -\frac{\mathbf{z}_{\alpha_2}}{2|\mathbf{z}_{\alpha_2}|^2} + \omega_1(\alpha) \tag{3.33}$$

$$= \frac{\mathbf{z}_{\alpha_2}}{2|\mathbf{z}_{\alpha_2}|^2} + \omega_2(\alpha) \ , \tag{3.34}$$

where ω_1 and ω_2 are defined in (3.26) and (3.29).

Remarks: So far we have derived the jump condition based on the three-dimensional vortex sheet equation. In particular, by comparing (3.33) and (3.34) to (3.13) and (3.14),

we find that the three-dimensional problem has the identical local terms as that of the two-dimensional problem using the special coordinates (α_1, α_2) satisfying (3.30) and (3.31).

It is also interesting to consider the two-dimensional problem as a special case of the three-dimensional problem. In this case, the coordinate satisfies:

$$\mathbf{z}(\alpha_1, \alpha_2, t) = (\alpha_1, f_2(\alpha_2, t), f_3(\alpha_2, t)) \ , \tag{3.35}$$

and

$$\mu = \mu(\alpha_2) \ . \tag{3.36}$$

Our main observation is that the three-dimensional vortex sheet problem can be reduced to a two-dimensional vortex sheet problem, along the α_2-direction, to the leading order approximation. This observation suggests that the three-dimensional problem develop the same type of singularities along the space curves $\mathbf{z}(\alpha_1, \cdot, t)$ as we complexify α_2. The detailed derivation will be presented in the next section.

3.3 Singularities at $t = 0+$ near $|\mathbf{z}_{\alpha_2}| = 0$

In this section, we show that along the space curves $\mathbf{z}(\alpha_1, \cdot, t)$, by continuing $\mathbf{z}$ into the complex α_2-domain, 3/2 singularities on the α_2-direction form at $t = 0+$.

The structure of the proof is described as follows.

1. At time $t = 0$, by fixing α_1, we calculate the mean curvature H and the square of the

arclength G along the α_2-direction by the following formulas,

$$G = \mathbf{z}_{\alpha_2} \cdot \mathbf{z}_{\alpha_2} \ , \tag{3.37}$$

and

$$H = \frac{EN - 2FM + GL}{2(EG - F^2)}, \tag{3.38}$$

where

$$\begin{aligned} E &= \mathbf{z}_{\alpha_1} \cdot \mathbf{z}_{\alpha_1}, \\ F &= \mathbf{z}_{\alpha_1} \cdot \mathbf{z}_{\alpha_2}, \\ \mathbf{z}^N &= \frac{\mathbf{z}_{\alpha_1} \times \mathbf{z}_{\alpha_2}}{|\mathbf{z}_{\alpha_1} \times \mathbf{z}_{\alpha_2}|}, \\ L &= \mathbf{z}_{\alpha_1\alpha_1} \cdot \mathbf{z}^N, \\ M &= \mathbf{z}_{\alpha_1\alpha_2} \cdot \mathbf{z}^N, \\ N &= \mathbf{z}_{\alpha_2\alpha_2} \cdot \mathbf{z}^N. \end{aligned}$$

2. Using $\sqrt{G}(t = 0)$ as the arc length and $H(t = 0)$ as the curvature, we can construct a unique planar curve up to a constant. We denote this curve as $(x^0_{GH}(\alpha_2), y^0_{GH}(\alpha_2))$.

3. Taking $(x^0_{GH}(\alpha_2), y^0_{GH}(\alpha_2))$ as the initial condition, we can solve the Birkhoff-Rott equation in time to obtain a family of plane curves (denoted as $(x_{GH}(\alpha_2, t), y_{GH}(\alpha_2, t))$).

4. By complexifying the parameter α_2 in $(x_{GH}(\alpha_2, t), y_{GH}(\alpha_2, t))$, Cowley, Baker & Tanveer [12] showed that 3/2 singularities can spontaneously form at $t = 0+$ in the complex α_2-domain. As a result, the two-dimensional square of arclength function

$G_2(\alpha_2, t)$ defined by

$$G_2(\alpha_2, t) = x^2_{GH_{\alpha_2}}(\alpha_2, t) + y^2_{GH_{\alpha_2}}(\alpha_2, t) \ , \tag{3.39}$$

forms 1/2 singularities in the extended complex domain at the same position as that of $(x_{GH}(\alpha_2, t), y_{GH}(\alpha_2, t))$.

5. We define the square of arclength function on α_2 direction of the three-dimensional vortex sheet interface G_3 as

$$G_3(\alpha_1, \alpha_2, t) = x^2_{\alpha_2}(\alpha_1, \alpha_2, t) + y^2_{\alpha_2}(\alpha_1, \alpha_2, t) + z^2_{\alpha_2}(\alpha_1, \alpha_2, t) \ . \tag{3.40}$$

By showing that the evolution equations of both G_2 and G_3 have the identical leading order terms around the points where singularities of G_2 develop, we show that G_3 also form singularities around the same α_2 position with the same power on the α_2-direction.

6. The result of Step 5 implies that the solution to the three-dimensional vortex sheet equation form 3/2 singularities on the α_2-direction spontaneously at $t = 0+$.

The key in our analysis is to justify Step 5. We divide the analysis into three sub-steps.

1. Derive the evolution equations of G_2 and G_3.

2. Show that around the α_2 locations where the singularities of G_2 form, the two equations share the same leading order terms in the evolution equations.

3. Show that $G_3(\alpha, t)$ develops the same type of singularity at the same locations where $G_2(\alpha, t)$ develops singularity.

Sub-step 1: It is sufficient to derive the evolution equation for G_3 only, because G_2 can be considered as a special case of G_3 from the last remark in the last section.

At time $t = 0$, the motion of a three-dimensional interface $\mathbf{z}(\alpha_1, \alpha_2, t)$ is governed by

$$\frac{\partial \mathbf{z}}{\partial t}(\alpha) = -\frac{\mathbf{z}_{\alpha_2}}{2|\mathbf{z}_{\alpha_2}|^2} + \omega_1(\alpha) \ , \tag{3.41}$$

where $\alpha = (\alpha_1, \alpha_2)$. The equation which describes the α_2-direction arclength square G can be derived as

$$\begin{aligned} G_t &= 2\mathbf{z}_{\alpha_2} \cdot \mathbf{z}_{\alpha_2 t} = 2\mathbf{z}_{\alpha_2} \cdot \left(\frac{\mathbf{z}_{\alpha_2}}{2G} + \omega_1(\alpha)\right)_{\alpha_2} \\ &= \frac{1}{G}\mathbf{z}_{\alpha_2} \cdot \mathbf{z}_{\alpha_2\alpha_2} + 2G\left(\frac{1}{2G}\right)_{\alpha_2} + 2\mathbf{z}_{\alpha_2} \cdot \omega_{1_{\alpha_2}}(\alpha) \\ &= -\frac{1}{2G}G_{\alpha_2} + 2\mathbf{z}_{\alpha_2} \cdot \omega_{1_{\alpha_2}}(\alpha) \end{aligned} \tag{3.42}$$

at time $t = 0$.

Similarly, if the governing equation for the interface is

$$\frac{\partial \mathbf{z}}{\partial t}(\alpha) = \frac{\mathbf{z}_{\alpha_2}}{2|\mathbf{z}_{\alpha_2}|^2} + \omega_2(\alpha) \ , \tag{3.43}$$

the equation for G can be shown to be

$$G_t = \frac{1}{2G}G_{\alpha_2} + 2\mathbf{z}_{\alpha_2} \cdot \omega_{2_{\alpha_2}}(\alpha) \ . \tag{3.44}$$

Remarks: 1. Note that (3.42) and (3.44) can be applied to both G_2 and G_3 with different ω terms because two-dimensional vortex sheet problems can be considered as special cases of three-dimensional vortex sheet problems.

2. Essentially, equation (3.42) and equation (3.44) describe a jump condition for the evolution equation of the arclength square function. What we need to mention here is that both (3.42) and (3.44) can only be analytically continued to half of the complex α_2 plane because of the jump condition. Following the idea used in studying the two-dimensional problem, we analytically continue equation (3.42) to the lower half complex α_2 domain and equation (3.44) to the upper half complex α_2 domain.

Sub-step 2: We need to show that around the α_2 locations where the G_2 forms singularity, the evolution equations of G_2 and G_3 share the same leading order terms.

First of all, it is necessary to derive the α_2 locations where $G_2(\alpha_2, t)$ develops singularities. Cowley, Baker & Tanveer [12], by applying asymptotic analysis to (3.8) and (3.11), showed that the 3/2 type singularities appear in the neighborhood of α_{20} in which

$$1 + s_{\alpha_2}(\alpha_{20}, 0) = 0 \qquad \text{or} \qquad 1 + s^*_{\alpha_2}(\alpha_{20}, 0) = 0 \ . \tag{3.45}$$

Note that the analytic continuation of $G_2(\alpha_2, t)$ takes the form

$$G_2(\alpha_2, t) = (1 + s_{\alpha_2}(\alpha_2, t))(1 + s^*_{\alpha_2}(\alpha_2, t)) \ .$$

Therefore, (3.45) implies that the singularities form around α_{20} such that

$$G_2(\alpha_{20}, 0) = 0 \ .$$

Furthermore, from Step 2 in the outline, with α_1 being fixed, the following equality is

satisfied for real α_2:

$$G_2(\alpha_2, 0) = G_3(\alpha_2, 0) \ .$$

This also implies that $G_2(\alpha_2, 0) = G_3(\alpha_2, 0)$ for complex α_2 as long as G_2 and G_3 are analytic. Together with Sub-step 1, we conclude that around the α_2's where the singularity formation takes place, the evolution equations of G_2 and G_3 have the same leading order terms.

Sub-step 3: We need to show that at the α_2 locations where G_2 develops singularities, G_3 also develops the same type of singularities.

In [12], the singularities of s and s^* defined in (3.4) and (3.5) are analyzed in two cases, the case in which there exists a α_{20} such that $1 + s_{\alpha_2}(\alpha_{20})$ and $1 + s^*_{\alpha_2}(\alpha_{20})$ vanish simultaneously, and the case in which there exist a α_{20} such that one of them vanish at the point but the other does not. We take the same approach as well. However, from the similarity of these two cases, it is sufficient for us to show only one of them in detail. The result of the other case can be derived similarly. We choose the case where there exists a α_{20} so that

$$1 + s_{\alpha_2}(\alpha_{20}) = 0 \ ,$$

but

$$1 + s^*_{\alpha_2}(\alpha_{20}) \neq 0 \ .$$

Since

$$G_2(\alpha_2) = (1 + s_{\alpha_2}(\alpha_2))(1 + s^*_{\alpha_2}(\alpha_2)) \ ,$$

for all α_2, it is appropriate to combine the expansion of s_{α_2} and $s^*_{\alpha_2}$ around α_{20} in powers of the time t to obtain the expansion of $G_2(\alpha_2, t)$ for $t \ll 1$.

Since direct expansion of s and s^* in powers of t breaks down in the neighborhood of α_{20}, Cowley, Baker & Tanveer [12] took $\zeta = \alpha_2 - \alpha_{20}$ and used the asymptotic scaling for small ζ when $t \ll 1$ as

$$\zeta = \eta \Omega t^{\frac{1}{2}} \quad \text{where} \quad \Omega = \left(\frac{2}{s_{02}(1 + s^*_{01})} \right)^{\frac{1}{2}} \ ,$$

where

$$s_{0n} = \frac{\partial s}{\partial \alpha_2^n}(\alpha_{20}, 0), \quad s^*_{0n} = \frac{\partial s^*}{\partial \alpha_2^n}(\alpha_{20}, 0),$$

and

$$K_{00} = K(\alpha_{20}, 0)$$

which was defined in (3.12). In this way, they obtained the expansion of s and s^* as

$$s = s_{00} - \eta \Omega t^{\frac{1}{2}} + \left(\frac{1}{2} + K_{00} + \frac{1}{1 + s^*_{01}} A(\eta) \right) t + \cdots \ , \tag{3.46}$$

$$s^* = s^*_{00} + ((1 + s^*_{01}) B(\eta) - \eta) \Omega t^{\frac{1}{2}} + \cdots \ , \tag{3.47}$$

by solving $A(\eta)$ and $B(\eta)$ from the evolution equations of s and s^*. As a result, they showed that $A(\eta)$ and $B(\eta)$ have a 3/2 branch point singularity at certain point η_0. In particular, $A(\eta)$ and $B(\eta)$ have the expansions

$$A(\eta) = A_0 + A_1(\eta - \eta_0) + A_p(\eta - \eta_0)^p + \cdots , \tag{3.48}$$

$$B(\eta) = B_0 + B_1(\eta - \eta_0) + B_p(\eta - \eta_0)^p + \cdots , \tag{3.49}$$

in the neighborhood of η_0 with $A_1 B_1 \neq 0$, $p = \frac{3}{2}$.

Since

$$\frac{\partial}{\partial \alpha_2} = (\Omega^{-1} t^{-\frac{1}{2}}) \frac{\partial}{\partial \eta} ,$$

from the rescaling, $G_2(\alpha_2)$ has the expansion

$$\begin{aligned} G_2(\alpha_2, t) &= (1 + s_{\alpha_2}(\alpha_2, t))(1 + s^*_{\alpha_2}(\alpha_2, t)) \\ &= \frac{A'(\eta)\Omega^{-1} t^{\frac{1}{2}}}{1 + s^*_{01}} \cdot (1 + s^*_{01}) B'(\eta) + \cdots \\ &= A'(\eta) B'(\eta) \Omega^{-1} t^{\frac{1}{2}} + \cdots \\ &= (A_1 B_1 + (p A_1 B_p + p B_1 A_p)(\eta - \eta_0)^{p-1}) \Omega^{-1} t^{\frac{1}{2}} + \cdots . \end{aligned} \tag{3.50}$$

We conclude that G_2 develops a 1/2 singularity at the same η_0 from the term of order $t^{1/2}$.

Now, we show that G_3 develops the same type of singularity at the same α_2 location. Our approach is to expand G_2 and G_3 around the α_{20} in powers of t and ζ, by using the rescaling of $\zeta = O(t^{1/2})$, to show that G_2 and G_3 have identical expansions to the order of $O(t^{1/2})$. To perform our analysis, we make the same assumption as in [12], that when we complexify α_2 in (3.26) and (3.29), the integrals are bounded in the complex α_2 domain.

From our assumption of α_{20}, G_2 vanishes in the upper half complex α_2-domain. Therefore, from the remarks at the end of Sub-step 1, we use (3.44) to expand both G_2 and G_3 in powers of t and $\zeta = \alpha_2 - \alpha_{20}$. Taking G_2 as an example, we get

$$\begin{aligned} G_2(\alpha_2, t) &= G_2(\alpha_2, 0) + G_{2t}(\alpha_2, 0)t + \cdots \\ &= G_2(\alpha_{20}, 0) + G_{2_{\alpha_2}}(\alpha_{20}, 0)\zeta + \frac{1}{2}G_{2_{\alpha_2\alpha_2}}(\alpha_{20}, 0)\zeta^2 + \cdots \\ &\quad + \left(\frac{G_{2_{\alpha_2}}(\alpha_2, 0)}{2G_{2_{\alpha_2}}(\alpha_{20}, 0)\zeta} + 2(\mathbf{z}_{\alpha_2} \cdot \omega_{2_{\alpha_2}})(\alpha_{20}, 0) \right) t + \cdots \end{aligned} \tag{3.51}$$

from equation (3.44). As expected, the expansion breaks down near $\zeta \sim 0$. Following the scaling in the expansions of s and s^*, we use $\zeta = \eta\Omega t^{1/2}$ and expand G_2 as

$$G_2(\alpha_2, t) = G_2(\alpha_{20}, 0) + \left(G_{2_{\alpha_2}}(\alpha_{20}, 0)\Omega\eta + \frac{G_{2_{\alpha_2}}(\alpha_2, 0)}{2G_{2_{\alpha_2}}(\alpha_{20}, 0)\Omega} C(\eta) \right) t^{\frac{1}{2}} + \cdots .$$

On the other hand, from equation (3.50), G_2 has the expansion up to order $O(t^{1/2})$ of

$$G_2(\alpha_2, t) = (A_1 B_1 + (pA_1 B_p + pB_1 A_p)(\eta - \eta_0)^{p-1})\Omega^{-1} t^{\frac{1}{2}} + \cdots .$$

We conclude that equation (3.50) satisfies the evolution equation of G_2 up to the order $O(t^{\frac{1}{2}})$.

Similarly, G_3 has the expansion in powers of t and ζ

$$\begin{aligned} G_3(\alpha_2,t) &= G_3(\alpha_2,0) + G_{3t}(\alpha_2,0)t + \cdots \\ &= G_3(\alpha_{20},0) + G_{3_{\alpha_2}}(\alpha_{20},0)\zeta + \frac{1}{2}G_{3_{\alpha_2\alpha_2}}(\alpha_{20},0)\zeta^2 + \cdots \\ &\quad + \left(\frac{G_{3_{\alpha_2}}(\alpha_2,0)}{2G_{3_{\alpha_2}}(\alpha_{20},0)\zeta} + 2(\mathbf{z}_{\alpha_2}\cdot\omega_{2_{\alpha_2}})(\alpha_{20},0)\right)t + \cdots . \end{aligned} \tag{3.52}$$

The expansion also breaks down near $\zeta \sim 0$. We use the same scaling function $\zeta = \eta\Omega t^{1/2}$ as in the case of G_2 and also expand G_3 as

$$G_3(\alpha_2,t) = G_3(\alpha_{20},0) + \left(G_{3_{\alpha_2}}(\alpha_{20},0)\Omega\eta + \frac{G_{3_{\alpha_2}}(\alpha_2,0)}{2G_{3_{\alpha_2}}(\alpha_{20},0)\Omega}C(\eta)\right)t^{\frac{1}{2}} + \cdots .$$

Since G_2 and G_3 have the same initial condition and the same leading order terms in their evolution equations, their expansions share identical terms up to $O(t^{1/2})$ which is the term that generates a singularity at G_2. Thus, G_3 also has the expansion

$$G_3(\alpha_2,t) = (A_1B_1 + (pA_1B_p + pB_1A_p)(\eta-\eta_0)^{p-1})\Omega^{-1}t^{\frac{1}{2}} + \cdots . \tag{3.53}$$

This shows that G_3 develops the same type of singularities at the same α_2 position. Moreover, if we complexify α_2 in the three-dimensional vortex sheet equation, singularities of power 3/2 on the α_2 direction form spontaneously at $t = 0+$. This completes our derivation of the singularity formation in the three-dimensional vortex sheet problem.

Existence of orthogonal coordinates satisfying (3.30) and (3.31): Throughout the analysis, we have assumed that (α_1,α_2) satisfies (3.30) and (3.31). Now we prove that given an orthogonal coordinates (α_1,α_2) and a reasonably large class of μ, we can always find another coordinate system (β_1,β_2) such that equation (3.30) and (3.31) are satisfied.

Lemma 3.3.1 *Assume that the interface is a small perturbation of a flat plane, and there exists orthogonal coordinates* (α_1, α_2) *for* $\mathbf{z}$. *Furthermore, we assume that*

$$\mu = \gamma_1 \alpha_1 + \gamma_2 \alpha_2 + O(\varepsilon)$$

where $(\alpha_1, \alpha_2) \in R \times R$. *Then there exists a change of variables* $\alpha = \alpha(\beta)$, *such that:*

$$\mathbf{z}_{\beta_1} \cdot \mathbf{z}_{\beta_2} = 0 \tag{3.54}$$

$$\frac{\partial \mu}{\partial \beta_1} = 0 \tag{3.55}$$

$$\frac{\partial \mu}{\partial \beta_2} = 1 \tag{3.56}$$

Proof: Starting from (α_1, α_2), we need to find another set of coordinates (β_1, β_2) as functions of (α_1, α_2). Furthermore, we need to show that the map from (α_1, α_2) to (β_1, β_2) is a one-to-one map, which means that for any (β_{10}, β_{20}), there is one and only one pair $(\alpha_{10}, \alpha_{20})$ which maps to (β_{10}, β_{20}), and vice versa.

Assume that the map from (β_1, β_2) to (α_1, α_2) has the following form:

$$\begin{aligned} \alpha_1 &= \alpha_1(\beta_1, \beta_2) \ , \\ \alpha_2 &= \alpha_2(\beta_1, \beta_2) \ . \end{aligned}$$

Write down the Jacobian matrix for (β_1, β_2) as

$$\frac{\partial(\beta_1, \beta_2)}{\partial(\alpha_1, \alpha_2)} = \begin{pmatrix} \beta_{1_{\alpha_1}} & \beta_{1_{\alpha_2}} \\ \beta_{2_{\alpha_1}} & \beta_{2_{\alpha_2}} \end{pmatrix} . \tag{3.57}$$

Consequently, the Jacobian matrix for (α_1, α_2) will be:

$$\frac{\partial(\alpha_1, \alpha_2)}{\partial(\beta_1, \beta_2)} = \frac{1}{\triangle} \begin{pmatrix} \beta_{2_{\alpha_2}} & -\beta_{1_{\alpha_2}} \\ -\beta_{2_{\alpha_1}} & \beta_{1_{\alpha_1}} \end{pmatrix} , \tag{3.58}$$

where

$$\triangle = \beta_{1_{\alpha_1}} \beta_{2_{\alpha_2}} - \beta_{1_{\alpha_2}} \beta_{2_{\alpha_1}} . \tag{3.59}$$

From equation (3.56), it is natural to choose

$$\beta_2(\alpha_1, \alpha_2) = \mu(\alpha_1, \alpha_2) . \tag{3.60}$$

With this choice, we can show that

$$\begin{aligned} \frac{\partial \mu}{\partial \beta_1} &= \mu_{\alpha_1} \alpha_{1_{\beta_1}} + \mu_{\alpha_2} \alpha_{2_{\beta_1}} \\ &= \frac{1}{\triangle} (\mu_{\alpha_1} \beta_{2_{\alpha_2}} - \mu_{\alpha_2} \beta_{2_{\alpha_1}}) \\ &= 0 , \end{aligned} \tag{3.61}$$

provided that $\triangle \neq 0$, which will be verified later.

Therefore, by choosing $\beta_2 = \mu$, equation (3.55) and (3.56) are satisfied. The next step is to use equation (3.54) to solve for β_1.

From equation (3.54), we get

$$[z_{\alpha_1}\frac{\partial\alpha_1}{\partial\beta_1}+z_{\alpha_2}\frac{\partial\alpha_2}{\partial\beta_1}]\cdot[z_{\alpha_1}\frac{\partial\alpha_1}{\partial\beta_2}+z_{\alpha_2}\frac{\partial\alpha_2}{\partial\beta_2}]=0\ . \tag{3.62}$$

Define $\lambda(\alpha_1,\alpha_2)$ as

$$\lambda(\alpha_1,\alpha_2)=\frac{z_{\alpha_1}\cdot z_{\alpha_1}}{z_{\alpha_2}\cdot z_{\alpha_2}}\ . \tag{3.63}$$

Note that in the case that the interface is a small perturbation of a flat plane, λ is a small perturbation of a constant. By substituting (3.63) into equation (3.62) and using $z_{\alpha_1}\cdot z_{\alpha_2}=0$, we get

$$\lambda\frac{\partial\alpha_1}{\partial\beta_1}\frac{\partial\alpha_1}{\partial\beta_2}+\frac{\partial\alpha_2}{\partial\beta_1}\frac{\partial\alpha_2}{\partial\beta_2}=0\ .$$

By applying (3.58), we obtain

$$\cdot\lambda\frac{\partial\beta_2}{\partial\alpha_2}\frac{\partial\beta_1}{\partial\alpha_2}+\frac{\partial\beta_2}{\partial\alpha_1}\frac{\partial\beta_2}{\partial\alpha_2}=0\ .$$

Furthermore, substituting (3.60) to the above equality leads to

$$\lambda\frac{\partial\mu}{\partial\alpha_2}\frac{\partial\beta_1}{\partial\alpha_2}+\frac{\partial\mu}{\partial\alpha_1}\frac{\partial\beta_1}{\partial\alpha_1}=0\ . \tag{3.64}$$

Thus, we have derived an equation for β_1. Under the assumption of lemma 3.3.1, λ, μ_{α_1} and μ_{α_2} are all small perturbation of some constants. Therefore, we can solve the linear hyperbolic equation.

Furthermore, under the assumption of current lemma, it is easy to verify that Δ will

always be a small perturbation of some nonzero constant. That concludes the proof of the lemma.

Remark: The assumption of the lemma can be relaxed to include more general initial conditions far from the equilibrium. Since it is our main interest to study the singularities near equilibrium state, we do not present the more general result here.

3.4 Motion of the singularities

In the previous section, we have shown that with a wide range of initial conditions, 3/2 singularities on the α_2 direction develop at the complex α_2 domain around the positions where $G_3(\alpha_1, \alpha_2, t) = 0$. This implies that the singularities develop simultaneously along one or several one-dimensional curves parametrized by α_1, i.e., $\alpha_2(\alpha_1, t)$. As time increases, each point of these one-dimensional curves moves around in the complex α_2 domain. The physical singularity time is the first time when these curves hit the real α_2 axis.

In this section, we show that at any time t before the singularity time, the one-dimensional curve $\alpha_2(\alpha_1, t)$ is always an analytical function of α_1. Due to the analyticity of $\alpha_2(\alpha_1, t)$ as a function of α_1, the curve $\alpha_2(\alpha_1, t)$ cannot intersect with the real (α_1, α_2) plane in a segment, for if this were the case it would imply the entire curve has zero imaginary part by analytic continuation. Therefore, its intersection with the real (α_1, α_2) plane contains either isolated points, or the entire $\alpha_2(\alpha_1, t)$ curve. In the latter case, the vortex sheet surface becomes singular along a one-dimensional curve at the singularity time.

At time $t = 0+$, from the results of the previous section, $\alpha_2(\alpha_1, 0)$ is defined implicitly by $G_3(\alpha_1, \alpha_2, 0) = 0$. Since the initial condition is assumed to be analytic in both α_1 and α_2, we conclude that $\alpha_2(\alpha_1, 0)$ is an analytic function of α_1. Let us parameterize the curve $alpha_2(\alpha_1, t)$ in the complex (α_1, α_2) plane as $(\alpha_1, \alpha_2(\alpha_1, t))$. Furthermore, we expand the

square of the arc length function $G_3(\alpha_1, \alpha_2, t)$ around $(\alpha_{10}, \alpha_2(\alpha_{10}, t))$ in the following form by factoring out the square root singularity explicitly:

$$G_3(\alpha_1, \alpha_2, t) = A_1 + A_{21}(\alpha_1 - \alpha_{10})^{\frac{1}{2}} + A_{22}(\alpha_2 - \alpha_2(\alpha_{10}, t))^{\frac{1}{2}} + \cdots \tag{3.65}$$

where A_1, A_{21} and A_{22} are functions of α_{10} and t. Since we have singled out the singular factor in the expansion, it is reasonable to assume that the coefficients, A_1, A_{21} and A_{22} are analytic functions of α_{10}.

To derive the equation which governs the motion of $\alpha_2(\alpha_1, t)$, we substitute (3.65) into either (3.42) or (3.44) based on whether the singularities are in the upper complex α_2 domain or in the lower complex α_2 domain. Without loss of generality, we assume that the singularities are in the upper half complex α_2 domain, and we use equation (3.44). By extracting the $(\alpha_2 - \alpha_2(\alpha_{10}, t))^{-\frac{1}{2}}$ terms, we get

$$\frac{\partial \alpha_2}{\partial t}(\alpha_{10}, t) = -\frac{1}{A_1(\alpha_{10}, t)} \ . \tag{3.66}$$

Note that for $t > 0$, the singularity trajectory departs from the trajectory of $G_3(\alpha_1, \alpha_2, t) = 0$. Thus A_1 does not vanish at $(\alpha_{10}, \alpha_2(\alpha_{10}, t)$, and the above equation for $\alpha_2(\alpha_1, t)$ is well defined. From equation (3.66), we conclude that $\alpha_2(\alpha_1, t)$ is an analytic function of α_1 up to time t since the right hand side is analytic (at least within this leading order asymptotic analysis). As a result, we conclude that when physical singularities appear, they appear either at some isolated points, or along the entire one-dimensional curve in the real (α_1, α_2) plane. It is not possible for the interface to develop finite time singularities along a segment of a one-dimensional curve. [1] This result will be confirmed by our numerical results.

[1] We thank Prof. Oscar Bruno for kindly suggesting the idea of proving analyticity of $\alpha_2(\alpha_1, t)$ as a way

3.5 The Local Form of the Curvature Singularity

Our arguments in the previous sections show that with a large class of initial conditions, 3/2 singularities on the α_2 direction develop at the complex α_2 domain where $|Im(\alpha_2)| \gg 1$. As time increases, the singularities propagate in the extended complex domain. The first time at which their trajectories intersect the real α_2 axis gives the time that a physical singularity appears. In this section, we study the local form of the interface shape in the neighborhood of the physical singularity.

Without loss of generality, we assume that the singularity forms at $t = 0$ and $(\alpha_1, \alpha_2) = (0, 0)$, and that the surface is moving with a velocity of $\dot{\mathbf{z}}$ at that point. We also assume that at the time of singularity formation, the surface is locally flat in the neighborhood of the singularity, with $\mathbf{z} \sim \mathbf{z}_0(\alpha_1, \alpha_2)$, where $\mathbf{z}_0$ is a plane. Moreover, we assume that (α_1, α_2) satisfies (3.54) and (3.55) at time $t = 0$.

We seek an asymptotic expansion of the solution of the three-dimensional vortex sheet equation

$$\frac{\partial \mathbf{z}}{\partial t}(\mathbf{z}) = \int_{-\infty}^{\infty}\int_{-\infty}^{\infty} |\nabla_\alpha \mu(\alpha')^T, \nabla_\alpha \mathbf{z}(\alpha')^T| \times \nabla_{\mathbf{z}'} G(\mathbf{z}(\alpha) - \mathbf{z}(\alpha'))\, d\alpha' \,, \tag{3.67}$$

where we have used the notation

$$|\nabla_\alpha \mu(\alpha')^T, \nabla_\alpha \mathbf{z}(\alpha')^T| = \frac{\partial \mu}{\partial \alpha_1}\mathbf{z}_{\alpha_2} - \frac{\partial \mu}{\partial \alpha_2}\mathbf{z}_{\alpha_1} \,,$$

to exclude the possibility of the singularity formation along a segment of a one dimensional curve.

and

$$\begin{aligned} G(\mathbf{z}-\mathbf{z}') &= -\frac{1}{4\pi|\mathbf{z}-\mathbf{z}'|}\,, \\ \nabla_{z'}G(\mathbf{z}-\mathbf{z}(\alpha')) &= -\frac{\mathbf{z}-\mathbf{z}}{4\pi|\mathbf{z}-\mathbf{z}'|^3}\,. \end{aligned}$$

Following the idea of Cowley, Baker & Tanveer [12], we separate the integral on the right-hand side of (3.67) into two regions: a local region where $|\alpha'| = O(t)$ and an outer region covering the rest of the sheet,

$$\frac{\partial \mathbf{z}}{\partial t}(\mathbf{z}) = \left(\int_{|\alpha'|>\delta} + \int_{|\alpha'|\le\delta}\right) |\nabla_\alpha \mu(\alpha')^T, \nabla_\alpha \mathbf{z}(\alpha')^T| \times \nabla_{\mathbf{z}'} G(\mathbf{z}(\alpha)-\mathbf{z}(\alpha'))\, d\alpha' \,. \tag{3.68}$$

In order to determine the local shape of the vortex sheet near the singularity, it is not necessary to consider the first integral in detail, other than to note that in the Taylor expansion of $\mathbf{z}(\alpha,t)$ in powers of t, the first two terms of the asymptotic expansion can be assumed to be $O(t^0)$ and $O(t^1)$, as in [12]. This means that the leading order contribution from the first integral is of order $O(t^0)$. It also suggests that the leading order correction terms from the first integral is smaller than that of the second integral, as we will show later. Therefore, the shape of the vortex sheet in the neighborhood of the singularity is essentially determined by the second integral. In order to approximate the singularity, it is convenient to write $\mathbf{z}$ in the form of components on the two tangential and one normal directions.

$$\mathbf{z} = \dot{\mathbf{z}}_0 t + \begin{pmatrix} \mathbf{z}_0^{T_1} \\ \mathbf{z}_0^{T_2} \\ \mathbf{z}_0^{N} \end{pmatrix} + \begin{pmatrix} P_1(\alpha,t) \\ P_2(\alpha,t) \\ P_3(\alpha,t) \end{pmatrix} \,, \tag{3.69}$$

where

$$\begin{aligned} z_0^{T_1} &= z_0 \cdot T_1 \ , \\ z_0^{T_2} &= z_0 \cdot T_2 \ , \\ z_0^{N} &= z_0 \cdot N \ , \end{aligned}$$

and

$$T_1 = \frac{z_{0_{\alpha_1}}}{|z_{0_{\alpha_1}}|} \ , \qquad T_2 = \frac{z_{0_{\alpha_2}}}{|z_{0_{\alpha_2}}|} \ ,$$

$$N = \frac{z_{0_{\alpha_1}} \times z_{0_{\alpha_2}}}{|z_{0_{\alpha_1}} \times z_{0_{\alpha_2}}|} \ ,$$

where P_1, P_2, and P_3 are small perturbations of the interface from the tangent plane in the T_1, T_2, and N directions respectively.

We substitute (3.69) into the second integral of the three-dimensional vortex sheet equation and seek asymptotic expansions of P_i's. We follow the analysis in [17] where Hou & Zhang, among other results, studied the growth rate for the linearized motion about an arbitrary smooth solution to the three-dimensional vortex sheet equation. In our case, we can use their result directly because a flat plane is an equilibrium state of equation (3.67), and therefore, the leading order terms extracted from the asymptotic expansion coincide with the leading order terms in the linearized equation.

By introducing ϕ_1 and ϕ_2 as

$$\phi_1 = (\sigma_2)^{-1}\tilde{H}_2 P_1 - (\sigma_1)^{-1}\tilde{H}_1 P_2 \,, \tag{3.70}$$

$$\phi_2 = (\sigma_1)^{-1}\tilde{H}_1 P_1 + (\sigma_2)^{-1}\tilde{H}_2 P_2 \,, \tag{3.71}$$

where $\tilde{H}_1$ and $\tilde{H}_2$ are the Riesz transforms defined on the interface,

$$(\tilde{H}_l f)(\alpha) = \frac{1}{2\pi}\int \frac{(\alpha_l - \alpha_l')f(\alpha')}{(|\mathbf{z}_{0_{\alpha_1}}(\alpha)|^2(\alpha_1-\alpha_1')^2 + |\mathbf{z}_{0_{\alpha_2}}(\alpha)|^2(\alpha_2-\alpha_2')^2)^{3/2}}d\alpha' \,,$$

and denoting

$$\sigma_l^{-1} = |\mathbf{z}_{0_{\alpha_l}}| \,,$$

with $l = 1, 2$, Hou & Zhang [17] showed that

$$\frac{\partial \phi_1}{\partial t} = E_1(\phi_1, \phi_2, P_3) \,, \tag{3.72}$$

$$\frac{\partial \phi_2}{\partial t} = \frac{1}{2}\sigma_1\sigma_2\frac{\partial P_3}{\partial \alpha_2} + E_2(\phi_1, \phi_2, P_3) \,, \tag{3.73}$$

$$\frac{\partial P_3}{\partial t} = -\frac{1}{2}\sigma_1^3\sigma_2^3\frac{\partial \phi_2}{\partial \alpha_2} + \frac{1}{2}\sigma_1^2\sigma_2^4\frac{\partial \phi_1}{\partial \alpha_1} + E_3(\phi_1, \phi_2, P_3) \,, \tag{3.74}$$

where E_1, E_2, and E_3 are the general representations of terms that are either smaller or smoother than the leading order terms, provided that ϕ_1, ϕ_2, and P_3 are of small amplitude. More importantly, E_1, E_2, and E_3 do not contain terms with higher order differentiations.

Following the idea by Cowley, Baker & Tanveer [12], we introduce a rescaling by

$$\alpha_2 = (-t)\chi \,, \tag{3.75}$$

and seek similarity solutions of the form

$$\phi_1 = (-t)^q F_1(\alpha_1, \chi) + \cdots , \tag{3.76}$$

$$\phi_2 = (-t)^q F_2(\alpha_1, \chi) + \cdots , \tag{3.77}$$

$$P_3 = (-t)^q F_3(\alpha_1, \chi) + \cdots , \tag{3.78}$$

where $q > 1$ in order to be consistent with the assumption of the sheet being locally flat in the neighborhood of singularity. Since we have showed that branch point singularities on the α_2 direction develop at $t = 0+$, we anticipate that $F_i \sim F_{i_\pm}|\chi|^q$ as $\chi \to \infty$, in order to match with the 'outer' region where $\alpha_2 = O(1)$. For the initial conditions analyzed in the last section, we have $q = 3/2$.

With the rescaling of (3.75), we substitute (3.76), (3.77), and (3.78) into (3.72), (3.73), and (3.74) and extract the $O((-t)^{-q+1})$ terms. It leads to

$$\chi F_{1_\chi} - qF_1 = 0 , \tag{3.79}$$

$$\chi F_{2_\chi} - qF_2 = \frac{1}{2}\sigma_1\sigma_2 F_{3_\chi} , \tag{3.80}$$

$$\chi F_{3_\chi} - qF_2 = -\frac{1}{2}\sigma_1^3\sigma_2^3 F_{2_\chi} + \frac{-t}{2}\sigma_1^2\sigma_2^4 F_{1_{\alpha_1}} . \tag{3.81}$$

Note that (3.79) has zero forcing term. This suggests that there is no qth order singularity in the ϕ_1 term. We conclude that $F_1 = 0$. Moreover, substituting this result into (3.80) and (3.81) leads to

$$\chi F_{2_\chi} - qF_2 = \frac{1}{2}\sigma_1\sigma_2 F_{3_\chi} , \tag{3.82}$$

$$\chi F_{3_\chi} - qF_2 = -\frac{1}{2}\sigma_1^3\sigma_2^3 F_{2_\chi} . \tag{3.83}$$

Since σ_1 and σ_2 are nearly constants in the neighborhood of the singularity, without loss of generality, we may assume that $\sigma_1 = 1$ and $\sigma_2 = 1$. Note that in equations (3.82) and (3.83), α_1 can be considered as a parameter, which shows that the essential direction in which singularities form is the α_2 direction.

To solve (3.82) and (3.83), by taking $\sigma_1 = \sigma_2 = 1$, we define

$$F = F_2 + iF_3 \ , \tag{3.84}$$

so that we can combine the system and derive

$$\chi F' - qF = -\frac{1}{2}iF' \ . \tag{3.85}$$

By solving F from (3.85), we get

$$\begin{aligned} F &= C\left(\chi + \frac{1}{2}i\right)^q \\ &= C2^{-q}(4\chi^2+1)^{\frac{q}{2}} \exp(iq \arctan((2\chi)^{-1})) \ , \end{aligned} \tag{3.86}$$

where C is a function of α_1 only.

In summary, we conclude that near the physical singularity time, by transferring $(\mathbf{z}^{T_1}, \mathbf{z}^{T_2}, \mathbf{z}^N)$ into $(\phi_1, \phi_2, \mathbf{z}^N)$, the curvature singularity does not appear on the ϕ_1 function to the leading order. For ϕ_2 and $\mathbf{z}^N$, the curvature singularity can be observed on at least one of the two functions.

Remark: We show that our result is consistent with that of Brady & Pullin's [7]. In [7], Brady & Pullin studied a three-dimensional vortex sheet with cylindrical shape and strength distribution at the same time. In particular, they assume that initially, the interface has a

normal mode disturbance of the form

$$h(x,y) = A\exp[i(mx+ny)]\ , \tag{3.87}$$

with uniform velocity jump U in the x-direction. By rotating from (x,y,z) axes to (x',y',z') axes

$$kx' = mx+ny\ , \qquad ky' = -nx+my\ , \qquad z' = z\ , \tag{3.88}$$

where $k^2 = m^2+n^2$, they showed that the singularity evolution in this special case is equivalent to that of a two-dimensional vortex sheet with velocity jump of $U\frac{m}{k}$.

To apply our analysis to this special case, we take $x = \alpha_1$ and $y = \alpha_2$ at the initial time to fit the initial coordinates taken by Brady & Pullin in [7]. Under this choice of coordinates, the transformations (3.70) and (3.71) applied to the normal mode is equivalent to a rotation of the axes. This is because the the Fourier representations of the Riesz transforms are:

$$\frac{-i\xi_k}{(\xi_1^2+\xi_2^2)^{1/2}} \tag{3.89}$$

where $k = 1,2$ and (ξ_1,ξ_2) are the Fourier mode. Since the normal mode functions only have one Fourier mode, applying the Riesz transforms is equivalent to multiplying constants to such functions. Specifically, the transformations (3.70) and (3.71) applied to normal mode initial condition (3.87) is equivalent to the axis rotation of (3.88). In this particular case, ϕ_1 defined by (3.70) turns out to be zero, as has been proved in [7]. This shows that our analysis is consistent with Brady & Pullin's result when we apply our analysis to their initial data.

We would also like to point out that even though Brady & Pullin [7] have shown that the singularity appears in both α_1 and α_2 direction, the singularity in the α_2 direction is the essential singularity. This can be seen from rotating the normal mode in the (m, n) plane. When we take $m = 0$, which means that the direction that the wave propagates is orthogonal to the x-direction, the singularity disappears. However, if we take $n = 0$, which means that the direction along which the wave propagates is parallel to the x-direction, the singularity still exists, and in addition, the physical singularity time is smaller than any other combinations of (m, n). This confirms that the velocity jump direction is the fundamental direction for the singularity development, and the tangential velocity jump is the driving force of singularity formation for vortex sheets.

Chapter 4 Existence Proof of the Three-dimensional Vortex Sheet Problem

In this chapter, we prove the long time existence of a three-dimensional vortex sheet slightly perturbed from an equilibrium state and in the absence of surface tension.

The sections of this chapter are arranged as follows. Section 1 provides a general introduction to the formulation of this problem, and states our main result. In Section 2, we derive a nonlinear system with linear leading order terms. This system is our platform of the existence proof. We devote Section 3 to the outline of the proof without details of energy estimates and the estimates of the nonlinear terms in our derived system. In Section 4, we provide the technical details omitted in Section 3.

4.1 Formulation and Main Result

4.1.1 General Formulation

We consider an interface S separating two infinite layers of incompressible, inviscid, irrotational and identical fluids in the absence of surface tension. Using the Lagrangian frame, the interface location at any instant t is given by:

$$\mathbf{z}(\alpha_1, \alpha_2, t) = (x(\alpha_1, \alpha_2, t)\ , y(\alpha_1, \alpha_2, t), z(\alpha_1, \alpha_2, t))^T\ , \tag{4.1}$$

where (α_1, α_2) is the Lagrangian surface parameter. Thus, the normalized tangential vectors to the surface, $\mathbf{T}_1$ and $\mathbf{T}_2$, are defined by

$$\mathbf{T}_1 = \frac{\mathbf{z}_{\alpha_1}}{|\mathbf{z}_{\alpha_1}|} , \qquad \mathbf{T}_2 = \frac{\mathbf{z}_{\alpha_2}}{|\mathbf{z}_{\alpha_2}|} , \tag{4.2}$$

and the normal vector to the surface $\mathbf{N}$ is defined by

$$\mathbf{N} = \frac{\mathbf{z}_{\alpha_1} \times \mathbf{z}_{\alpha_2}}{|\mathbf{z}_{\alpha_1} \times \mathbf{z}_{\alpha_2}|} . \tag{4.3}$$

We label the region below the interface as Region 1 and the region above the interface as Region 2. Therefore, the velocity field $\mathbf{u}_1$ ($\mathbf{u}_2$) is the velocity below (above) the interface. We define $\mathbf{u}_+$ to be the limit of $\mathbf{u}_2$ approaching the interface from Region 2 and $\mathbf{u}_-$ to be the limit of $\mathbf{u}_1$ approaching the interface from Region 1.

Since the flow in each region is irrotational, we can introduce the velocity potentials ϕ_1 and ϕ_2 so that

$$\mathbf{u}_1 = \nabla\phi_1 , \qquad \mathbf{u}_2 = \nabla\phi_2 . \tag{4.4}$$

Furthermore, since the flows are incompressible, the velocity potentials satisfy the Laplace equation:

$$\nabla^2\phi_1 = 0 \quad \text{and} \quad \nabla^2\phi_2 = 0 . \tag{4.5}$$

Therefore, the potentials in the fluid domain can be written in the following dipole

representation [2]:

$$\phi(\mathbf{z}) = \int_{S'} \mu(\alpha')(\mathbf{z}_{\alpha_1} \times \mathbf{z}_{\alpha_2})(\alpha') \cdot \nabla_{z'} G(\mathbf{z} - \mathbf{z}(\alpha'))d\alpha' \ , \tag{4.6}$$

where

$$\begin{aligned} G(\mathbf{z} - \mathbf{z}') &= -\frac{1}{4\pi|\mathbf{z} - \mathbf{z}'|} \ , \\ \nabla_{z'} G(\mathbf{z} - \mathbf{z}(\alpha')) &= -\frac{\mathbf{z} - \mathbf{z}}{4\pi|\mathbf{z} - \mathbf{z}'|^3} \ . \end{aligned}$$

and $\mu(\alpha) = \phi_- - \phi_+$.

By differentiating equation (4.6) with respect to $\mathbf{z}$ and then integrating by parts, we obtain

$$\nabla\phi(\mathbf{z}) = \int_{S'} |\nabla_\alpha \mu(\alpha')^T, \nabla_\alpha \mathbf{z}(\alpha')^T| \times \nabla_{\mathbf{z}'} G(\mathbf{z} - \mathbf{z}(\alpha'))\, d\alpha' \ , \tag{4.7}$$

where we have used the notation

$$|\nabla_\alpha \mu(\alpha')^T, \nabla_\alpha \mathbf{z}(\alpha')^T| = \frac{\partial \mu}{\partial \alpha_1}\mathbf{z}_{\alpha_2} - \frac{\partial \mu}{\partial \alpha_2}\mathbf{z}_{\alpha_1} \ .$$

The motion of the interface is governed by

$$\frac{\partial \mathbf{z}}{\partial t} = \mathbf{u} \ ,$$

where $\mathbf{u} = (u, v, w)$ is the velocity of fluid particles on the interface. The kinematic condition that ensures that the interface moves with the fluid requires that the normal component of the velocity be continuous at the interface. However, the tangential velocity at the interface

is arbitrary and can be chosen at our convenience.

For the vortex sheet problem, we apply Bernoulli's equation to the upper and lower layer of fluid respectively. Based on the continuity of the normal stress, and combining with equation (4.6) and equation (4.7), we can show that with $\mathbf{u} = \frac{1}{2}(\mathbf{u}_+ + \mathbf{u}_-)$,

$$\frac{\partial \mu}{\partial t} = 0 \tag{4.8}$$

holds [4]. Equation (4.8) says that the circulation stays constant along the trajectories whose motions are determined by the average fluid velocity.

With this particular choice of tangential velocity, the velocity of the vortex sheet interface can be obtained by the average of the limiting velocities in equation (4.7) approaching from the upper and lower layer of fluid. The equation of the surface particle motion can be written as:

$$\frac{\partial \mathbf{z}}{\partial t}(\mathbf{z}) = \int_{S'} |\nabla_\alpha \mu(\alpha')^T, \nabla_\alpha \mathbf{z}(\alpha')^T| \times \nabla_{\mathbf{z}'} G(\mathbf{z}(\alpha) - \mathbf{z}(\alpha'))\, d\alpha' \,, \tag{4.9}$$

where $\mathbf{z} \in S$ and the integral takes Cauchy principal value.

4.1.2 Main Result

Throughout this chapter, we study the long time existence of a unique solution to the initial value problem (4.9). The main result is to prove the existence of such a solution given a slightly perturbed periodic initial condition from an equilibrium flat state. More precisely,

$\mathbf{z}$ is written as

$$\mathbf{z} = \begin{pmatrix} x \\ y \\ z \end{pmatrix} = \begin{pmatrix} \alpha_1 \\ \alpha_2 \\ 0 \end{pmatrix} + \begin{pmatrix} P_1 \\ P_2 \\ P_3 \end{pmatrix} , \tag{4.10}$$

where P_1, P_2 and P_3 are periodic functions with period of $(2\pi \times 2\pi)$ and small analytic initial values. Furthermore, without loss of generality, we assume $\mu = \gamma_1\alpha_1 + \gamma_2\alpha_2$, with γ_1 and γ_2 being two constants. The existence of such a set of coordinates was proved in the last chapter where we studied the early time singularity formation of three-dimensional vortex sheets.

Similar to the two-dimensional problem, there is no existence result in the Sobolev norm (Caflisch & Orellana, [9]). Therefore, we establish the well-posedness in an analytic norm. Particularly, we choose the Lipschitz norm within a certain complex strip following the idea of Caflisch and Orellana [9]. The following theorem is our main result.

Theorem 4.1.1 *(Long Time Existence of 3D Vortex Sheet Solutions) Let* $0 < \kappa < 1$, $0 < \alpha < 1$, *and* $\rho_0 > 0$. *Assume that* $\mathbf{z}$ *has the form of (4.10) with* $S_i(\beta_1, \beta_2, 0)$ *satisfying*

$$\sup_{\substack{|Im(\beta_1)|<\rho_0 \\ |Im(\beta_2)|<\rho_0}} \Big(|S_i(\beta_1,\beta_2,0)| + |\nabla S_i(\beta_1,\beta_2,0)| + \sum_{k=1}^{2}\sum_{j=1}^{2} |(\partial_{\beta_k}\partial_{\beta_j} S_i(\beta_1,\beta_2,0))| \Big) < \varepsilon , \tag{4.11}$$

where $i = 1, 2, 3$ *and* ε *is sufficiently small.*

Then there exists a solution $\mathbf{z} = (\beta_1, \beta_2, 0)^T + (S_1, S_2, S_3)^T$ *for a time* $0 \le t \le T$, *where*

T satisfies

$$T < \frac{\rho_0}{\frac{1}{2}+\kappa} \ , \ \textit{and} \ \ \kappa^{-2}\varepsilon T \ll 1 \ .$$

Moreover, $S_i(t)$ satisfies:

$$\begin{aligned} \sum_{i=1}^{3} \|S_i(t)\|_{\alpha\rho} &\leq c(\kappa^{-1}t)\varepsilon \\ &\leq c(\kappa^{-1}T)\varepsilon \ , \end{aligned}$$

for any ρ and t such that

$$0 < \rho < \rho_0 - \frac{t}{\frac{1}{2}+\kappa} \ ,$$

where c is independent of ε, κ and ρ_0. And the Lipschitz norm is defined by

$$\|f\|_{\alpha\rho} = \sup_{\substack{|Im(\kappa_1)|<\rho \\ |Im(\kappa_2)|<\rho}} |f(\kappa_1,\kappa_2)| + \sup_{\substack{|Im(\kappa_1)|<\rho, \ \ |Im(\kappa_2)|<\rho \\ |Im(\kappa_1')|<\rho, \ \ |Im(\kappa_2')|<\rho \\ (\kappa_1,\kappa_2)\neq(\kappa_1',\kappa_2')}} \frac{|f(\kappa_1,\kappa_2)-f(\kappa_1',\kappa_2')|}{|(\kappa_1,\kappa_2)-(\kappa_1',\kappa_2')|^{\alpha}} \ .$$

Remarks: This result is similar to the two-dimensional result proved by Caflisch and Orellana [9]. Particularly, the existence times in the two results are same up to the leading order term $2\rho_0$. Besides, a linear time growth rate is observed in both results even though it is bounded over all by the product of ϵ and the maximum existence time, εT.

4.2 A Nonlinear System with Linear Leading Order Terms

In this section, we derive a nonlinear system with linear leading order terms from equation (4.9). The linear terms constitute an elliptic system, whose initial value problem leads to Kelvin-Helmholtz instability. The nonlinear terms are small in the Lipschitz norm for analytic solutions within a strip in the complex domain. The bounds of the nonlinear terms are proved rigorously in the next section.

To overcome the instability from the Cauchy-Riemann structure, we extend the independent variables into the complex domain. With this complexification, the system can be considered as a hyperbolic system with complex characteristic speeds. With its characteristic lines propagating within the complex domain, the ill-posed problem in the physical domain becomes a well-posed problem in the extended complex domain with shrinking analytic strip.

Before we start deriving the system, it is necessary to introduce the Riesz transforms, which will be used extensively throughout this chapter.

Define:

$$H_1(f) = \frac{1}{2\pi}\iint \frac{(\alpha_1-\alpha_1')f(\alpha')}{((\alpha_1-\alpha_1')^2+(\alpha_2-\alpha_2')^2)^{\frac{3}{2}}}\,d\alpha' , \tag{4.12}$$

$$H_2(f) = \frac{1}{2\pi}\iint \frac{(\alpha_2-\alpha_2')f(\alpha')}{((\alpha_1-\alpha_1')^2+(\alpha_2-\alpha_2')^2)^{\frac{3}{2}}}\,d\alpha' , \tag{4.13}$$

for $f \in L^p(\Re^2)$, where $1 < p < \infty$, $\alpha' = (\alpha_1', \alpha_2')$. The integrals take the Cauchy principal value.

In [30], Stein proved that the Riesz transformations have the following spectral repre-

sentations:

$$\widehat{H_1 f} = \frac{-i\xi_1}{(\xi_1^2+\xi_2^2)^{1/2}}\hat{f} \ , \tag{4.14}$$

$$\widehat{H_2 f} = \frac{-i\xi_2}{(\xi_1^2+\xi_2^2)^{1/2}}\hat{f} \ , \tag{4.15}$$

in which $\hat{f}$ stands for the Fourier transformation of $f \in L^2(\Re^2)$.

From (4.14) and (4.15), the following Lemma can be shown straightforwardly.

Lemma 4.2.1 *For $f(\alpha_1, \alpha_2) \in H^1(\Re^2)$ and $\hat{f}(0) = 0$, where $H^1(\Re^2)$ is the Sobolev H^1 space on $\Re^2$ and $\hat{f}$ is the Fourier transform of f. The following equalities hold:*

$$H_1 H_2(f) = H_2 H_1(f) \ ,$$

$$H_1 D_2(f) = H_2 D_1(f) \ ,$$

$$(H_1 H_1 + H_2 H_2)(f) = -f \ ,$$

where D_1 (D_2) stands for derivative operator with respect to α_1 (α_2).

Throughout the derivation, we will encounter the following singular operators:

$$\Lambda(f) = \frac{1}{2\pi}\int\int \frac{f(\alpha)-f(\alpha')}{((\alpha_1-\alpha_1')^2+(\alpha_2-\alpha_2')^2)^{\frac{3}{2}}}\, d\alpha' \ , \tag{4.16}$$

$$\Lambda^{11}(f) = \frac{1}{2\pi}\int\int \frac{(\alpha_1-\alpha_1')^2(f(\alpha)-f(\alpha'))}{((\alpha_1-\alpha_1')^2+(\alpha_2-\alpha_2')^2)^{\frac{5}{2}}}\, d\alpha' \ , \tag{4.17}$$

$$\Lambda^{12}(f) = \frac{1}{2\pi} \int\int \frac{(\alpha_1 - \alpha_1')(\alpha_2 - \alpha_2')(f(\alpha) - f(\alpha'))}{((\alpha_1 - \alpha_1')^2 + (\alpha_2 - \alpha_2')^2)^{\frac{5}{2}}} d\alpha' , \tag{4.18}$$

$$\Lambda^{22}(f) = \frac{1}{2\pi} \int\int \frac{(\alpha_2 - \alpha_2')^2(f(\alpha) - f(\alpha'))}{((\alpha_1 - \alpha_1')^2 + (\alpha_2 - \alpha_2')^2)^{\frac{5}{2}}} d\alpha' . \tag{4.19}$$

Hou & Zhang [16] proved the following lemma:

Lemma 4.2.2 *For* $f(\alpha_1, \alpha_2) \in H^1(\Re^2)$,

$$\begin{aligned}
\Lambda(f) &= (H_1 D_1 + H_2 D_2)(f) , \\
\Lambda^{11}(f) &= \frac{1}{3}(2H_1 D_1 + H_2 D_2)(f) , \\
\Lambda^{12}(f) &= \frac{1}{3} H_1 D_2(f) , \\
\Lambda^{22}(f) &= \frac{1}{3}(H_1 D_1 + 2H_2 D_2)(f) .
\end{aligned}$$

Up to now, we have defined the Riesz transforms for L^2 functions in the infinite domain. We would like to extend the definition to periodic functions. This can be implemented in two ways. One is to use the Fourier representations, in which the Fourier transforms in (4.14) and (4.15) will be written in the form of Fourier coefficients for periodic functions. This can be done for Lipschitz continuous functions $Lip_\alpha([0, 2\pi] \times [0, 2\pi])$ because of the fact that $Lip_\alpha([0, 2\pi] \times [0, 2\pi]) \subset L^2([0, 2\pi] \times [0, 2\pi])$.

Another way to extend the definition is through the kernel. We denote $K(\alpha_1, \alpha_2)$ the integral kernel of the Riesz transform, and assume that f is periodic with period of $2\pi \times 2\pi$ and

$$\int_{-\pi}^{\pi}\int_{-\pi}^{\pi} f(\alpha_1, \alpha_2) d\alpha_1 d\alpha_2 = 0 . \tag{4.20}$$

The Riesz transform with kernel $K(\alpha_1, \alpha_2)$ can be written as:

$$\begin{aligned}
H_i(f)(\zeta) &= \int_{-\infty}^{\infty}\int_{-\infty}^{\infty} f(\zeta-\alpha)K(\alpha)d\alpha_1 d\alpha_2 \\
&= \lim_{n_1,n_2\to\infty} \int_{-(2n_1+1)\pi}^{(2n_1+1)\pi}\int_{-(2n_2+1)\pi}^{(2n_2+1)\pi} f(\zeta-\alpha)K(\alpha)d\alpha_1 d\alpha_2 \\
&= \lim_{n_1,n_2\to\infty} \sum_{k_1=-n_1}^{n_1}\sum_{k_2=-n_2}^{n_2} \int_{(2k_1-1)\pi}^{(2k_1+1)\pi}\int_{(2k_2-1)\pi}^{(2k_2+1)\pi} f(\zeta-\alpha)K(\alpha)d\alpha_1 d\alpha_2 \\
&= \lim_{n_1,n_2\to\infty} \int_{-\pi}^{\pi}\int_{-\pi}^{\pi} f(\zeta-\alpha)[K(\alpha) \\
&\qquad + \sum_{\substack{(k_1,k_2)=(-n_1,-n_2)\\(k_1,k_2)\neq(0,0)}}^{(n_1,n_2)} K(\alpha_1-2k_1\pi, \alpha_2-2k_2\pi)]d\alpha_1 d\alpha_2 \\
&= \lim_{n_1,n_2\to\infty} \int_{-\pi}^{\pi}\int_{-\pi}^{\pi} f(\zeta-\alpha)[K(\alpha) \\
&\qquad + \sum_{\substack{(k_1,k_2)=(-n_1,-n_2)\\(k_1,k_2)\neq(0,0)}}^{(n_1,n_2)} (K(\alpha-2k\pi)-K(-2k\pi))]d\alpha_1 d\alpha_2 \ ,
\end{aligned} \tag{4.21}$$

where $\alpha = (\alpha_1, \alpha_2)$, $\zeta = (\zeta_1, \zeta_2)$, and $k = (k_1, k_2)$ with k_1, k_2 both being integers. We have used the fact that $\int f(\alpha)\, d\alpha = 0$ in the last step.

If for the kernel $K(\alpha)$,

$$\sum_{\substack{(k_1,K_2)=(-n_1,-n_2)\\(k_1,k_2)\neq(0,0)}}^{(n_1,n_2)} (K(\alpha-2k\pi)-K(-2k\pi))]$$

converges absolutely and uniformly for $\alpha \in [0, 2\pi] \times [0, 2\pi]$, we can take the limit into the integral and define:

$$\begin{aligned}
K^*(\alpha) &= K(\alpha) + \sum_{k\neq(0,0)} [K(\alpha+2k\pi) - K(2k\pi)] \\
&= K(\alpha) + \overline{K}(\alpha) \ ,
\end{aligned} \tag{4.22}$$

for each $(\alpha_1, \alpha_2) \in [0, 2\pi] \times [0, 2\pi]$.

It is well-known [11] that the sum $\overline{K}(\alpha_1, \alpha_2)$ does converge absolutely and uniformly to a bounded function for $(\alpha_1, \alpha_2) \in [0, 2\pi] \times [0, 2\pi]$. Particularly, K^* converges to $\frac{1}{2}\cot(\frac{1}{2}\alpha)$ if K is the kernel of the Hilbert transform in one dimension. This shows that the Riesz transform for periodic functions is well-defined. It can be written so that its integration interval is either the function period or the infinite domain; both forms are equivalent.

We derive similarly the periodic kernel of the vortex sheet integral. The result is analogous to obtaining the kernel $\frac{1}{2}\cot(\frac{z-z'}{2})$ in one-dimensional space.

Denote:

$$K_z^1(\alpha, \alpha - \zeta) = \frac{\zeta_1}{|\mathbf{z}(\alpha) - \mathbf{z}(\alpha - \zeta)|^3} , \tag{4.23}$$

where $\alpha = (\alpha_1, \alpha_2)$ and $\zeta = (\zeta_1, \zeta_2)$. Since $\mathbf{z}$ has the form of (4.10), the denominator can be re-written as:

$$|\mathbf{z}(\alpha) - \mathbf{z}(\alpha - \zeta)|^3 = \left| \begin{pmatrix} \zeta_1 \\ \zeta_2 \\ 0 \end{pmatrix} + \begin{pmatrix} S_1(\alpha) - S_1(\alpha - \zeta) \\ S_2(\alpha) - S_2(\alpha - \zeta) \\ S_3(\alpha) - S_3(\alpha - \zeta) \end{pmatrix} \right|^3 . \tag{4.24}$$

Using the periodicity of S_1, S_2 and S_3, one can show that

$$|\mathbf{z}(\alpha) - \mathbf{z}(\alpha - (\zeta + 2k\pi))|^3 = \left| \begin{pmatrix} \zeta_1 + 2k_1\pi \\ \zeta_2 + 2k_2\pi \\ 0 \end{pmatrix} + \begin{pmatrix} S_1(\alpha) - S_1(\alpha - \zeta) \\ S_2(\alpha) - S_2(\alpha - \zeta) \\ S_3(\alpha) - S_3(\alpha - \zeta) \end{pmatrix} \right|^3 , \tag{4.25}$$

where $k = (k_1, k_2)$. Consequently, we can define:

$$\begin{aligned} & K_z^{1*}(\alpha, \alpha - \zeta) \\ &= K_z^1(\alpha, \alpha - \zeta) + \sum_{k \neq (0,0)} (K_z^1(\alpha, \alpha - (\zeta + 2k\pi)) - K^1(2k\pi)) \\ &= K_z^1(\alpha, \alpha - \zeta) + \overline{K_z^1}(\alpha, \alpha - \zeta) \end{aligned} \tag{4.26}$$

where K^1 is the kernel of Riesz transform in the α_1-direction,

$$K^1(\zeta) = \frac{\zeta_1}{|\zeta|^3} .$$

Similar to equation (4.22), $\overline{K_z^1}$ converges absolutely and uniformly to a bounded function for every $(\alpha_1, \alpha_2) \in [0, 2\pi] \times [0, 2\pi]$ provided that the perturbation from $\mathbf{z}$ to a flat plane is sufficiently small.

The idea can be illustrated in the case of Hilbert transform, where

$$\begin{aligned} K_z(\alpha, \alpha - \zeta) &= \frac{1}{z(\alpha) - z(\alpha - \zeta)} \\ &= \frac{1}{\zeta + s(\alpha) - s(\alpha - \zeta)} , \end{aligned}$$

and

$$K(\alpha) = \frac{1}{\alpha} .$$

In this particular case, there is a closed form of $K_z^*(\alpha, \alpha-\zeta)$:

$$\begin{aligned} & K_z^*(\alpha, \alpha-\zeta) \\ = \; & K_z(\alpha, \alpha-\zeta) + \sum_{k\neq 0}(K_z(\alpha, \alpha-(\zeta+2k\pi)) - K(2k\pi)) \\ = \; & \frac{1}{z(\alpha)-z(\alpha-\zeta)} + \sum_{k\neq 0}\left(\frac{1}{2k\pi + z(\alpha) - z(\alpha-\zeta)} - \frac{1}{2k\pi}\right) \\ = \; & \frac{1}{2}\cot\left(\frac{1}{2}(z(\alpha)-z(\alpha-\zeta))\right) . \end{aligned} \tag{4.27}$$

Remarks: 1. The definition shows that the vortex sheet integral can be applied to the periodic functions as well. In addition, similar to the result of the Riesz transform, it can be written so that the integration interval is either the period of the function or the infinite domain as well.

2. As we will show rigorously in last section, if $\mathbf{z}$ is a small perturbation of a flat plane under the Lipschitz norm, i.e. ,

$$\mathbf{z} \sim (\alpha_1, \alpha_2, 0)^T + O(\varepsilon) ,$$

the vortex sheet kernel $K_z^{1*}(\alpha, \alpha-\zeta)$ defined in (4.26) is close to the Riesz transform kernel $K^{1*}(\alpha)$ defined in (4.22) under the same Lipschitz norm. This observation will be used extensively in the following derivation.

3. All the derivations in this section are formal. We write the remaining terms as $O(\varepsilon^2)$ since they are, as we will show later, of smaller amplitude, during the derivation. At the end of this section, we denote them as R_1, R_2 and R_3 respectively.

4. Since we have defined the Riesz transforms for periodic functions, the other singular integral operators mentioned before can be defined by Lemma 4.2.2.

Next we derive our target system. Based on the assumptions stated in the last section, equation (4.9) can be re-written as:

$$\begin{aligned}
\frac{\partial \mathbf{z}}{\partial t} &= -\frac{1}{4\pi}\iint \frac{(\gamma_1 \mathbf{z}'_{\alpha_2} - \gamma_2 \mathbf{z}'_{\alpha_1}) \times (\mathbf{z} - \mathbf{z}')}{|\mathbf{z} - \mathbf{z}'|^3}\, d\mathbf{z}' \\
&= -\frac{1}{4\pi}\iint \left[\gamma_1 \begin{pmatrix} S'_{1\alpha_2} \\ 1 + S'_{2\alpha_2} \\ S'_{3\alpha_2} \end{pmatrix} - \gamma_2 \begin{pmatrix} 1 + S'_{1\alpha_1} \\ S'_{2\alpha_1} \\ S'_{3\alpha_1} \end{pmatrix} \right] \\
&\quad \times \begin{pmatrix} \alpha_1 - \alpha'_1 + S_1 - S'_1 \\ \alpha_2 - \alpha'_2 + S_2 - S'_2 \\ S_3 - S'_3 \end{pmatrix} \frac{d\alpha'}{|\mathbf{z} - \mathbf{z}'|^3} \cdot
\end{aligned}$$

Since $S_i \sim O(\varepsilon)$, it is reasonable to consider the linear terms in the integral as the leading order terms. By writing down every component separately and only keeping the linear terms, equations for S_1, S_2 and S_3 can be obtained.

$$\begin{aligned}
\frac{\partial S_1}{\partial t} &= -\frac{1}{4\pi}\iint \frac{(\gamma_1(1 + S'_{2\alpha_2}) - \gamma_2 S'_{2\alpha_1})(S_3 - S'_3)}{|\ \mathbf{z} - \mathbf{z}'|^3} \\
&\quad - \frac{(\gamma_1 S'_{3\alpha_2} - \gamma_2 S'_{3\alpha_1})(\alpha_2 - \alpha'_2 + S_2 - S'_2)}{|\mathbf{z} - \ \mathbf{z}'|^3}\, d\alpha' \\
&= -\frac{1}{4\pi}\iint \frac{\gamma_1(S_3 - S'_3) - (\gamma_1 S'_{3\alpha 2} - \gamma_2 S'_{3\alpha_1})(\alpha_2 - \alpha'_2)}{|\mathbf{z} - \mathbf{z}'|^3}\, d\alpha' \\
&\quad + O(\varepsilon^2)\ ,
\end{aligned} \tag{4.28}$$

$$\begin{aligned}\frac{\partial S_2}{\partial t} &= -\frac{1}{4\pi}\int\int \frac{(\gamma_1 S'_{3\alpha_2} - \gamma_2 S'_{3\alpha_1})(\alpha_1 - \alpha'_1 + S_1 - S'_1)}{|\mathbf{z}-\mathbf{z}'|^3} \\ &\quad - \frac{(\gamma_1 S'_{1\alpha_2} - \gamma_2(1+S'_{1\alpha_1}))(S_3 - S'_3)}{|\mathbf{z}-\mathbf{z}'|^3}\, d\alpha' \\ &= -\frac{1}{4\pi}\int\int \frac{\gamma_2(S_3 - S'_3) + (\gamma_1 S'_{3\alpha 2} - \gamma_2 S'_{3\alpha_1})(\alpha_1 - \alpha'_1)}{|\mathbf{z}-\mathbf{z}'|^3}\, d\alpha' \\ &\quad + O(\epsilon^2)\ , \end{aligned} \tag{4.29}$$

and

$$\begin{aligned}\frac{\partial S_3}{\partial t} &= -\frac{1}{4\pi}\int\int \frac{(\gamma_1 S'_{1\alpha_2} - \gamma_2(1+S'_{1\alpha_1}))(\alpha_2 - \alpha'_2 + S_2 - S'_2)}{|\mathbf{z}-\mathbf{z}'|^3} \\ &\quad - \frac{(\gamma_1(1+S'_{2\alpha_2}) - \gamma_2 S'_{2\alpha_1})(\alpha_1 - \alpha'_1 + S_1 - S'_1)}{|\mathbf{z}-\mathbf{z}'|^3}\, d\alpha' \\ &= -\frac{1}{4\pi}\int\int \frac{(\gamma_1 S'_{1\alpha_2} - \gamma_2 S'_{1\alpha_1})(\alpha_2 - \alpha'_2)}{|\mathbf{z}-\mathbf{z}'|^3} \\ &\quad - \frac{(\gamma_1 S'_{2\alpha_2} - \gamma_2 S'_{2\alpha_1})(\alpha_1 - \alpha'_1)}{|\mathbf{z}-\mathbf{z}'|^3} \\ &\quad - \frac{\gamma_1(\alpha_1 - \alpha'_1 + S_1 - S'_1) + \gamma_2(\alpha_2 - \alpha'_2 + S_2 - S'_2)}{|\mathbf{z}-\mathbf{z}'|^3}\, d\alpha' \\ &\quad + O(\epsilon^2)\ . \end{aligned} \tag{4.30}$$

To understand the instability mechanism in the system, it is helpful to introduce the following change of variables.

$$\psi_1 = H_2(S_1) - H_1(S_2)\ , \tag{4.31}$$

$$\psi_2 = H_1(S_1) + H_2(S_2)\ . \tag{4.32}$$

The ill-posedness or instability will become more apparent using these new variables. Furthermore, from Lemma 4.2.1, (S_1, S_2) can be represented by (ψ_1, ψ_2) through the following

equations:

$$S_1 = -H_2(\psi_1) - H_1(\psi_2) \,, \tag{4.33}$$

$$S_2 = H_1(\psi_1) - H_2(\psi_2) \,. \tag{4.34}$$

Therefore, it follows from differentiating equation (4.31) and (4.32) with respect to time t that

$$\frac{\partial \psi_1}{\partial t} = H_2(\frac{\partial S_1}{\partial t}) - H_1(\frac{\partial S_2}{\partial t}) \,, \tag{4.35}$$

$$\frac{\partial \psi_2}{\partial t} = H_1(\frac{\partial S_1}{\partial t}) + H_2(\frac{\partial S_2}{\partial t}) \,. \tag{4.36}$$

To derive the leading order terms of the evolution equation for ψ_1, we substitute (4.28) and (4.29) into (4.35), so that

$$\begin{aligned} \frac{\partial \psi_1}{\partial t} &= H_2(\frac{\partial S_1}{\partial t}) - H_1(\frac{\partial S_2}{\partial t}) \\ &= H_2(-\frac{1}{4\pi}\int \frac{\gamma_1(S_3 - S_3') - (\gamma_1 S'_{3\alpha_2} - \gamma_2 S'_{3\alpha_1})(\alpha_2 - \alpha_2')}{|\mathbf{z} - \mathbf{z}'|^3}\, d\alpha') \\ &\quad - H_1(-\frac{1}{4\pi}\int \frac{\gamma_2(S_3 - S_3') + (\gamma_1 S'_{3\alpha_2} - \gamma_2 S'_{3\alpha_1})(\alpha_1 - \alpha_1')}{|\mathbf{z} - \mathbf{z}'|^3}\, d\alpha') \\ &\quad + O(\varepsilon^2) \,. \end{aligned} \tag{4.37}$$

By further using the observation that the vortex sheet kernel is close to the Riesz transform

kernel under Lipschitz norm, one can show that

$$\begin{aligned}
\frac{\partial \psi_1}{\partial t} &= -\frac{1}{2}H_2(\gamma_1 \Lambda S_3 - \gamma_1 H_2 D_2 S_3 + \gamma_2 H_2 D_1 S_3) \\
&\quad + \frac{1}{2}H_1(\gamma_2 \Lambda S_3 + \gamma_1 H_1 D_2 S_3 - \gamma_2 H_1 D_1 S_3) + O(\varepsilon^2) \\
&= -\frac{1}{2}H_2(\gamma_1 H_1 D_1 S_3 + \gamma_2 H_2 D_1 S_3) \\
&\quad + \frac{1}{2}H_1(\gamma_1 H_1 D_2 S_3 + \gamma_2 H_2 D_2 S_3) + O(\varepsilon^2) \\
&= O(\varepsilon^2)\ , \qquad (4.38)
\end{aligned}$$

where we have applied Lemma 4.2.1 and 4.2.2 in the last step.

Similarly, to derive the leading order terms in the evolution equation of ψ_2, we substitute (4.28) and (4.29) into (4.36) and get

$$\begin{aligned}
\frac{\partial \psi_2}{\partial t} &= H_1(\frac{\partial S_1}{\partial t}) + H_2(\frac{\partial S_2}{\partial t}) \\
&= H_1(-\frac{1}{4\pi}\int \frac{\gamma_1(S_3 - S_3') - (\gamma_1 S'_{3\alpha_2} - \gamma_2 S'_{3\alpha_1})(\alpha_2 - \alpha_2')}{|\mathbf{z} - \mathbf{z}'|^3}\, d\alpha') \\
&\quad + H_2(-\frac{1}{4\pi}\int \frac{\gamma_2(S_3 - S_3') + (\gamma_1 S'_{3\alpha_2} - \gamma_2 S'_{3\alpha_1})(\alpha_1 - \alpha_1')}{|\mathbf{z} - \mathbf{z}'|^3}\, d\alpha') \\
&\quad + O(\varepsilon^2)\ , \qquad (4.39)
\end{aligned}$$

which by our observation further implies that:

$$\begin{aligned}
\frac{\partial \psi_2}{\partial t} &= -\frac{1}{2}H_1(\gamma_1 \Lambda S_3 - \gamma_1 H_2 D_2 S_3 + \gamma_2 H_2 D_1 S_3) \\
&\quad - \frac{1}{2}H_2(\gamma_2 \Lambda S_3 + \gamma_1 H_1 D_2 S_3 - \gamma_2 H_1 D_1 S_3) + O(\varepsilon^2) \\
&= -\frac{1}{2}H_1(\gamma_1 H_1 D_1 S_3 + \gamma_2 H_2 D_1 S_3) \\
&\quad - \frac{1}{2}H_2(\gamma_1 H_1 D_2 S_3 + \gamma_2 H_2 D_2 S_3) + O(\varepsilon^2)\ . \qquad (4.40)
\end{aligned}$$

By applying Lemma 4.2.1 and 4.2.2, we simplify the above equation to

$$\begin{aligned}\frac{\partial \psi_2}{\partial t} &= -\frac{1}{2}\gamma_1 D_1(H_1H_1 + H_2H_2)S_3 \\ &\quad -\frac{1}{2}\gamma_2 D_2(H_1H_1 + H_2H_2)S_3 + O(\varepsilon^2) \\ &= \frac{1}{2}(\gamma_1 D_1 + \gamma_2 D_2)S_3 + O(\varepsilon^2)\ . \end{aligned} \tag{4.41}$$

For the evolution equation of S_3, we substitute (4.33) and (4.34) into (4.30), and extract the leading order terms:

$$\begin{aligned}\frac{\partial S_3}{\partial t} &= -\frac{1}{4\pi}\iint \frac{\gamma_1(-H_2(\psi_1') - H_1(\psi_2'))_{\alpha_2})(\alpha_2 - \alpha_2')}{|\mathbf{z}-\mathbf{z}'|^3} \\ &\quad + \frac{\gamma_2(H_2(\psi_1') + H_1(\psi_2')_{\alpha_1}(\alpha_2 - \alpha_2')}{|\mathbf{z}-\mathbf{z}'|^3} \\ &\quad + \frac{\gamma_2(H_1(\psi_1') - H_2(\psi_2'))_{\alpha_1}(\alpha_1 - \alpha_1')}{|\mathbf{z}-\mathbf{z}'|^3} \\ &\quad - \frac{\gamma_1(H_1(\psi_1') - H_2(\psi_2')_{\alpha_2}(\alpha_1 - \alpha_1')}{|\mathbf{z}-\mathbf{z}'|^3} \\ &\quad - \frac{\gamma_2(H_1(\psi_1 - \psi_1') - H_2(\psi_2 - \psi_2'))}{|\mathbf{z}-\mathbf{z}'|^3} \\ &\quad - \frac{\gamma_1(-H_2(\psi_1 - \psi_1') - H_1(\psi_2 - \psi_2'))}{|\mathbf{z}-\mathbf{z}'|^3} \\ &\quad - \frac{\gamma_1(\alpha_1 - \alpha_1') + \gamma_2(\alpha_2 - \alpha_2')}{|\mathbf{z}-\mathbf{z}'|^3}\, d\alpha' + O(\varepsilon^2)\ . \end{aligned} \tag{4.42}$$

By using Lemma 4.2.1 and 4.2.2, and the fact that $|\mathbf{z}-\mathbf{z}'| \sim |\alpha - \alpha'|$ to the leading order,

we obtain

$$\begin{aligned}
\frac{\partial S_3}{\partial t} &= \frac{1}{2}\gamma_1 H_2^2 D_2\psi_1 + \frac{1}{2}\gamma_1 H_2 H_1 D_2\psi_2 - \frac{1}{2}\gamma_2 H_2^2 D_1\psi_1 - \frac{1}{2}\gamma_2 H_2 H_1 D_1\psi_2 \\
&\quad + \frac{1}{2}\gamma_1 H_1^2 D_2\psi_1 - \frac{1}{2}\gamma_1 H_1 H_2 D_2\psi_2 - \frac{1}{2}\gamma_2 H_1^2 D_1\psi_1 + \frac{1}{2}\gamma_2 H_1 H_2 D_1\psi_2 \\
&\quad + \frac{1}{2}\gamma_2 \Lambda H_1\psi_1 - \frac{1}{2}\gamma_2 \Lambda H_2\psi_2 - \frac{1}{2}\gamma_1 \Lambda H_2\psi_1 - \frac{1}{2}\gamma_1 \Lambda H_1\psi_2 \\
&\quad + \frac{1}{4\pi}\int \frac{\gamma_2(\alpha_2 - \alpha_2') + \gamma_1(\alpha_1 - \alpha_1')}{|\mathbf{z} - \mathbf{z}'|^3}\, d\alpha' + O(\varepsilon^2) \\
&= \frac{1}{2}(\gamma_1 D_1 + \gamma_2 D_2)\psi_2 \\
&\quad + \frac{1}{4\pi}\int \frac{\gamma_2(\alpha_2 - \alpha_2') + \gamma_1(\alpha_1 - \alpha_1')}{|\mathbf{z} - \mathbf{z}'|^3}\, d\alpha' + O(\varepsilon^2)\,. \qquad (4.43)
\end{aligned}$$

It is necessary to analyze the integral term of equation (4.43) and extract the leading order contributions. By further expanding the integral in terms of S_i's, we find that the leading order terms are:

$$\begin{aligned}
&\frac{1}{4\pi}\int \frac{\gamma_2(\alpha_2 - \alpha_2') + \gamma_1(\alpha_1 - \alpha_1')}{|\mathbf{z} - \mathbf{z}'|^3}\, d\alpha' \\
&= -\frac{3}{4\pi}\int \frac{\gamma_2(\alpha_2 - \alpha_2')[(S_1 - S_1')(\alpha_1 - \alpha_1') + (S_2 - S_2')(\alpha_2 - \alpha_2')]}{|\mathbf{z} - \mathbf{z}'|^5}\,, \qquad (4.44)
\end{aligned}$$

where we applied the matrix equality of

$$\nabla_{z'}\nabla_{z'} G(\mathbf{z} - \mathbf{z}') = \frac{1}{4\pi}\Big(\frac{I}{|\mathbf{z} - \mathbf{z}'|^3} - \frac{3(\mathbf{z} - \mathbf{z}')(\mathbf{z} - \mathbf{z}')^T}{|\mathbf{z} - \mathbf{z}'|^5}$$

from [15]. Then, it follows from Lemma 4.2.1 and 4.2.2 that

$$\begin{aligned}
&\frac{1}{4\pi}\int \frac{\gamma_2(\alpha_2-\alpha_2')+\gamma_1(\alpha_1-\alpha_1')}{|\mathbf{z}-\mathbf{z}'|^3}\,d\alpha' \\
&\qquad +\frac{\gamma_1(\alpha_1-\alpha_1')[(S_1-S_1')(\alpha_1-\alpha_1')+(S_2-S_2')(\alpha_2-\alpha_2')]}{|\mathbf{z}-\mathbf{z}'|^5}+O(\varepsilon^2) \\
&= -\frac{3}{2}\gamma_2(\Lambda^{12}(S_1)+\Lambda^{22}(S_2))+-\frac{3}{2}\gamma_1(\Lambda^{11}(S_1)+\Lambda^{12}(S_2))+O(\varepsilon^2) \\
&= -\frac{1}{2}\gamma_2(H_1D_2(S_1)+(2H_2D_2+H_1D_1)(S_2)) \\
&\quad -\frac{1}{2}\gamma_1((2H_1D_1+H_2D_2)(S_1)+H_1D_2(S_2))+O(\varepsilon^2)\,. \qquad (4.45)
\end{aligned}$$

By substituting (4.33) and (4.34) into (4.45), we write the leading order terms in ψ_1 and ψ_2.

$$\begin{aligned}
&\frac{1}{4\pi}\int \frac{\gamma_2(\alpha_2-\alpha_2')+\gamma_1(\alpha_1-\alpha_1')}{|\mathbf{z}-\mathbf{z}'|^3}\,d\alpha' \\
&= -\frac{1}{2}\gamma_2(H_1D_2)(-H_2\psi_1-H_1\psi_2) \\
&\quad -\frac{1}{2}\gamma_2(2H_2D_2+H_1D_1)(H_1\psi_1-H_2\psi_2) \\
&\quad -\frac{1}{2}\gamma_1(2H_1D_1+H_2D_2)(-H_2\psi_1-H_1\psi_2) \\
&\quad -\frac{1}{2}\gamma_1H_1D_2(H_1\psi_1-H_2\psi_2)+O(\varepsilon^2)\,, \qquad (4.46)
\end{aligned}$$

which can be further simplified to

$$\begin{aligned}
&\frac{1}{4\pi}\int \frac{\gamma_2(\alpha_2-\alpha_2')+\gamma_1(\alpha_1-\alpha_1')}{|\mathbf{z}-\mathbf{z}'|^3}\,d\alpha' \\
&= -\frac{1}{2}(H_1D_1+H_2D_2)(-\gamma_1H_2+\gamma_2H_1)\psi_1 \\
&\quad +(H_1D_1+H_2D_2)(\gamma_1H_1+\gamma_2H_2)\psi_2+O(\varepsilon^2) \\
&= -(\gamma_1D_1+\gamma_2D_2)\psi_2-\frac{1}{2}(\gamma_1D_2-\gamma_2D_1)\psi_1+O(\varepsilon^2)\,. \qquad (4.47)
\end{aligned}$$

To unify our notations, we define

$$\psi_3 = S_3 \tag{4.48}$$

Combining (4.28), (4.29), and (4.43) into a system we get

$$\frac{\partial \psi_1}{\partial t} = O(\varepsilon^2) , \tag{4.49}$$

$$\frac{\partial \psi_2}{\partial t} = \frac{1}{2}(\gamma_1 D_1 + \gamma_2 D_2)\psi_3 + O(\varepsilon^2) . \tag{4.50}$$

$$\frac{\partial \psi_3}{\partial t} = -\frac{1}{2}(\gamma_1 D_1 + \gamma_2 D_2)\psi_2 + \frac{1}{2}(\gamma_2 D_1 - \gamma_1 D_2)\psi_1 + O(\varepsilon^2) , \tag{4.51}$$

where D_1 (D_2) stands for differentiation with respect to the α_1 (α_2) variable.

We compare our leading order terms to the linearized system derived in the article of Hou & Zhang [17]. Their linearized system is

$$\frac{\partial \dot{\psi}_1}{\partial t} = 0 ,$$

$$\frac{\partial \dot{\psi}_2}{\partial t} = \frac{1}{2}(\gamma_1 D_1 + \gamma_2 D_2)\dot{z} ,$$

$$\frac{\partial \dot{z}}{\partial t} = -\frac{1}{2}(\gamma_1 D_1 + \gamma_2 D_2)\dot{\psi}_2 + \frac{1}{2}(\gamma_2 D_1 - \gamma_1 D_2)(\dot{\psi}_1) ,$$

where $\dot{\psi}_1$,$\dot{\psi}_2$ and $\dot{z}$ are perturbations of ψ_1, ψ_2 and z respectively. This comparison confirms that our linear system does capture the leading order terms of the three-dimensional vortex sheet equation when perturbed around an equilibrium state.

Since γ_1 and γ_2 are constants, we introduce a change of variables from (α_1, α_2) to (β_1, β_2)

as follows:

$$\beta_1 = \frac{1}{\sqrt{\gamma_1^2+\gamma_2^2}}(-\gamma_2\alpha_1+\gamma_1\alpha_2)\ , \tag{4.52}$$

$$\beta_2 = \frac{1}{\sqrt{\gamma_1^2+\gamma_2^2}}(\gamma_1\alpha_1+\gamma_2\alpha_2)\ . \tag{4.53}$$

Substitute this variable change into system (4.49) – (4.51); the leading order terms become

$$\frac{\partial\psi_1}{\partial t} = O(\varepsilon^2)\ , \tag{4.54}$$

$$\frac{\partial\psi_2}{\partial t} = \frac{1}{2}\gamma D_{\beta_2}\psi_3 + O(\varepsilon^2)\ , \tag{4.55}$$

$$\frac{\partial\psi_3}{\partial t} = -\frac{1}{2}\gamma D_{\beta_2}\psi_2 - \frac{1}{2}\gamma D_{\beta_1}\psi_1 + O(\varepsilon^2)\ , \tag{4.56}$$

where $\gamma = \sqrt{\gamma_1^2+\gamma_2^2}$.

In the new coordinates, we can see that the system will suffer the Kelvin-Helmholtz instability because of the coupling of (4.55) and (4.56). It also shows that the β_2 direction is the unstable direction responsible for generating Kelvin-Helmholtz instability. Moreover, since the β_2 direction is the tangential velocity jump direction between the upper and lower layers of fluid, the leading order terms confirm that the tangential velocity jump is the physical driving force of the instability of the three-dimensional vortex sheet.

During the derivation, the only terms written down explicitly were the leading order terms. This is because, as we will see in later sections, the remaining terms on the right-hand side of the equations are of smaller magnitude. We denote them as R_1, R_2, and R_3

and define them as:

$$R_1(\psi_1, \psi_2, \psi_3) = \frac{\partial \psi_1}{\partial t} , \tag{4.57}$$

$$R_2(\psi_1, \psi_2, \psi_3) = \frac{\partial \psi_2}{\partial t} - \frac{1}{2}\gamma D_{\beta_2}\psi_3 , \tag{4.58}$$

$$R_3(\psi_1, \psi_2, \psi_3) = \frac{\partial \psi_3}{\partial t} + \frac{1}{2}\gamma D_{\beta_2}\psi_2 + \frac{1}{2}\gamma D_{\beta_1}\psi_1 . \tag{4.59}$$

Next, we extend the independent variables β_1 and β_2 into the complex domain. As a result, we can analytically continue the system into the two-dimensional complex domain. Following Caflisch & Orellana [9], we assume that S_1, S_2, and S_3 are initially small analytic functions within a strip of $\max(|Im(\alpha_1)|, |Im(\alpha_2)|) < \rho$, where the strip width ρ depends on their initial amplitude ϵ. Since ψ_1, ψ_2 are Riesz transforms of S_1 and S_2, it can be shown that ψ_1 and ψ_2 are also analytic functions within the strip, since the Riesz transforms preserve analyticity. Therefore, from the fact that γ_1 and γ_2 are constants, we conclude that ψ_1, ψ_2, and ψ_3 are initially analytic functions in the strip of $\max(|Im(\beta_1)|, |Im(\beta_2)|) < \rho_0$, where ρ_0 and ρ are of the same order.

By analytically extending system (4.57) – (4.59) into the complex domain, the system can be considered as a hyperbolic system with characteristic lines in the complex domain. Furthermore, simple calculations show that the characteristic speeds of the linear system are 0 and $\pm\frac{i\gamma}{2}$. Later, we will prove that these are the leading order terms of the characteristic speed of the nonlinear system.

Remark: Even though we will analyze a complex system instead of a real system, the domain that interests us the most is still the real (β_1, β_2) plane. This means that we have the flexibility to shrink the imaginary strip without affecting the physical solution.

Following the idea by Caflisch & Orellana [9], we construct a quasi-linear system from

(4.57) – (4.59). Seemingly, we are deriving a more complicated system. In fact, it is more amendable for error control for the high order terms.

To construct a quasi-linear system, we differentiate (4.57) – (4.59) in space and derive a system of the space derivatives of ψ_1, ψ_2 and ψ_3. Specifically, define:

$$\psi_{11} = \frac{\partial \psi_1}{\partial \beta_1} , \qquad \psi_{12} = \frac{\partial \psi_1}{\partial \beta_2} , \tag{4.60}$$

$$\psi_{21} = \frac{\partial \psi_2}{\partial \beta_1} , \qquad \psi_{22} = \frac{\partial \psi_2}{\partial \beta_2} , \tag{4.61}$$

$$\psi_{31} = \frac{\partial \psi_3}{\partial \beta_1} , \qquad \psi_{32} = \frac{\partial \psi_3}{\partial \beta_2} . \tag{4.62}$$

(4.57) – (4.59) then becomes:

$$\frac{\partial \psi_{11}}{\partial t} = \frac{\partial}{\partial \beta_1} R_1(\psi_1, \psi_2, \psi_3) , \tag{4.63}$$

$$\frac{\partial \psi_{12}}{\partial t} = \frac{\partial}{\partial \beta_2} R_1(\psi_1, \psi_2, \psi_3) , \tag{4.64}$$

$$\frac{\partial \psi_{21}}{\partial t} = \frac{\gamma}{2} D_{\beta_1} \psi_{32} + \frac{\partial}{\partial \beta_1} R_2(\psi_1, \psi_2, \psi_3) , \tag{4.65}$$

$$\frac{\partial \psi_{22}}{\partial t} = \frac{\gamma}{2} D_{\beta_2} \psi_{32} + \frac{\partial}{\partial \beta_2} R_2(\psi_1, \psi_2, \psi_3) , \tag{4.66}$$

$$\frac{\partial \psi_{31}}{\partial t} = -\frac{\gamma}{2} D_{\beta_1} \psi_{22} - \frac{\gamma}{2} D_{\beta_1} \psi_{11} + \frac{\partial}{\partial \beta_1} R_3(\psi_1, \psi_2, \psi_3) , \tag{4.67}$$

$$\frac{\partial \psi_{32}}{\partial t} = -\frac{\gamma}{2} D_{\beta_2} \psi_{22} - \frac{\gamma}{2} D_{\beta_2} \psi_{11} + \frac{\partial}{\partial \beta_3} R_3(\psi_1, \psi_2, \psi_3) . \tag{4.68}$$

This is our target nonlinear system.

In (4.63) – (4.68), if we take

$$E_{11} = \frac{\partial}{\partial \beta_1} R_1, \qquad E_{12} = \frac{\partial}{\partial \beta_2} R_1,$$

$$E_{21} = \frac{\partial}{\partial \beta_1} R_2, \qquad E_{22} = \frac{\partial}{\partial \beta_2} R_2,$$

$$E_{31} = \frac{\partial}{\partial \beta_1} R_3, \qquad E_{32} = \frac{\partial}{\partial \beta_2} R_3,$$

and assume that they are known forcing functions, in order to solve system (4.63) – (4.68), we can first solve system (4.63), (4.64), (4.66), (4.68) by integrating along the characteristic lines, and then substituting the calculated solutions into system (4.65), (4.67) and solve the resulting O.D.E.. The procedure will be used in the last section where we prove a lemma on energy estimates. Furthermore, without loss of generality, we assume that $\gamma = 1$ for the rest of the chapter. In this case, the leading order term of the characteristic speed becomes $\frac{1}{2}$.

4.3 Long Time Existence Proof

In this section, we prove the main result of this chapter, the long time existence theorem of the three-dimensional vortex sheet equation.

The idea is to apply the extension of the abstract Cauchy-Kowalewski Theorem introduced by Caflisch & Orellana [9]. It requires estimates of the nonlinear terms in system (4.63) – (4.68). Since the estimation itself is rather technical, to show a clearer outline of our main proof, we just state the results here and leave the detailed derivation to the next section.

For technical purposes, we split the solution of (4.63) – (4.68) into two parts. One satisfies a linear system with the initial condition of the full nonlinear system, while the other satisfies a nonlinear system with vanishing initial condition. The existence of the first part of the solution is straight-forward, while we use the extension of the abstract Cauchy-Kowalewski theorem to prove the existence of the second part.

The subsections in this section are arranged as follows. In the next subsection, we present two lemmas about error estimates and energy estimates respectively. The proofs of the lemmas are deferred to the next section. In subsection 2, we state the extended

abstract Cauchy-Kowalewski theorem. Furthermore, we devote subsection 3 to solving the linear system with full initial condition as the first part of the solution to the full nonlinear system. The existence of the second part of the solution will be proved in the last subsection.

4.3.1 Results on Error Estimates and Linear Systems

In this subsection, we state two lemmas related to the error estimates and energy estimates respectively. First of all, it is necessary to define the following Lipschitz norms:

$$|f|_\rho = \sup_{\substack{|Im(\kappa_1)|<\rho \\ |Im(\kappa_2)|<\rho}} |f(\kappa_1,\kappa_2)| \ , \tag{4.69}$$

$$\|f\|_{\alpha\rho} = |f|_\rho + \sup_{\substack{|Im(\kappa_1)|<\rho,\ |Im(\kappa_2)|<\rho \\ |Im(\kappa_1')|<\rho,\ |Im(\kappa_2')|<\rho \\ (\kappa_1,\kappa_2)\neq(\kappa_1',\kappa_2')}} \frac{|f(\kappa_1,\kappa_2)-f(\kappa_1',\kappa_2')|}{|(\kappa_1,\kappa_2)-(\kappa_1',\kappa_2')|^\alpha} \ , \tag{4.70}$$

$$\|f\|_{\alpha\rho+} = |f|_\rho + \sup_{\substack{|Im(\kappa_1)|<\rho,\ |Im(\kappa_2)|<\rho \\ |Im(\kappa_1')|<\rho,\ |Im(\kappa_2')|<\rho \\ Im(\kappa_1)=Im(\kappa_1'),\ Im(\kappa_2)=Im(\kappa_2') \\ (\kappa_1,\kappa_2)\neq(\kappa_1',\kappa_2')}} \frac{|f(\kappa_1,\kappa_2)-f(\kappa_1',\kappa_2')|}{|(\kappa_1,\kappa_2)-(\kappa_1',\kappa_2')|^\alpha} \ , \tag{4.71}$$

where $0<\alpha<1$ and $|(\kappa_1,\kappa_2)-(\kappa_1',\kappa_2')| = \sqrt{(\kappa_1-\kappa_1')^2+(\kappa_2-\kappa_2')^2}$.

Also define $\|\cdot\|_{\alpha_1\rho}$ and $\|\cdot\|_{\alpha_2\rho}$ as the $\|\cdot\|_{\alpha\rho}$ norm on the β_1 and β_2 direction respectively:

$$\|f\|_{\alpha_1\rho} = |f|_\rho + \sup_{\substack{\max(|Im(\kappa_1)|,|Im(\kappa_1')|,|Im(\kappa_2)|)<\rho \\ \kappa_1\neq\kappa_1'}} \frac{|f(\kappa_1,\kappa_2)-f(\kappa_1',\kappa_2)|}{|(\kappa_1-\kappa_1')|^\alpha}\ , \tag{4.72}$$

$$\|f\|_{\alpha_2\rho} = |f|_\rho + \sup_{\substack{\max(|Im(\kappa_1)|,|Im(\kappa_2)|,|Im(\kappa_2')|)<\rho \\ \kappa_2\neq\kappa_2'}} \frac{|f(\kappa_1,\kappa_2)-f(\kappa_1,\kappa_2')|}{|(\kappa_2-\kappa_2')|^\alpha}\ . \tag{4.73}$$

Similarly, we can define $\|\cdot\|_{\alpha_1\rho+}$ and $\|\cdot\|_{\alpha_2\rho+}$ for the $\|\cdot\|_{\alpha\rho+}$ norm on the β_1 and β_2 directions respectively:

$$\|f\|_{\alpha_1\rho+} = |f|_\rho + \sup_{\substack{\max(|Im(\kappa_1)|,|Im(\kappa_1')|,|Im(\kappa_2)|)<\rho \\ Im(\kappa_1)=Im(\kappa_1') \\ \kappa_1\neq\kappa_1'}} \frac{|f(\kappa_1,\kappa_2)-f(\kappa_1',\kappa_2)|}{|(\kappa_1-\kappa_1')|^\alpha}\ , \tag{4.74}$$

$$\|f\|_{\alpha_2\rho+} = |f|_\rho + \sup_{\substack{\max(|Im(\kappa_1)|,|Im(\kappa_2)|,|Im(\kappa_2')|)<\rho \\ Im(\kappa_2)=Im(\kappa_2') \\ \kappa_2\neq\kappa_2'}} \frac{|f(\kappa_1,\kappa_2)-f(\kappa_1,\kappa_2')|}{|(\kappa_2-\kappa_2')|^\alpha}\ . \tag{4.75}$$

Note that for $\kappa_1 \neq \kappa_1'$ and $\kappa_2 \neq \kappa_2'$,

$$\begin{aligned}
&\frac{|f(\kappa_1,\kappa_2)-f(\kappa_1',\kappa_2')|}{|(\kappa_1,\kappa_2)-(\kappa_1',\kappa_2')|^\alpha} \\
&\leq \frac{|f(\kappa_1,\kappa_2)-f(\kappa_1',\kappa_2)|}{|(\kappa_1,\kappa_2)-(\kappa_1',\kappa_2')|^\alpha} + \frac{|f(\kappa_1',\kappa_2)-f(\kappa_1',\kappa_2')|}{|(\kappa_1,\kappa_2)-(\kappa_1',\kappa_2')|^\alpha} \\
&\leq \frac{|f(\kappa_1,\kappa_2)-f(\kappa_1',\kappa_2)|}{|(\kappa_1,\kappa_2)-(\kappa_1',\kappa_2)|^\alpha} + \frac{|f(\kappa_1',\kappa_2)-f(\kappa_1',\kappa_2')|}{|(\kappa_1',\kappa_2)-(\kappa_1',\kappa_2')|^\alpha} \\
&= \frac{|f(\kappa_1,\kappa_2)-f(\kappa_1',\kappa_2)|}{|\kappa_1-\kappa_1'|^\alpha} + \frac{|f(\kappa_1',\kappa_2)-f(\kappa_1',\kappa_2')|}{|\kappa_2'-\kappa_2'|^\alpha}\ .
\end{aligned} \tag{4.76}$$

We conclude that $\|\cdot\|_{\alpha\rho}$ is equivalent to $(\|\cdot\|_{\alpha_1\rho} + \|\cdot\|_{\alpha_2\rho})$. Similarly, we can show that

$\|\cdot\|_{\alpha\rho+}$ is equivalent to $(\|\cdot\|_{\alpha_1\rho+} + \|\cdot\|_{\alpha_2\rho+})$. This property will be used extensively in the later analysis.

Definitions (4.72), (4.73), (4.74), and (4.75) are natural extensions from the corresponding one-dimensional norm. In particular, Caflisch and Orellana [9] have proved that for one-dimensional analytic functions:

$$\|f\|_{\alpha_1\rho} \leq c\|f\|_{\alpha_1\rho+} ,$$

$$\|f\|_{\alpha_2\rho} \leq c\|f\|_{\alpha_2\rho+} .$$

Therefore, for two-dimensional analytic functions, the following inequality holds,

$$\|f\|_{\alpha\rho} \leq (\|f\|_{\alpha_1\rho} + \|f\|_{\alpha_2\rho}) \leq c(\|f\|_{\alpha_1\rho+} + \|f\|_{\alpha_2\rho+}) \leq 2c\|f\|_{\alpha\rho+} . \tag{4.77}$$

In the next section, we prove that

Lemma 4.3.1 *Assuming that x, y, z defined in (4.1) are small perturbations of a flat plane, and S_1, S_2, S_3 satisfy*

1. *S_1, S_2, S_3 are analytic functions within the strip*

$$\{(\beta_1, \beta_2) | \max(|Im(\beta_1)|, |Im(\beta_2)|) < \rho\} .$$

2. *S_1, S_2, S_3 are periodic functions with period of $(2\pi, 2\pi)$.*

3.

$$\|S_j\|_\alpha(\cdot + i\mu_1, \cdot + i\mu_2) \quad \leq \quad \frac{1}{8} ,$$

where $j = 1, 2, 3$ *with* (μ_1, μ_2) *satisfying* $|\mu_1| < \rho$ *and* $|\mu_2| < \rho$.

Furthermore, we assume that ψ_{ij} *and* $\tilde{\psi}_{ij}$ *are defined in (4.31), (4.32), and (4.60) – (4.62). Then, for* $0 < \rho' < \rho$ *and* $0 < \alpha < 1$, *the following inequalities hold:*

$$\|E_{ij}\|_{\alpha\rho'} \leq c(\rho - \rho')^{-1} \left(\sum_{k_1=1}^{3} \sum_{k_2=1}^{2} \|\psi_{k_1 k_2}\|_{\alpha\rho} \right)^2 , \tag{4.78}$$

and

$$\begin{aligned} \|E_{ij} - \tilde{E}_{ij}\|_{\alpha\rho'} \quad \leq \quad & c(\rho - \rho')^{-1} \left(\sum_{k_1=1}^{3} \sum_{k_2=1}^{2} (\|\psi_{k_1 k_2}\|_{\alpha\rho} + \|\tilde{\psi}_{k_1 k_2}\|_{\alpha\rho} \right) \\ & \cdot \left(\sum_{k_1=1}^{3} \sum_{k_2=1}^{2} \|\psi_{k_1 k_2} - \tilde{\psi}_{k_1, k_2}\|_{\alpha\rho} \right) , \end{aligned} \tag{4.79}$$

where $i, j = 1, 2, 3$.

Lemma 4.3.2 *Consider the following system of*

$$\mathbf{u} = (u_{11}, u_{12}, u_{21}, u_{22}, u_{31}, u_{32})^T$$

with analytic forcing terms

$$\mathbf{g} = (g_{11}, g_{12}, g_{21}, g_{22}, g_{31}, g_{32})^T$$

$$\frac{\partial u_{11}}{\partial t} = g_{11} \ , \tag{4.80}$$

$$\frac{\partial u_{12}}{\partial t} = g_{12} \ , \tag{4.81}$$

$$\frac{\partial u_{21}}{\partial t} = \frac{1}{2} D_{\beta_1} u_{32} + g_{21} \ , \tag{4.82}$$

$$\frac{\partial u_{22}}{\partial t} = \frac{1}{2} D_{\beta_2} u_{32} + g_{22} \ , \tag{4.83}$$

$$\frac{\partial u_{31}}{\partial t} = -\frac{1}{2} D_{\beta_1} u_{22} - \frac{1}{2} D_{\beta_1} u_{11} + g_{31} \ , \tag{4.84}$$

$$\frac{\partial u_{32}}{\partial t} = -\frac{1}{2} D_{\beta_2} u_{22} - \frac{1}{2} D_{\beta_2} u_{11} + g_{32} \ , \tag{4.85}$$

with

$$\mathbf{u}(t=0) = 0 \ . \tag{4.86}$$

Then, the following inequality holds,

$$\|\mathbf{u}\|_{\alpha\rho} \leq c\kappa^{-1} \int_0^t \|\mathbf{g}(\cdot,\cdot,\tau)\|_{\alpha(\rho+(\frac{1}{2}+\kappa)(t-\tau))} d\tau \ , \tag{4.87}$$

for any $0 < \kappa < 1$, $0 < \alpha < 1$, *with* c *being a constant.*

4.3.2 Extended Abstract Cauchy-Kowalewski Theorem

In this subsection, we state the result of the extended abstract Cauchy-Kowalewski theorem for future use.

Consider the equation

$$\frac{\partial}{\partial t} u + L[u,t] = G[u,t] \ , \tag{4.88}$$

with

$$u(t=0) = 0 \ , \tag{4.89}$$

in which L is a linear operator on u, and G may be nonlinear. Assume that there are positive functions $\rho_0(t)$, $\rho_1(\tau, t, \rho)$, $d_1(\tau, t)$, $d_2(t)$ and positive scalars c_1, c_2, c_3, R and K that satisfy the following conditions:

1. If u solves $(\partial/\partial t)u + L[u,t] = g(t)$, with $u(t=0) = 0$ for some g, then for any $\rho < \rho_0(t)$,

$$\|u(t)\|_\rho \leq c_1 \int_0^t d_1(\tau, t) \|g(\cdot, \tau)\|_{\rho_1(\tau,t,\rho)} d\tau \ . \tag{4.90}$$

2. If $\|u(t)\|_\rho \leq R$, $\|\tilde{u}(t)\|_\rho \leq R$, and $0 < \rho' < \rho < \rho_0(t)$, then

$$\|G[u,t] - G[\tilde{u},t]\|_{\rho'} \leq$$
$$c_2(\rho - \rho')^{-1}(d_2(t) + \|u(t)\|_\rho + \|\tilde{u}(t)\|_\rho)\|(u - \tilde{u})(t)\|_\rho \ , \tag{4.91}$$

   in which d_2 is an increasing function of t.

3. $\|G[u=0,t]\|_\rho \leq K d_2(t)(\rho_0(t) - \rho)^{-1}$ if $\rho < \rho_0(t)$.

4. ρ is positive and decreasing for $0 < t < T_0$; $\rho_1(\tau, t, \rho)$ is decreasing in τ and increasing in ρ. Moreover, if $0 < \tau < t$ and $0 < \rho < \rho_0(t)$

$$\rho < \rho_0(\tau, t, \rho) \leq \rho_0(\tau) - (\rho_0(t) - \rho) \ . \tag{4.92}$$

5. If $0 \leq \tau \leq t < T_0$, then

$$d_1(\tau, t) d_2(\tau) < d_2(t) < c_3 \ . \tag{4.93}$$

Theorem 4.3.1 *(Extended Abstract Cauchy-Kowalewski Theorem) Under assumption (1)-(5) above, equation (4.88) with initial condition (4.89) has a unique solution u for the time interval $0 \leq t \leq T$. The solution satisfies*

$$\|u(t)\|_\rho < \beta d_2(t) < R \tag{4.94}$$

for all ρ and $t < T$ for which $0 < t < a(\rho_0(t) - \rho)$, where a, β, and T are any numbers satisfying

$$\gamma(1 + 2\beta)a < 1 \tag{4.95}$$

$$2ac_1 K(3 - \gamma(1 + 2\beta)a)(1 - \gamma(1 + 2\beta)a)^{-3} < \beta \tag{4.96}$$

$$T = \min(T_0, \max(t : 2\beta d_2(t) < R)) \tag{4.97}$$

with $\gamma = 8c_1c_2c_3$ and $R, d_2, K, c_1, c_2, c_3, T_0$ defined in (1)-(5).

Remark: 1. In the proof provided by Caflisch & Orellana [9], they used Condition (2)

as:

$$\|G[u,t] - G[\tilde{u},t]\|_{\rho'} \leq$$

$$c_2(\rho - \rho')^{-1}(d_2(t) + \|u(t)\|_{\rho'} + \|\tilde{u}(t)\|_{\rho'})\|(u - \tilde{u})(t)\|_{\rho} \,, \tag{4.98}$$

The same proof can be carried out using the Condition (2) in our statement, and this does not effect the result.

2. The proof uses the iteration method since the system is basically a linear system with weak nonlinear terms. Among all the constraints, Condition (1) provides the energy estimates in every step of the iteration. Condition (2) controls the nonlinear terms during the iteration. Condition (3) describes the nonlinear terms at the initial moment.

3. In our case, $\rho_0(t)$ is to describe the outer boundary where ψ_{ij} are still small at time t for our nonlinear problem. The function $\rho_1(\tau, t, \rho)$ corresponds to the downwards moving characteristic for the linear problem in Condition (1). Condition (4) says that the linear characteristic stays within the domain of dependence for the nonlinear problem.

4. The inequalities (4.95), (4.96), and (4.97) are due to some technical estimates in the proof. These inequalities set a bound on a, which is the speed in which the complex domain shrinks in addition to $\rho_0(t)$.

4.3.3 Linear System with Full Initial Condition

Consider the following linear system:

$$\frac{\partial \tilde{\psi}_{11}}{\partial t} = 0 , \tag{4.99}$$

$$\frac{\partial \tilde{\psi}_{12}}{\partial t} = 0 , \tag{4.100}$$

$$\frac{\partial \tilde{\psi}_{21}}{\partial t} = -\frac{i}{2}\gamma D_{\beta_1}\tilde{\psi}_{32} , \tag{4.101}$$

$$\frac{\partial \tilde{\psi}_{22}}{\partial t} = -\frac{i}{2}\gamma D_{\beta_2}\tilde{\psi}_{32} , \tag{4.102}$$

$$\frac{\partial \tilde{\psi}_{31}}{\partial t} = \frac{i}{2}\gamma D_{\beta_1}\tilde{\psi}_{22} + \frac{i}{2}\gamma D_{\beta_1}\tilde{\psi}_{11} , \tag{4.103}$$

$$\frac{\partial \tilde{\psi}_{32}}{\partial t} = \frac{i}{2}\gamma D_{\beta_2}\tilde{\psi}_{22} + \frac{i}{2}\gamma D_{\beta_2}\tilde{\psi}_{11} , \tag{4.104}$$

with

$$\tilde{\psi}_{ij}|_{t=0} = \psi_{ij}|_{t=0}, \quad i = 1,2,3, \quad j = 1,2.$$

If we change variables, letting $\psi'_{ij} = \tilde{\psi}_{ij} - \tilde{\psi}_{ij}|_{t=0}$ and still write them as $\tilde{\psi}_{ij}$, we get a system as (4.80) – (4.85) in Lemma 4.3.2. Therefore, we can apply Lemma 4.3.2 to prove the existence and estimate the boundness of $\tilde{\psi}_{ij}$.

Assume the $\psi_{ij}|_{t=0}$'s are analytic within the strip $\max(|Im(\beta_1)|, |Im(\beta_2)|) < \rho_0$ with their Lipschitz norms satisfying:

$$\|\nabla \psi_{ij}|_{t=0}\|_{\alpha\rho_0} < \epsilon , \tag{4.105}$$

where $i = 1,2,3$; and $j = 1,2$.

From Lemma 4.3.2, we know that $\tilde{\psi}_{ij}$ is analytic within a shrinking domain of width

$$\rho_0(t) = \rho_0 - (\frac{1}{2} + \kappa)t \ , \tag{4.106}$$

where $0 < \kappa < 1$. As we will see later, κ could be taken as small as pleased provided that ε is sufficiently small. Furthermore, the estimates in Lemma 4.3.2 show that

$$\begin{aligned} \|\tilde{\psi}_{ij}(t)\|_{\alpha\rho_0(t)} &\leq c\kappa^{-1} \int_0^t \|\nabla(\psi_{ij}|_{t=0})\|_{\alpha\rho_0} d\tau \\ &\leq c\varepsilon(\kappa^{-1}t) \ . \end{aligned} \tag{4.107}$$

We remark that $\rho_0(t)$ in the three-dimensional problem has an expression similar to the corresponding two-dimensional problem in [9], when κ is small and $\kappa^{-1}\varepsilon \ll 1$. In addition, similar linear growth rate with respect to time is observed in both the two-dimensional and the three-dimensional problem if $\varepsilon t \ll 1$.

4.3.4 Long Time Existence Theorem

To split the solution into two parts, we define:

$$\psi'_{ij} = \psi_{ij} - \tilde{\psi}_{ij} \ ,$$

where $i = 1, 2, 3$, $j = 1, 2$ and ψ_{ij}'s are the solution for our target system.

By substituting it into the system and deriving equations for ψ'_{ij}, we get

$$\frac{\partial \psi'_{11}}{\partial t} = \frac{\partial}{\partial \beta_1} R_1(\psi_1, \psi_2, \psi_3) \ , \tag{4.108}$$

$$\frac{\partial \psi'_{12}}{\partial t} = \frac{\partial}{\partial \beta_2} R_1(\psi_1, \psi_2, \psi_3) \ , \tag{4.109}$$

$$\frac{\partial \psi'_{21}}{\partial t} = \frac{1}{2} D_{\beta_1} \psi'_{32} + \frac{\partial}{\partial \beta_1} R_2(\psi_1, \psi_2, \psi_3) \ , \tag{4.110}$$

$$\frac{\partial \psi'_{22}}{\partial t} = \frac{1}{2} D_{\beta_2} \psi'_{32} + \frac{\partial}{\partial \beta_2} R_2(\psi_1, \psi_2, \psi_3) \ , \tag{4.111}$$

$$\frac{\partial \psi'_{31}}{\partial t} = -\frac{1}{2} D_{\beta_1} \psi'_{22} - \frac{1}{2} D_{\beta_1} \psi'_{11} + \frac{\partial}{\partial \beta_1} R_3(\psi_1, \psi_2, \psi_3) \ , \tag{4.112}$$

$$\frac{\partial \psi'_{32}}{\partial t} = -\frac{1}{2} D_{\beta_2} \psi'_{22} - \frac{1}{2} D_{\beta_2} \psi'_{11} + \frac{\partial}{\partial \beta_3} R_3(\psi_1, \psi_2, \psi_3) \ , \tag{4.113}$$

with

$$\psi'_{ij}(t=0) = 0 \quad i = 1,2,3 \ \ j = 1,2.$$

The existence of ψ'_{ij}'s implies the existence of S_i's. Moreover, the following theorem implies Theorem (4.1.1).

Theorem 4.3.2 *(Theorem of Long Time Existence) Let* $0 < \kappa < 1$, $0 < \alpha < 1$, *and* $\rho_0 > 0$. *Assume that* $S_i(\beta_1, \beta_2, 0)$ *satisfy*

$$\sup_{\substack{|Im(\alpha_1)|<\rho_0 \\ |Im(\alpha_2)|<\rho_0}} (|S_i(\alpha_1, \alpha_2, 0)| + |\nabla(S_i(\alpha_1, \alpha_2, 0))| + |\sum_{k=1}^{2} \sum_{j=1}^{2} (\partial_{\alpha_k} \partial_{\alpha_j} S_i(\alpha_1, \alpha_2, 0))|) < \varepsilon \ , \tag{4.114}$$

where $i = 1,2,3$, *and* ε *is sufficiently small. Then system (4.63) - (4.68) with* $\mathbf{z} =$

$(\alpha_1, \alpha_2, 0) + (s_1, s_2, s_3)$ *has a solution for a time* $0 \leq t \leq T$ *where* T *satisfies*

$$T =< \frac{\rho_0}{\frac{1}{2} + \kappa} \ , \ \textit{and} \ \ \kappa^{-2}\varepsilon T \ll 1 \ .$$

Moreover, the corresponding functions ψ_{ij} *satisfy*

$$\sum_{i=1,2,3;j=1,2} \|\psi_{ij}(t) - \tilde{\psi}_{ij}(t)\|_{\alpha\rho} \leq c\varepsilon\kappa^{-1}t < \frac{1}{8} \ , \tag{4.115}$$

for any ρ, t *satisfying*

$$0 < \rho < \rho_0 - \frac{t}{\frac{1}{2} + \kappa} \ ,$$

where the functions $\tilde{\psi}_{ij}$ *are solutions of the linear system (4.99) - (4.104) with initial data corresponding to* $S_i(t = 0)$, *and* c *is independent of* ε, κ *and* ρ_0.

Proof: From equation (4.106) in the last section, we have that

$$\rho_0(t) = \rho_0 - (\frac{1}{2} + \kappa)t \ .$$

From Lemma 4.3.2, choosing any fixed $\kappa' > \kappa$, we can always derive inequality (4.90) such that

$$\rho_1(\rho, t, \tau) = \rho + (\frac{1}{2} + \kappa')(t - \tau) \ .$$

From Lemma 4.3.1, the following inequalities hold:

$$\begin{aligned} \|E_{ij}(0,t)\|_{\alpha\rho'} &\leq c(\rho-\rho')^{-1}\left(\sum_{k_1=1}^{3}\sum_{k_2=1}^{2}\|\tilde{\psi}_{k_1k_2}\|_{\alpha\rho}\right)^2 \\ &\leq c(\rho-\rho')^{-1}(\varepsilon\kappa^{-1}t)^2\,, \end{aligned} \tag{4.116}$$

$$\begin{aligned} &\|E_{ij}(\psi'_{ij},t)-E_{ij}(\tilde{\psi'}_{ij},t)\|_{\alpha\rho'} \\ &\leq c(\rho-\rho')^{-1}\left[c\varepsilon\kappa^{-1}t+\left(\sum_{k_1=1}^{3}\sum_{k_2=1}^{2}(\|\psi_{k_1k_2}\|_{\alpha\rho}+\|\tilde{\psi}_{k_1k_2}\|_{\alpha\rho}\right)\right] \\ &\quad\cdot\left[\sum_{k_1=1}^{3}\sum_{k_2=1}^{2}\|\psi'_{k_1k_2}-\tilde{\psi'}_{k_1,k_2}\|_{\alpha\rho}\right]\,, \end{aligned} \tag{4.117}$$

for any $0<\rho'<\rho<\rho_0(t)$.

Thus, the assumptions (1) to (5) in the statement of Theorem (4.3.1) are satisfied with our choice of $\rho_0(t)$, $\rho_1(\tau,t,\rho)$ as above and with

$$d_1(\tau,t)=1;\quad c_1=c\kappa^{-1};\quad c_2=c;$$

$$d_2(t)=c\varepsilon t\kappa^{-1};\quad K=\varepsilon T\kappa^{-1};\quad c_3=c\varepsilon T\kappa^{-1}.$$

We can simply take $\beta=1$ and any constant a for ε sufficiently small. In particular, we take $a=\kappa'-\kappa$ to fulfill the conditions on $\rho_0(t)$ and $\rho_1(\rho,t,\tau)$. Therefore, it is straightforward to apply the Cauchy-Kowalewski theorem to our system. This guarantees the existence of the solution to (4.9) throughout the time interval. It also proves that the magnitude of the solution remains small since the ψ_{ij}'s are always of order $o(1)$ with the choice of T for sufficiently small ε.

4.4 Estimate on the Error Terms

Our goal in this section is to provide proofs for Lemma 4.3.1 and 4.3.2. Since the proof for lemma 4.3.2 is quite straightforward, we present it in the first subsection. The proof for lemma 4.3.1 is much more complicated and we divide it into three subsubsections.

4.4.1 Bounds on a Linear System

Consider the linear, spatially inhomogeneous complex $N \times N$ system

$$\frac{\partial}{\partial t}\mathbf{u} + F\frac{\partial}{\partial y}\mathbf{u} = \mathbf{g}(x, y, t) \ , \tag{4.118}$$

with

$$\mathbf{u}(t = 0) = 0 \ ,$$

in which the complex N-vector $\mathbf{g}$ and the complex $N \times N$ matrix F are given. Further assume that F is constant matrix and can be diagonalized as:

$$F = P^{-1}\Lambda P \ ,$$

$$\Lambda = diag(\lambda_1, \cdots, \lambda_n) \ .$$

Define the backward characteristics by

$$\frac{\partial}{\partial \tau}Y_i(\tau, t, y) = \lambda_i \ , \tag{4.119}$$

where

$$Y_i(t,t,y) = y \ , \tag{4.120}$$

and for $\tau < t$, define the dependence set $\Omega(\tau,t,y)$ as those y' which can be reached at time τ going backwards along characteristics starting from y at time t, i.e. ,

$$\Omega(t,t,y) = \{y\} \ , \tag{4.121}$$

$$\begin{aligned} \Omega(\tau,t,y) \quad = \quad & \{y' : y' = Y_i(\tau,t,y'') \text{ for some } i \text{ and} \\ & \text{for some } y'' \in \Omega(t_1,t,y), \tau < t_1 < t\} \ . \end{aligned} \tag{4.122}$$

Lemma 4.4.1 *Suppose that* g *is analytic in* x *and* y *and, that*

$$|P| + |P^{-1}| < p \ , \tag{4.123}$$

where $|P|$ *is the maximal norm of matrix* P.

Then the solution u *of (4.118) is analytic and satisfies*

$$|u_i(x,y,t)| \leq c \int_0^t \sup_{\bar{y} \in \Omega(\tau,t,y)} |g(x,\bar{y},\tau)| d\tau \ , \tag{4.124}$$

$$\begin{aligned}\frac{|u_i(x,y,t)-u_i(x,y',t)|}{|y-y'|^\alpha} &\leq c\int_0^t \sup_{\bar{y}\in\Omega(\tau,t,y)\cup\Omega(\tau,t,y')} |g(x,\bar{y},\tau)|d\tau \ , \\ &+ c\int_0^t \sup_{\substack{\bar{y}\in\Omega(\tau,t,x,y)\\ \bar{y}'\in\Omega(\tau,t,x,y')\\ \bar{y}\neq\bar{y}'}} \left(\frac{|g(x,\bar{y},\tau)-g(x,\bar{y}',\tau)|}{|\bar{y}-\bar{y}'|}\right) d\tau \ ,\end{aligned} \tag{4.125}$$

$$\frac{|u_i(x,y,t)-u_i(x',y,t)|}{|x-x'|^\alpha} \leq c\int_0^t \sup_{\bar{y}\in\Omega(\tau,t,y)} \frac{|g(x,\bar{y},\tau)-g(x',\bar{y},\tau)|}{|x-x'|^\alpha} d\tau \ , \tag{4.126}$$

where c only depends on p.

Proof: The proof of inequality (4.124) and (4.125) can be obtained by directly applying Proposition B.1 in (Caflisch & Orellana [9]).

Therefore, we only need to prove (4.126). Note that in equation (4.118), x is only a parameter. Therefore, if $u(x,y,t)$ is a solution of (4.118),

$$\frac{u(x,y,t)-u(x',y,t)}{|x-x'|^\alpha}$$

is a solution of

$$\frac{\partial}{\partial t}\mathbf{u} + F\frac{\partial}{\partial y}\mathbf{u} = \frac{\mathbf{g}(x,y,t)-\mathbf{g}(x',y,t)}{|x-x'|^\alpha} \ .$$

And thus, by applying inequality (4.124), we get (4.126).

As we mentioned at the end of last section, if we treat the error terms in system (4.63)

– (4.68) as given functions, we can solve the equation by first solving system (4.63), (4.64), (4.66), (4.68) by integrating along the characteristic lines, and then substituting the solution into system (4.65), (4.67) to solve the resulting O.D.E. This was the procedure used in the proof of the extended abstract Cauchy-Kowalewski theorem in which the following results are used to carry over the iteration [9].

Using Lemma 4.4.1 as a tool, we can prove Lemma 4.3.2.

Proof of Lemma 4.3.2: Considering the following matrix

$$F = \begin{pmatrix} 0 & 0 & 0 & 0 \\ 0 & 0 & 0 & 0 \\ 0 & 0 & 0 & \frac{1}{2} \\ -\frac{1}{2} & 0 & -\frac{1}{2} & 0 \end{pmatrix},$$

Straightforward calculation shows that its eigenvalues are $0, 0, \frac{i}{2}$, and $-\frac{i}{2}$. By applying Lemma (4.4.1), we can show that

$$\begin{aligned} \|u_{11}(t), u_{12}(t), u_{22}(t), u_{32}(t)\|_{\alpha\rho} &\leq c\int_0^t \|\mathbf{g}(\cdot,\cdot,\tau)\|_{\alpha(\rho+\frac{1}{2}(t-\tau))}d\tau \\ &\leq c\int_0^t \|\mathbf{g}(\cdot,\cdot,\tau)\|_{\alpha(\rho+(\frac{1}{2}+\kappa)(t-\tau))}d\tau \ . \end{aligned} \tag{4.127}$$

Furthermore, we can solve the remaining two equations as O.D.E.'s. Taking u_{21} as example, we can show that

$$\begin{aligned} \|u_{21}\|_{\alpha\rho} &\leq \int_0^t \frac{1}{2}\|D_{\beta_1}u_{32}(\cdot,\cdot,\tau)\|_{\alpha\rho} + \|g_{21}(\cdot,\cdot,\tau)\|_{\alpha\rho}d\tau \\ &\leq \int_0^t \frac{1}{2}\kappa^{-1}t^{-1}\|u_{32}(\cdot,\cdot,\tau)\|_{\alpha(\rho+\kappa t)}d\tau + \int_0^t \|g_{21}(\cdot,\cdot,\tau)\|_{\alpha\rho}d\tau \ , \end{aligned} \tag{4.128}$$

by applying the Cauchy Inequality. Then, it follows from the estimates on the first integral that

$$\begin{aligned}
\|u_{21}\|_{\alpha\rho} &\leq \frac{1}{2}\kappa^{-1} \max_{0<t'<t} \|u_{32}(\cdot,\cdot,t')\|_{\alpha(\rho+\kappa t)} + \int_0^t \|g_{21}(\cdot,\cdot,\tau)\|_{\alpha\rho} d\tau \\
&\leq \frac{1}{2}\kappa^{-1} \max_{0<t'<t} \int_0^{t'} c\|g(\cdot,\cdot,\tau)\|_{\alpha(\rho+\kappa t+\frac{1}{2}(t'-\tau))} d\tau \\
&\quad + \int_0^t \|g_{21}(\cdot,\cdot,\tau)\|_{\alpha\rho} d\tau \ ,
\end{aligned} \tag{4.129}$$

where we used inequality (4.127) in the last step. Moreover, using the monotonicity of the Lipschitz norm, we have

$$\begin{aligned}
\|u_{21}\|_{\alpha\rho} &\leq \frac{c}{2}\kappa^{-1} \int_0^t \|g(\cdot,\cdot,\tau)\|_{\alpha(\rho+\kappa t+\frac{1}{2}(t-\tau))} d\tau + \int_0^t \|g_{21}(\cdot,\cdot,\tau)\|_{\alpha\rho} d\tau \\
&\leq c\kappa^{-1} \int_0^t \|g(\cdot,\cdot,\tau)\|_{\alpha(\rho+\kappa t+\frac{1}{2}(t-\tau))} d\tau \\
&\leq c\kappa^{-1} \int_0^t \|g(\cdot,\cdot,\tau)\|_{\alpha(\rho+(\frac{1}{2}+\kappa)(t-\tau))} d\tau \ .
\end{aligned} \tag{4.130}$$

The estimate on u_{32} can be obtained similarly.

4.4.2 Bound on E_{ij}

The error terms E_{ij} are defined in system (4.63) – (4.68), which are space derivatives of the R_k's. Since we can apply the Cauchy inequality for analytic functions in the complex plane [1], it is sufficient to obtain the bounds for R_k. Moreover, since the R_k's are combinations of the Riesz transforms of the error terms in the equations for $\partial S_i/\partial t$'s, from the boundedness of the Riesz transforms which we show later, we are able to derive the bounds of E_{ij} from the bounds in the $\partial S_i/\partial t$ equations.

Along this line, we perform the error estimates in three steps: the error estimates on the Riesz transforms, the error estimates on the R_i terms, and the error estimates on theE_{ij} terms.

First of all, we define a special Lipschitz norm, which will be used only in this section.

$$\|f(\cdot + i\mu_1, \cdot + i\mu_2)\|_0 = \sup_{\kappa_1,\kappa_2 \in R} |f(\kappa_1 + i\mu_1, \kappa_2 + i\mu_2)| \ , \tag{4.131}$$

$$\begin{aligned} \|f(\cdot + i\mu_1, \cdot + i\mu_2)\|_\alpha &= \|f(\cdot + i\mu_1, \cdot + i\mu_2)\|_0 \\ &+ \sup_{\substack{(\kappa_1,\kappa_2),(\kappa_1',\kappa_2') \in R\times R \\ (\kappa_1,\kappa_2)\neq(\kappa_1',\kappa_2')}} \frac{|f(\kappa_1 + i\mu_1, \kappa_2 + i\mu_2) - f(\kappa_1' + i\mu_1, \kappa_2' + i\mu_2)|}{|(\kappa_1,\kappa_2) - (\kappa_1',\kappa_2')|^\alpha} \ . \end{aligned} \tag{4.132}$$

Bounds on the Hilbert Transform

The following lemma has been proved by Calderon & Zygmund [11] and Taibleson [31]:

Lemma 4.4.2 *If f has period of $2\pi \times 2\pi$, and satisfies*

$$\int_{-\pi}^{\pi}\int_{\pi}^{\pi} f(\beta_1 + i\mu_1, \beta_2 + i\mu_2) d\beta_1 d\beta_2 = 0 \ ,$$

for any μ_1 and μ_2, then

$$\|H_k f(\cdot + i\mu_1, \cdot + i\mu_2)\|_\alpha \leq c\|f(\cdot + i\mu_1, \cdot + i\mu_2)\|_\alpha \tag{4.133}$$

where H^k is the Riesz transform in the k-th variable, $k = 1, 2$, $0 < \alpha < 1$, and c depends only on α.

4.4.3 Bounds on the R_i Terms in System (4.57) – (4.59)

The R_i terms are defined in (4.57) – (4.59). Taking equation (4.57) as an example, we see that R_1 is the sum of the Riesz transforms of the residue terms in the $\frac{\partial S_1}{\partial t}$ and the $\frac{\partial S_2}{\partial t}$ equations. The same is true for equation (4.58). Therefore, by the boundedness of the Riesz transform, we claim that the boundedness of the residue terms in equations (4.28), (4.29), (4.30) are equivalent to the boundness of the R_i terms. Moreover, taking equation (4.28) as an example, it is sufficient to prove the following lemmas.

Lemma 4.4.3 *Given x, y, z defined as small perturbations of a flat plane, assume that (μ_1, μ_2), satisfying $|\mu_1| < \rho$ and $|\mu_2| < \rho$ and f, S_1, S_2, S_3 satisfy:*

1. *f, S_1, S_2, S_3 are analytic functions within the strip*

$$\{(\beta_1, \beta_2) | \max(|Im(\beta_1)|, |Im(\beta_2)|) < \rho\} .$$

2. *f, S_1, S_2, S_3 are periodic functions with period of $(2\pi, 2\pi)$.*

3.

$$\begin{aligned} \|f\|_\alpha(\cdot + i\mu_1, \cdot + i\mu_2) &\leq \frac{1}{8} , \\ \|S_j\|_\alpha(\cdot + i\mu_1, \cdot + i\mu_2) &\leq \frac{1}{8} , \end{aligned}$$

where $j = 1, 2, 3$.

We define:

$$Diff^k[f, S_1, S_2, S_3](\beta_1 + i\mu_1, \beta_2 + i\mu_2) =$$
$$H_k f(\beta_1 + i\mu_1, \beta_2 + i\mu_2) - \frac{1}{2\pi} \int \frac{(\beta_k - \beta'_k) f(\beta'_1 + i\mu_1, \beta'_2 + i\mu_2)}{|\mathbf{z} - \mathbf{z}'|^3} \, d\beta' \ , \tag{4.134}$$

where

$$\begin{aligned} \mathbf{z} &= (\beta_1 + S_1(\beta + i\mu), \beta_2 + S_2(\beta + i\mu), S_3(\beta + i\mu))^T \ , \\ \mathbf{z}' &= (\beta'_1 + S_1(\beta' + i\mu), \beta'_2 + S_2(\beta' + i\mu), S_3(\beta' + i\mu))^T \ , \end{aligned}$$

and

$$\begin{aligned} \beta + i\mu &= (\beta_1 + i\mu_1, \beta_2 + i\mu_2) \ , \\ \beta' + i\mu &= (\beta'_1 + i\mu_1, \beta'_2 + i\mu_2) \ . \end{aligned}$$

Then the following inequality holds

$$\|Diff^k[f, S_1, S_2, S_3](\cdot + i\mu_1, \cdot + i\mu_2)\|_\alpha \leq$$
$$c(\|\nabla S_1\|_\alpha + \|\nabla S_2\|_\alpha + \|\nabla S_3\|_\alpha) \|f\|_\alpha(\cdot + i\mu_1, \cdot + i\mu_2) \ , \tag{4.135}$$

$$\|(Diff^k[f,S_1,S_2,S_3] - Diff^k[\tilde{f},\tilde{S}_1,\tilde{S}_2,\tilde{S}_3])(\cdot+i\mu_1,\cdot+i\mu_2)\|_\alpha \leq cN(\alpha,\mu_1,\mu_2) \ , \tag{4.136}$$

for $0<\alpha<1$, *where*

$$\begin{aligned} N(\alpha,\mu_1,\mu_2) &= (\|f\|_\alpha + \|\tilde{f}\|_\alpha + \sum_{j=1}^{3}(\|\nabla S_j\|_\alpha + \|\nabla \tilde{S}_j\|_\alpha)) \cdot \\ &\quad (\|f-\tilde{f}\|_\alpha + \sum_{j=1}^{3}(\|\nabla(S_j-\tilde{S}_j)\|_\alpha))(\cdot+i\mu_1,\cdot+i\mu_2) \ , \end{aligned} \tag{4.137}$$

and $k=1,2$.

Lemma 4.4.4 *Let* f, x, y, z *be defined as in Lemma 4.4.3, then the same inequalities hold if we re-define Diff as,*

$$\begin{aligned} &Diff^k[f,S_1,S_2,S_3](\beta_1+i\mu_1,\beta_2+i\mu_2) = \\ &\quad \frac{1}{2\pi}\int \frac{(S_k - S_k')f'}{|\mathbf{z}-\mathbf{z}'|^3}\,d\beta' - \frac{1}{2\pi}\int \frac{[(\beta_1-\beta_1')S_{k_{\beta_1}} + (\beta_2-\beta_2')S_{k_{\beta_2}}]f'}{|(\beta_1,\beta_2)-(\beta_1',\beta_2')|^3}\,d\beta' \ , \end{aligned} \tag{4.138}$$

where $k=1,2,3$.

Lemma 4.4.5 *Let x, y, z be given as in Lemma (4.4.3), define*

$$\begin{aligned} &Diff[S_1,S_2,S_3](\beta_1+i\mu_1,\beta_2+i\mu_2) = \\ &\quad \frac{1}{2\pi}\int \frac{\gamma_1(\beta_1-\beta_1')+\gamma_2(\beta_2-\beta_2')}{|\mathbf{z}(\beta+i\mu)-\mathbf{z}(\beta'+i\mu')|^3}\,d\beta' \\ &\quad + \gamma_2(H_1D_2(S_1)+(2H_2D_2+H_1D_1)(S_2))(\beta+i\mu) \\ &\quad + \gamma_1((2H_1D_1+H_2D_2)(S_1)+H_1D_2(S_2))(\beta+i\mu)\ , \end{aligned} \tag{4.139}$$

where D_1 (D_2) stands for the space derivative on the β_1 (β_2) direction, and

$$\begin{aligned} \mathbf{z} &= (\beta_1+S_1(\beta+i\mu),\beta_2+S_2(\beta+i\mu),S_3(\beta+i\mu))^T\ , \\ \mathbf{z}' &= (\beta_1'+S_1(\beta'+i\mu),\beta_2'+S_2(\beta'+i\mu),S_3(\beta'+i\mu))^T\ , \end{aligned}$$

and

$$\begin{aligned} \beta+i\mu &= (\beta_1+i\mu_1,\beta_2+i\mu_2)\ , \\ \beta'+i\mu &= (\beta_1'+i\mu_1,\beta_2'+i\mu_2)\ . \end{aligned}$$

Then the following inequalities hold:

$$\begin{aligned} &\|Diff[S_1,S_2,S_3](\cdot+i\mu_1,\cdot+i\mu_2)\|_\alpha \le \\ &\quad c(\|\nabla S_1\|_\alpha+\|\nabla S_2\|_\alpha+\|\nabla S_3\|_\alpha)^2(\cdot+i\mu_1,\cdot+i\mu_2)\ , \end{aligned} \tag{4.140}$$

$$\|(Diff[S_1, S_2, S_3] - Diff[\tilde{S}_1, \tilde{S}_2, \tilde{S}_3])(\cdot + i\mu_1, \cdot + i\mu_2)\|_\alpha \leq cN(\alpha, \mu_1, \mu_2) \ , \tag{4.141}$$

for $0 < \alpha < 1$, *where*

$$\begin{aligned} N(\alpha, \mu_1, \mu_2) \quad = \quad & \sum_{j=1}^{3} (\|\nabla S_j\|_\alpha + \|\nabla \tilde{S}_j\|_\alpha) \cdot \\ & \sum_{j=1}^{3} (\|\nabla (S_j - \tilde{S}_j)\|_\alpha)(\cdot + i\mu_1, \cdot + i\mu_2) \ . \end{aligned} \tag{4.142}$$

Remarks: The above lemmas confirm our observation in the previous section where we derived our leading order system. We have proved that, if the interface is close to a flat plane, the vortex sheet kernel is close to the Riesz transform kernel. The difference is a smaller term in the Lipschitz norm.

Combining Lemma 4.4.3, 4.4.4, and Lemma 4.4.5, we get the following bound.

Lemma 4.4.6 *Let* x, y, z *be given as that in Lemma (4.4.3), then the following inequalities hold:*

$$\|R_k[S_1, S_2, S_3]\|_\alpha(\cdot + i\mu_1, \cdot + i\mu_2) \leq c \left(\sum_{j=1}^{3} \|\nabla S_j\|_\alpha \right)^2 (\cdot + i\mu_1, \cdot + i\mu_2) \ , \tag{4.143}$$

and

$$\|R_k[S_1,S_2,S_3]-R_k[\tilde{S}_1,\tilde{S}_2,\tilde{S}_3\|_\alpha(\cdot+i\mu_1,\cdot+i\mu_2)\leq$$
$$c\left(\sum_{j=1}^{3}(\|\nabla S_j\|_\alpha+\|\nabla\tilde{S}_j\|_\alpha)\right)\left(\sum_{j=1}^{3}\|\nabla(S_j-\tilde{S}_j)\|_\alpha\right)(\cdot+i\mu_1,\cdot+i\mu_2)\ , \tag{4.144}$$

where $k=1,2,3$.

Now that we have obtained the estimates of the R_i terms, we can derive the bounds of E_{ij} terms in the next subsubsection. Now, we provide the proof of above lemmas.

We just prove Lemma 4.4.3 here. Lemma 4.4.4 and Lemma 4.4.5 can be proved similarly. Lemma 4.4.6 is a natural extension of Lemma 4.4.3, Lemma 4.4.4, and Lemma 4.4.5.

Proof of Lemma 4.4.3: We only prove the inequalities for $Diff^1$. The inequalities of $Diff^2$ can be proved similarly. Furthermore, we suppress μ_1 and μ_2 and just keep the real part β_1 and β_2 throughout the proof.

Note that inequality (4.135) can be derived from inequality (4.136) by taking $\tilde{f}=0$, and $\tilde{S}_i=0$ for $i=1,2,3$. Therefore, it is sufficient to prove (4.136).

To perform our analysis, we first write the integrals in the periodic form as

$$\begin{aligned}
Diff^1[f,S_1,S_2,S_3] &= \frac{1}{2\pi}\int_{-\pi}^{\pi}\int_{-\pi}^{\pi}(K^{1*}(\zeta)-K_z^{1*}(\beta,\beta-\zeta))f(\beta-\zeta)d\zeta_1 d\zeta_2\\
&= \frac{1}{2\pi}\int_{-\pi}^{\pi}\int_{-\pi}^{\pi}(K^{1}(\zeta)-K_z^{1}(\beta,\beta-\zeta))f(\beta-\zeta)d\zeta_1 d\zeta_2\\
&\quad+\frac{1}{2\pi}\int_{-\pi}^{\pi}\int_{-\pi}^{\pi}(\overline{K^{1}}(\zeta)-\overline{K_z^{1}}(\beta,\beta-\zeta))f(\beta-\zeta)d\zeta_1 d\zeta_2\\
&\triangleq I_1[f,S_1,S_2,S_3](\beta)+I_2[f,S_1,S_2,S_3](\beta)\ .
\end{aligned} \tag{4.145}$$

What we need to do is to prove I_1 and I_2 both satisfy (4.136).

Since I_2 does not contain any singularity, it is just a regular integral on a bounded domain. Therefore, the maximum value of I_2 is bounded by the maximum value of f, and S_i's. In addition, the Hölder norm of I_2 is bounded by the Hölder norm of f, and ∇S_i's. Along this line, we can prove that I_2 satisfy (4.136).

We focus on the first integral I_1. What we need to prove is

$$|(I_1 - \tilde{I}_1)(\beta)| \leq cN(\alpha) \tag{4.146}$$

and

$$|(I_1 - \tilde{I}_1)(\beta) - (I_1 - \tilde{I}_1)(\beta')| \leq c|\beta - \beta'|^{\alpha} N(\alpha) \ , \tag{4.147}$$

where $N(\alpha)$ is defined in the statement of the lemma with $i\mu$ being suppressed.

We split the rest of our proof into three parts: the preparation, the proof of (4.146) and the proof of (4.147).

Preparation: Before we go on to prove (4.146) and (4.147), it is necessary to analyze the integrand of I_1 more and derive several inequalities for later use.

From the definition of I_1, we get:

$$\begin{aligned} I_1 &= \frac{1}{2\pi} \int_{-\pi}^{\pi} \int_{-\pi}^{\pi} (K^1(\zeta) - K_z^1(\beta, \beta - \zeta)) f(\beta - \zeta) d\zeta_1 d\zeta_2 \\ &= -\frac{1}{2\pi} \int_{-\pi}^{\pi} \int_{-\pi}^{\pi} f(\beta + \zeta) \left(\frac{\zeta_1}{|\zeta|^3} - \frac{\zeta_1}{|\mathbf{z}(\beta + \zeta) - \mathbf{z}(\beta)|^3} \right) d\zeta_1 d\zeta_2 \\ &= -\frac{1}{2\pi} \int_{-\pi}^{\pi} \int_{-\pi}^{\pi} \frac{\zeta_1 f(\beta + \zeta)}{|\zeta|^3} \left(\frac{|\mathbf{z}(\beta + \zeta) - \mathbf{z}(\beta)|^3 - |\zeta|^3}{|\mathbf{z}(\beta + \zeta) - \mathbf{z}(\beta)|^3} \right) d\zeta_1 d\zeta_2 \ , \end{aligned} \tag{4.148}$$

where $\beta = (\beta_1, \beta_2)$ and $\zeta = (\zeta_1, \zeta_2)$.

Define

$$G(\beta, \beta+\zeta) = f(\beta+\zeta) G_1(\beta, \beta+\zeta) \ , \tag{4.149}$$

where

$$G_1(\beta, \beta+\zeta) = \frac{|\mathbf{z}(\beta+\zeta) - \mathbf{z}(\beta)|^3 - |\zeta|^3}{|\mathbf{z}(\beta+\zeta) - \mathbf{z}(\beta)|^3} \ . \tag{4.150}$$

Naturally, we can also write down:

$$\tilde{G}(\beta, \beta+\zeta) = \tilde{f}(\beta+\zeta) \tilde{G}_1(\beta, \beta+\zeta) \ , \tag{4.151}$$

where

$$\tilde{G}_1(\beta, \beta+\zeta) = \frac{|\tilde{\mathbf{z}}(\beta+\zeta) - \tilde{\mathbf{z}}(\beta)|^3 - |\zeta|^3}{|\tilde{\mathbf{z}}(\beta+\zeta) - \tilde{\mathbf{z}}(\beta)|^3} \ . \tag{4.152}$$

Under the assumptions of Lemma 4.4.3, we can prove the following bounds:

$$|\mathbf{z}(\beta+\zeta) - \mathbf{z}(\beta)| \geq c|\zeta| \ , \tag{4.153}$$

$$|G_1(\beta, \beta+\zeta)| \leq c \sum_{i=1}^{3} \|\nabla S_i\|_0 \ , \tag{4.154}$$

$$|(G_1 - \tilde{G}_1)(\beta, \beta+\zeta)| \leq c \sum_{i=1}^{3} \|\nabla (S_i - \tilde{S}_i)\|_0 \ , \tag{4.155}$$

$$
\begin{aligned}
&|(G_1 - \tilde{G}_1)(\beta, \beta + \zeta) - (G_1 - \tilde{G}_1)(\beta, \beta - \zeta)| \\
&\leq \quad c|\zeta|^{\alpha} \left(\sum_{i=1}^{3} \|\nabla(S_i - \tilde{S}_i)\|_{\alpha} \right) , \qquad (4.156)
\end{aligned}
$$

$$
|\frac{\partial}{\partial S_i} G_1| \leq c|\zeta|^{-1} . \qquad (4.157)
$$

However, to focus on the main idea of the proof of Lemma 4.4.3, we will defer the verification of the above inequalities to the end.

From (4.154), it is straightforward to derive the following bound:

$$
\begin{aligned}
|G(\beta, \beta + \zeta)| &\leq |f(\beta + \zeta)||G_1(\beta, \beta + \zeta)| \\
&\leq c\|f\|_0 \sum_{i=1}^{3} \|\nabla S_i\|_0 . \qquad (4.158)
\end{aligned}
$$

Similarly, from (4.155), it can be shown that

$$
\begin{aligned}
&|(G - \tilde{G})(\beta, \beta + \zeta)| \\
&\leq |(f - \tilde{f})(\beta + \zeta)||G_1(\beta, \beta + \zeta)| + |\tilde{f}(\beta + \zeta)||(G_1 - \tilde{G}_1)(\beta, \beta + \zeta)| \\
&\leq c\|f - \tilde{f}\|_0 \sum_{i=1}^{3} \|\nabla S_i\|_0 + c\|f\|_0 \sum_{i=1}^{3} \|\nabla(S_i - \tilde{S}_i)\|_0 \\
&\leq cN(\alpha) , \qquad (4.159)
\end{aligned}
$$

where $N(\alpha)$ again is defined in the statement of the lemma as $N(\alpha, \mu_1, \mu_2)$.

Using an argument similar to (4.159), the following inequality can be shown from (4.156):

$$
|(G - \tilde{G})(\beta, \beta + \zeta) - (G - \tilde{G})(\beta, \beta - \zeta)| \leq c|\zeta|^{\alpha} N(\alpha) , \qquad (4.160)
$$

From (4.157), we can derive

$$|\nabla_\beta(G_1 - \tilde{G}_1)(\beta, \beta+\zeta)| \le c|\zeta|^{-1+\alpha} \sum_{i=1}^{3} \|\nabla(S_i - \tilde{S}_i)\|_\alpha \ , \tag{4.161}$$

which implies

$$\begin{aligned} &|(G_1 - \tilde{G}_1)(\beta, \beta+\zeta) - (G_1 - \tilde{G}_1)(\beta', \beta'+\zeta)| \\ &\le \ c|\beta - \beta'||\zeta|^{-1+\alpha} \sum_{i=1}^{3} \|\nabla(S_i - \tilde{S}_i)\|_\alpha \ . \end{aligned} \tag{4.162}$$

Proof of (4.146): We are ready to derive (4.146).

We split the integration domain in two regions as:

$$\begin{aligned} |I_1 - \tilde{I}_1| &= \frac{1}{2\pi} \left| \int_{-\pi}^{\pi}\int_{-\pi}^{\pi} \frac{\zeta_1}{|\zeta|^3}(G(\beta, \beta+\zeta) - \tilde{G}(\beta, \beta+\zeta))d\zeta \right| \\ &= \frac{1}{2\pi} \left| \left(\int_{-\pi}^{\pi}\int_{-\pi}^{0} + \int_{-\pi}^{\pi}\int_{0}^{\pi} \right) \right. \\ &\qquad \left. \frac{\zeta_1}{|\zeta|^3}(G(\beta, \beta+\zeta) - \tilde{G}(\beta, \beta+\zeta))d\zeta \right| . \end{aligned} \tag{4.163}$$

$$\tag{4.164}$$

From the oddness of the kernel $\frac{\zeta_1}{|\zeta|^3}$, we change the variable $\zeta' = -\zeta$ in the second integral and get

$$\begin{aligned} |I_1 - \tilde{I}_1| &= \frac{1}{2\pi} \left| \int_{-\pi}^{\pi}\int_{0}^{\pi} \frac{\zeta_1}{|\zeta|^3}[(G - \tilde{G})(\beta, \beta+\zeta) \right. \\ &\qquad \left. - (G - \tilde{G})(\beta, \beta-\zeta)]d\zeta_1 d\zeta_2 \right| \\ &\le \frac{c}{2\pi} \left| \int_{-\pi}^{\pi}\int_{0}^{\pi} \frac{\zeta_1}{|\zeta|^3}|\zeta|^\alpha d\zeta_1 d\zeta_2 \right| N(\alpha) \\ &\le \ cN(\alpha) \ , \end{aligned} \tag{4.165}$$

where we applied inequality (4.160) in the second step.

Proof of (4.147): Our next step is to prove

$$|(I_1 - \tilde{I}_1)(\beta) - (I_1 - \tilde{I}_1)(\beta')| \leq c|\beta - \beta'|^{\alpha} N(\alpha) \ . \tag{4.166}$$

For a complicated inequality like (4.166), we would like to break it down into several integrals and estimate them one by one. It can be shown that

$$\begin{aligned}
&|(I_1 - \tilde{I}_1)(\beta) - (I_1 - \tilde{I}_1)(\beta')| \\
&= \left| \int_{-\pi}^{\pi}\int_{-\pi}^{\pi} f(\beta+\zeta)G_1(\beta,\beta+\zeta) - \tilde{f}(\beta+\zeta)\tilde{G}_1(\beta,\beta+\zeta)\frac{\zeta_1}{|\zeta|^3}d\zeta \right. \\
&\quad \left. - \int_{-\pi}^{\pi}\int_{-\pi}^{\pi} f(\beta'+\zeta)G_1(\beta',\beta'+\zeta) - \tilde{f}(\beta'+\zeta)\tilde{G}_1(\beta',\beta'+\zeta)\frac{\zeta_1}{|\zeta|^3}d\zeta \right| \\
&\leq \left| \int_{-\pi}^{\pi}\int_{-\pi}^{\pi} [(f-\tilde{f})(\beta+\zeta)G_1(\beta,\beta+\zeta) - (f-\tilde{f})(\beta'+\zeta)G_1(\beta',\beta'+\zeta)]\frac{\zeta_1}{|\zeta|^3}d\zeta \right| \\
&\quad + \left| \int_{-\pi}^{\pi}\int_{-\pi}^{\pi} \tilde{f}(\beta'+\zeta)[(G_1-\tilde{G}_1)(\beta,\beta+\zeta) - (G_1-\tilde{G}_1)(\beta',\beta'+\zeta)]\frac{\zeta_1}{|\zeta|^3}d\zeta \right| \\
&\quad + \left| \int_{-\pi}^{\pi}\int_{-\pi}^{\pi} (\tilde{f}(\beta+\zeta) - \tilde{f}(\beta'+\zeta))(G_1-\tilde{G}_1)(\beta,\beta+\zeta)\frac{\zeta_1}{|\zeta|^3}d\zeta \right| \\
&\triangleq I_{11} + I_{12} + I_{13} \ .
\end{aligned} \tag{4.167}$$

We prove the inequalities of I_{11} and I_{12} in detail. The estimates of I_{13} can be obtained similar to that of I_{11}.

Bounds on I_{12}: To estimate I_{12}, we follow an idea by Caflisch & Orellana from [9] in their estimation for singular operator. First of all, we break the integration domain into

two regions, $|\zeta| < |\beta - \beta'|$ and $|\zeta| \geq |\beta - \beta'|$,

$$\begin{aligned}
&\left|\frac{1}{2\pi}\int_{-\pi}^{\pi}\int_{-\pi}^{\pi}\frac{\zeta_1}{|\zeta|^3}\tilde{f}(\beta'+\zeta)[(G_1-\tilde{G}_1)(\beta,\beta+\zeta)-(G_1-\tilde{G}_1)(\beta',\beta'+\zeta)]d\zeta\right| \\
&= \left|\frac{1}{2\pi}\left(\int_{|\zeta|<|\beta-\beta'|}+\int_{|\zeta|\geq|\beta-\beta'|}\right)\right. \\
&\quad \left.\frac{\zeta_1}{|\zeta|^3}\tilde{f}(\beta'+\zeta)[(G_1-\tilde{G}_1)(\beta,\beta+\zeta)-(G_1-\tilde{G}_1)(\beta',\beta'+\zeta)]d\zeta\right| . \qquad (4.168)
\end{aligned}$$

For the first integral we use the oddness of the kernel similar to the way we prove (4.165), while for the second integral, we apply inequality (4.162). Therefore, it follows that

$$\begin{aligned}
&\left|\frac{1}{2\pi}\int_{-\pi}^{\pi}\int_{-\pi}^{\pi}\frac{\zeta_1}{|\zeta|^3}\tilde{f}(\beta'+\zeta)[(G_1-\tilde{G}_1)(\beta,\beta+\zeta)-(G_1-\tilde{G}_1)(\beta',\beta'+\zeta)]d\zeta\right| \\
&\leq \frac{1}{2\pi}\left|\int_{\substack{|\zeta|<|\beta-\beta'| \\ \zeta_1>0}}\frac{\zeta_1}{|\zeta|^3}\cdot\right. \\
&\qquad [\tilde{f}(\beta'+\zeta)((G_1-\tilde{G}_1)(\beta,\beta+\zeta)-(G_1-\tilde{G}_1)(\beta',\beta'+\zeta)) \\
&\qquad \left.-\tilde{f}(\beta'-\zeta)((G_1-\tilde{G}_1)(\beta,\beta-\zeta)-(G_1-\tilde{G}_1)(\beta',\beta'-\zeta))]d\zeta\right| \\
&\qquad + \frac{1}{2\pi}\left|\int_{|\zeta|\geq|\beta-\beta'|}\frac{\zeta_1}{|\zeta|^3}\tilde{f}(\beta'+\zeta)[(G_1-\tilde{G}_1)(\beta,\beta+\zeta)\right. \\
&\qquad\qquad \left.-(G_1-\tilde{G}_1)(\beta',\beta'+\zeta)]d\zeta\right| \\
&\leq \frac{c}{2\pi}\int_{|\zeta|<|\beta-\beta'|}\frac{\zeta_1}{|\zeta|^3}|\zeta|^{\alpha}d\zeta N(\alpha) \\
&\qquad + \frac{c}{2\pi}\int_{|\zeta|\geq|\beta-\beta'|}\frac{\zeta_1}{|\zeta|^3}|\zeta|^{-1+\alpha}d\zeta|\beta-\beta'|N(\alpha) \\
&\leq c|\beta-\beta'|^{\alpha}N(\alpha) , \qquad (4.169)
\end{aligned}$$

where we have applied (4.160) and (4.162) in the above proof.

Therefore, we get

$$I_{12} \leq c|\beta-\beta'|^{\alpha}N(\alpha) . \qquad (4.170)$$

Bounds on I_{11}: It is sufficient to prove

$$\left|\int_{-\pi}^{\pi}\int_{-\pi}^{\pi} f(\beta+\zeta)G_1(\beta,\beta+\zeta)\frac{\zeta_1}{|\zeta|^3}d\zeta - \int_{-\pi}^{\pi}\int_{-\pi}^{\pi} f(\beta'+\zeta)G_1(\beta',\beta'+\zeta)\frac{\zeta_1}{|\zeta|^3}d\zeta\right| \leq c|\beta-\beta'|^\alpha \|f\|_\alpha \sum_{i=1}^{3}\|\nabla S_i\|_\alpha, \quad (4.171)$$

because by taking $f' = f - \tilde{f}$ and still writing as f in I_{11}, the bound satisfies

$$c|\beta-\beta'|^\alpha \|f-\tilde{f}\|_\alpha \sum_{i=1}^{3}\|\nabla S_i\|_\alpha \leq c|\beta-\beta'|^\alpha N(\alpha)\ .$$

From (4.169), by taking $\tilde{G}_1 = 0$ and $\tilde{f} = 1$, we get:

$$\left|f(\beta)\left(\int_{-\pi}^{\pi}\int_{-\pi}^{\pi} G_1(\beta,\beta+\zeta)\frac{\zeta_1}{|\zeta|^3}d\zeta - \int_{-\pi}^{\pi}\int_{-\pi}^{\pi} G_1(\beta',\beta'+\zeta)\frac{\zeta_1}{|\zeta|^3}d\zeta\right)\right| \leq c|\beta-\beta'|^\alpha \|f\|_0 \sum_{i=1}^{3}\|\nabla S_i\|_\alpha\ . \quad (4.172)$$

Therefore, to prove (4.171), we only need to prove that

$$\left|\int_{-\pi}^{\pi}\int_{-\pi}^{\pi} (f(\beta+\zeta)-f(\beta))G_1(\beta,\beta+\zeta)\frac{\zeta_1}{|\zeta|^3}d\zeta - \int_{-\pi}^{\pi}\int_{-\pi}^{\pi} (f(\beta'+\zeta)-f(\beta))G_1(\beta',\beta'+\zeta)\frac{\zeta_1}{|\zeta|^3}d\zeta\right| \leq c|\beta-\beta'|^\alpha \|f\|_0 \sum_{i=1}^{3}\|\nabla S_i\|_\alpha\ . \quad (4.173)$$

For simplicity, we denote $h = \beta' - \beta = (h_1, h_2)$. By changing variable from ζ to ζ' as

$$\zeta' = \zeta + h\ ,$$

and still writing it as ζ, we re-write the second integral above as

$$\int_{-\pi+h_1}^{\pi+h_1}\int_{-\pi+h_2}^{\pi+h_2}(f(\beta+\zeta)-f(\beta))G_1(\beta',\beta+\zeta)\frac{\zeta_1-h_1}{|\zeta-h|^3}d\zeta\ .$$

For h sufficiently small, the integral

$$\left(\int_{-\pi+h_1}^{\pi+h_1}\int_{-\pi+h_2}^{\pi+h_2}-\int_{-\pi}^{\pi}\int_{-\pi}^{\pi}\right)(f(\beta+\zeta)-f(\beta))G_1(\beta',\beta+\zeta)\frac{\zeta_1-h_1}{|\zeta-h|^3}d\zeta$$

does not contain any singular points for sufficiently small h. Because the integration area is of order $O(|h|)$, it can be shown that

$$\left(\int_{-\pi+h_1}^{\pi+h_1}\int_{-\pi+h_2}^{\pi+h_2}-\int_{-\pi}^{\pi}\int_{-\pi}^{\pi}\right)(f(\beta+\zeta)-f(\beta))G_1(\beta',\beta+\zeta)\frac{\zeta_1-h_1}{|\zeta-h|^3}d\zeta$$
$$\leq c|h|\|f\|_0\sum_{i=1}^{3}\|\nabla S_i\|_0\leq c|\beta-\beta'|^\alpha N(\alpha)\ .$$

Therefore, to prove (4.173), we only need to prove

$$\left|\int_{-\pi}^{\pi}\int_{-\pi}^{\pi}(f(\beta+\zeta)-f(\beta))\left[G_1(\beta,\beta+\zeta)\frac{\zeta_1}{|\zeta|^3}-G_1(\beta',\beta+\zeta)\frac{\zeta_1-h_1}{|\zeta-h|^3}\right]d\zeta\right|$$
$$\leq c|\beta-\beta'|^\alpha\|f\|_0\sum_{i=1}^{3}\|\nabla S_i\|_\alpha\ .$$

(4.174)

We denote the above integral as I_3 and split it into two parts:

$$\begin{aligned} I_3 &\leq \left| \int_{|\zeta|<3|h|} (f(\beta+\zeta)-f(\beta)) \left[G_1(\beta,\beta+\zeta)\frac{\zeta_1}{|\zeta|^3} - G_1(\beta',\beta+\zeta)\frac{\zeta_1-h_1}{|\zeta-h|^3} \right] d\zeta \right| \\ &\quad + \left| \int_{|\zeta|\geq 3|h|} (f(\beta+\zeta)-f(\beta)) \left[G_1(\beta,\beta+\zeta)\frac{\zeta_1}{|\zeta|^3} - G_1(\beta',\beta+\zeta)\frac{\zeta_1-h_1}{|\zeta-h|^3} \right] d\zeta \right| . \\ &\triangleq I_{31} + I_{32} . \end{aligned} \tag{4.175}$$

Because the integration area is of order $O(h^2)$, we get

$$I_{31} \leq c|\beta-\beta'|^\alpha \|f\|_\alpha \sum_{i=1}^{3} \|\nabla S_i\|_\alpha . \tag{4.176}$$

To estimate I_32, we further split I_{32} into two parts:

$$\begin{aligned} I_{32} &\leq \int_{|\zeta|\geq 3|h|} |\zeta|^\alpha \|f\|_\alpha \left| [G_1(\beta,\beta+\zeta)-G_1(\beta',\beta+\zeta)]\frac{\zeta_1}{|\zeta|^3} \right| d\zeta \\ &\quad + \int_{|\zeta|\geq 3|h|} |\zeta|^\alpha \|f\|_\alpha \left| G_1(\beta',\beta+\zeta) \left(\frac{\zeta_1}{|\zeta|^3} - \frac{\zeta_1-h_1}{|\zeta-h|^3} \right) \right| d\zeta \\ &\triangleq I_{321} + I_{322} , \end{aligned} \tag{4.177}$$

which were denoted as I_{321} and I_{322}.

We estimate them separately. First, it can be shown that

$$I_{322} \leq c|\beta-\beta'|^\alpha \|f\|_\alpha \sum_{i=1}^{3} \|\nabla S_i\|_\alpha , \tag{4.178}$$

since

$$\left| \frac{\zeta_1}{|\zeta|^3} - \frac{\zeta_1-h_1}{|\zeta-h|^3} \right| \leq c\frac{|h|}{|\zeta|^3} . \tag{4.179}$$

Furthermore, the following bound can be proved.

$$I_{321} \leq c|\beta - \beta'|^{\alpha} \|f\|_{\alpha} \sum_{i=1}^{3} \|\nabla S_i\|_{\alpha} \ , \tag{4.180}$$

since

$$|G_1(\beta, \beta + \zeta) - G_1(\beta', \beta + \zeta)| \leq c \frac{|h|}{|\zeta|} \sum_{i=1}^{3} \|\nabla S_i\|_0 \ , \tag{4.181}$$

where we have applied (4.154), (4.156), and (4.162). The derivation of (4.181) is similar to that of (4.179).

Moreover, as we mentioned earlier, by replacing f with $f - \tilde{f}$, we can prove

$$I_{11} \leq c|\beta - \beta'|^{\alpha} \|f - \tilde{f}\|_{\alpha} \sum_{i=1}^{3} \|\nabla S_i\|_{\alpha} \ ,$$

which further implies that

$$I_{11} \leq c|\beta - \beta'|^{\alpha} N(\alpha) \ .$$

In summary, we obtained inequality (4.136). Inequality (4.135) will follow if we take $\tilde{f} = \tilde{S}_k = 0$.

Up to now, the only thing left is to prove (4.153) – (4.157). Since the proofs are similar, we just prove the first two.

1. The proof of (4.153)

Basically, we need to prove

$$\frac{|\mathbf{z}(\beta+\zeta)-\mathbf{z}(\beta)|}{|\zeta|} \geq c \ ,$$

which is equivalent to

$$\frac{|\mathbf{z}(\beta+\zeta)-\mathbf{z}(\beta)|^2}{|\zeta|^2} \geq c^2 \ .$$

Substituting the formulation of x, y, and z into the left-hand side of the inequality, we get

$$\left(\frac{\zeta_1+S_1(\beta+\zeta)-S_1(\beta)}{|\zeta|}\right)^2+\left(\frac{\zeta_2+S_2(\beta+\zeta)-S_2(\beta)}{|\zeta|}\right)^2+\left(\frac{S_3(\beta+\zeta)-S_3(\beta)}{|\zeta|}\right)^2,$$

which is greater than

$$1-2(\|\nabla S_1\|_0+|\nabla S_2\|_0)-\sum_{i=1}^{3}\|\nabla S_i\|_0^2 \ .$$

The above quantity has a lower bound of $\frac{29}{64}$ if

$$\|\nabla S_i\|_0 \leq \frac{1}{8} \ .$$

2. The proof of (4.154)

Similarly to the proof of (4.153), we can show that

$$\frac{|\mathbf{z}(\beta+\zeta)-\mathbf{z}(\beta)|}{|\zeta|} \leq c \ .$$

Therefore, to prove (4.154), we only need to show that

$$\frac{|\mathbf{z}(\beta+\zeta)-\mathbf{z}(\beta)|^3-|\zeta|^3}{|\zeta|^3} \leq c\left(\sum_{i=1}^{3}\|\nabla S_i\|_0\right) .$$

This is true if

$$\frac{|\mathbf{z}(\beta+\zeta)-\mathbf{z}(\beta)|^2-|\zeta|^2}{|\zeta|^2} \leq c\left(\sum_{i=1}^{3}\|\nabla S_i\|_0\right) ,$$

because by denoting $Df = \mathbf{z}(\beta+\zeta)-\mathbf{z}(\beta)$, we have

$$\frac{|Df|^3-|\zeta|^3}{|\zeta|^3} = \frac{|Df|^2-|\zeta|^2}{|\zeta|^2}\cdot\frac{|Df|^2+|Df||\zeta|+|\zeta|^2}{|\zeta|(|Df|+|\zeta|)} .$$

It comes down to show that for each S_i

$$|S_i(\beta+\zeta)-S_i(\beta)| \leq c\left(\sum_{i=1}^{3}\|\nabla S_i\|_0\right)|\zeta|$$

holds, which is obviously true.

This concludes our proof.

4.4.4 Bounds on E_{ij}

The error terms E_{ij} are defined in system (4.63) – (4.68), which are space derivatives of the R_k's.

By the definition of the E_{ij}'s, using the Cauchy inequality for analytic functions, we get:

$$\begin{aligned}
\|E_{ij}\|_{\alpha\rho'} &\leq c\|E_{ij}\|_{\alpha\rho'+} \\
&\leq c \sup_{(\mu_1,\mu_2)<\rho'} \|\nabla R_k[S_1,S_2,S_3]\|_\alpha(\cdot + i\mu_1, \cdot + i\mu_2) \\
&\leq c(\rho-\rho')^{-1} \sup_{(\mu_1,\mu_2)<\rho} \|R_k[S_1,S_2,S_3]\|_\alpha(\cdot + i\mu_1, \cdot + i\mu_2) \ .
\end{aligned} \tag{4.182}$$

It further follows from Lemma 4.4.6 that

$$\begin{aligned}
\|E_{ij}\|_{\alpha\rho'} &\leq c(\rho-\rho')^{-1} \sup_{(\mu_1,\mu_2)<\rho} \left(\sum_{k=1}^{3} \|\nabla S_k\|_\alpha\right)^2 (\cdot + i\mu_1, \cdot + i\mu_2) \\
&\leq c(\rho-\rho')^{-1} \left(\sum_{k=1}^{3} \|\nabla S_k\|_{\alpha\rho}\right)^2 \\
&\leq c(\rho-\rho')^{-1} \left(\sum_{k_1=1}^{3}\sum_{k_2=1}^{2} \|\psi_{k_1k_2}\|_{\alpha\rho}\right) \ ,
\end{aligned} \tag{4.183}$$

where in the last step we used the definition of ψ_{ij}.

Similarly, we can get the bounds of $(E_{ij} - \tilde{E}_{ij})$. We conclude this part of the estimate with a final lemma which is identical to Lemma 4.3.1.

Lemma 4.4.7 *Let x, y, z be given as in Lemma 4.4.3. Suppose ϕ_{ij} and $\tilde{\phi}_{ij}$ are analytic in $\max(|Im(\kappa_1)|, |Im(\kappa_2)|) < \rho$. Then for $0 < \rho' < \rho$, and $0 < \alpha < 1$, the following inequalities hold:*

$$\|E_{ij}\|_{\alpha\rho'} \leq c(\rho-\rho')^{-1} \left(\sum_{k_1=1}^{3}\sum_{k_2=1}^{2} \|\psi_{k_1k_2}\|_{\alpha\rho}\right)^2 \ , \tag{4.184}$$

and

$$\|E_{ij} - \tilde{E}_{ij}\|_{\alpha\rho'} \leq c(\rho - \rho')^{-1} \left(\sum_{k_1=1}^{3} \sum_{k_2=1}^{2} (\|\psi_{k_1 k_2}\|_{\alpha\rho} + \|\tilde{\psi}_{k_1 k_2}\|_{\alpha\rho} \right) \left(\sum_{k_1=1}^{3} \sum_{k_2=1}^{2} \|\psi_{k_1 k_2} - \tilde{\psi}_{k_1, k_2}\|_{\alpha\rho} \right) , \quad (4.185)$$

where $i, j = 1, 2, 3$.

Chapter 5 Some Theoretical Results on Model Equations

In this chapter, we introduce model equations for two-dimensional and three-dimensional vortex sheet equations.

The sections of this chapter are arranged as follows. Section 1 provides some theoretical results for the three-dimensional model equation, where we show that our three-dimensional model equation preserve the singularity type and the local singularity structure near the singularity time of the full equation. We devote Section 2 to the theoretical work on two-dimensional model equation, which we present as a special case of our three-dimensional model equation.

5.1 Three-dimensional Model Equation

5.1.1 Formulation

Consider the three-dimensional vortex sheet equation on an interface denoted as S,

$$\frac{\partial \mathbf{z}}{\partial t}(\mathbf{z}) = \int_{S'} |\nabla_\alpha \mu(\alpha')^T, \nabla_\alpha \mathbf{z}(\alpha')^T| \times \nabla_{\mathbf{z}'} G(\mathbf{z}(\alpha) - \mathbf{z}(\alpha'))\, d\alpha' \,, \tag{5.1}$$

where

$$\begin{aligned} G(\mathbf{z} - \mathbf{z}') &= -\frac{1}{4\pi|\mathbf{z} - \mathbf{z}'|} \,, \\ \nabla_{z'} G(\mathbf{z} - \mathbf{z}(\alpha')) &= -\frac{\mathbf{z} - \mathbf{z}}{4\pi|\mathbf{z} - \mathbf{z}'|^3} \,, \end{aligned}$$

and

$$|\nabla_\alpha \mu(\alpha')^T, \nabla_\alpha \mathbf{z}(\alpha')^T| = \frac{\partial \mu}{\partial \alpha_1}\mathbf{z}_{\alpha_2} - \frac{\partial \mu}{\partial \alpha_2}\mathbf{z}_{\alpha_1} ,$$

where the integral takes the Cauchy principal value.

Our main purpose of introducing the model equation is to use it as a tool to numerically study the three-dimensional vortex sheet problem. As we have mentioned before, all theoretical results on the singularity development of vortex sheet equations are based on formal asymptotic analysis. To confirm the results, some numerical calculation is needed. However, because of the nature of integro-differential equations, the numerical computation of equation (5.1) could become prohibitively expensive. For this reason, we try to derive a model equation for (5.1). We hope that the model equation captures the essence of the vortex sheet singularity and, at the same time, can be solved efficiently.

Inspired by our two-dimensional model equation, we feel that the most singular part of the integral on the right-hand side of equation (5.1) is in the neighborhood of $\mathbf{z}(\alpha)$. Similar to the two-dimensional model equation, we propose to replace

$$\mathbf{z}(\alpha_1, \alpha_2) - \mathbf{z}(\alpha_1', \alpha_2') ,$$

by the first order Taylor expansion around $\mathbf{z}(\alpha')$

$$\mathbf{z}_{\alpha_1}(\alpha')(\alpha_1 - \alpha_1') + \mathbf{z}_{\alpha_2}(\alpha')(\alpha_2 - \alpha_2') .$$

Consequently, equation (5.1) becomes:

$$\begin{aligned}\frac{\partial \mathbf{z}}{\partial t}(\mathbf{z}) &= \int_{S'} |\nabla_\alpha \mu(\alpha')^T, \nabla_\alpha \mathbf{z}(\alpha')^T| \\ &\times \frac{\mathbf{z}_{\alpha_1}(\alpha')(\alpha_1 - \alpha_1') + \mathbf{z}_{\alpha_2}(\alpha')(\alpha_2 - \alpha_2')}{|\mathbf{z}_{\alpha_1}(\alpha')(\alpha_1 - \alpha_1') + \mathbf{z}_{\alpha_2}(\alpha')(\alpha_2 - \alpha_2')|^3} \, d\alpha' \ , \end{aligned} \tag{5.2}$$

with further leads to

$$\frac{\partial \mathbf{z}}{\partial t} = \frac{1}{4\pi} \int\int \frac{(\mu'_{\alpha_1}(\alpha_1 - \alpha_1') + \mu'_{\alpha_2}(\alpha_2 - \alpha_2'))|\mathbf{z}'_{\alpha_1} \times \mathbf{z}'_{\alpha_2}|\mathbf{N}(\alpha')}{|\mathbf{z}'_{\alpha_1}(\alpha_1 - \alpha_1') + \mathbf{z}'_{\alpha_2}(\alpha_2 - \alpha_2')|^3} d\alpha_1' d\alpha_2' \ , \tag{5.3}$$

where

$$\mathbf{N} = \frac{\mathbf{z}_{\alpha_1} \times \mathbf{z}_{\alpha_2}}{|\mathbf{z}_{\alpha_1} \times \mathbf{z}_{\alpha_2}|} \ .$$

Furthermore, in every time step, if we can find a coordinate system (α_1, α_2), such that

$$\mathbf{z}_{\alpha_1} \cdot \mathbf{z}_{\alpha_2} = C_1 \mathbf{z}_{\alpha_2} \cdot \mathbf{z}_{\alpha_2} \ , \tag{5.4}$$

$$\mathbf{z}_{\alpha_1} \cdot \mathbf{z}_{\alpha_1} = C_2 \mathbf{z}_{\alpha_2} \cdot \mathbf{z}_{\alpha_2} \ , \tag{5.5}$$

where C_1 and C_2 are independent of α_1 and α_2, the integral on the right hand side of equation (5.3) becomes a convolution operator with kernel

$$\frac{\alpha_k}{2\pi(C_2\alpha_1^2 + 2C_1\alpha_1\alpha_2 + \alpha_2^2)^{3/2}} \ , \tag{5.6}$$

where $k = 1, 2$. Therefore, we can use FFT to evaluate it. In particular, when $C_1 = 0$ as in

the case of our computation, the spectral representation of the operator is:

$$\frac{-i\xi_1}{C_2(\xi_1^2 + C_2\xi_2^2)^{1/2}} , \tag{5.7}$$

and

$$\frac{-i\xi_2}{(\xi_1^2 + C_2\xi_2^2)^{1/2}} . \tag{5.8}$$

In general, even if $C_1 \neq 0$, the spectral representation of the the kernel is still known. In this way, the computational complexity in each time step is reduced to $O(N^2 \log N)$ from $O(N^4)$, where N is the number of mesh points in each direction.

However, since the numerical computation is performed on our model equation instead of the full equation, it is important to understand how much our model equation can be used to represent the full equation. That is the topic of next subsection, where we show that our model equation does capture the singularity type of the full equation, while the physical singularity time and location could be different.

5.1.2 Early Time Singularity Formation

Our goal in this subsection is to show that our three-dimensional model equation preserves the singularity type of the full three-dimensional vortex sheet equation.

First, it is necessary to review the results of last chapter where we derived the early time singularity formation on the full equation.

We consider a vortex sheet interface S separating two layers of fluids. With the Lagrangian representation, we parameterize the interface using surface parameters α_1 and α_2,

so that

$$\mathbf{z}(\alpha_1, \alpha_2, t) = (x(\alpha_1, \alpha_2, t), y(\alpha_1, \alpha_2, t), z(\alpha_1, \alpha_2, t))^T \ .$$

In particular, according to Lemma (3.3.1) in the last chapter, it is reasonable to assume that the coordinates (α_1, α_2) satisfy

$$\mathbf{z}_{\alpha_1} \cdot \mathbf{z}_{\alpha_2} = 0 \ , \tag{5.9}$$

$$\frac{\partial \mu}{\partial \alpha_1} = 0 \ , \tag{5.10}$$

$$\frac{\partial \mu}{\partial \alpha_2} = 1 \ , \tag{5.11}$$

at time $t = 0$. Without loss of generality, we also assume that

$$\begin{aligned} x(\alpha_1, \alpha_2, t) &= \alpha_1 + S_1(\alpha_1, \alpha_2, t) \ , \\ y(\alpha_1, \alpha_2, t) &= \alpha_2 + S_2(\alpha_1, \alpha_2, t) \ , \\ z(\alpha_1, \alpha_2, t) &= S_3(\alpha_1, \alpha_2, t) \ , \end{aligned}$$

where S_1, S_2 and S_3 are small perturbations.

Under the above assumptions, we have shown in Chapter 3 that by considering α_1 as a parameter and complexifying α_2, $\mathbf{z}(\alpha_1, \cdot)$ develops $\frac{3}{2}$ singularities on the α_2-direction at $t = 0+$.

The key to the result is to derive a local term from the integro-differential equation. It can be shown from the full equation that:

$$\omega(\alpha) = -\omega_{loc}(\alpha) + \omega_1(\alpha) \ , \tag{5.12}$$

$$= \omega_{loc}(\alpha) + \omega_2(\alpha) \ , \tag{5.13}$$

where

$$\omega_{loc}(\alpha) = \frac{\mathbf{z}_{\alpha_2}}{2|\mathbf{z}_{\alpha_2}|^2} \ , \tag{5.14}$$

and $\omega_1(\alpha)$, $\omega_2(\alpha)$ stand for the limiting velocity approaching from the lower and upper layer fluid respectively.

Furthermore, the local term $2\omega_{loc}(\alpha)$ represents a tangential velocity jump from the upper layer limiting velocity to the lower layer limiting velocity across the sheet. The jump is the driving force of the development of singularities. To derive a similar local term from our model equation, we analyze the difference between the full equation and our model equation. We would like to show that the difference is a regular integral and does not generate any discontinuity when extended into the complex domain.

Define:

$$u^f(\alpha) = -\frac{1}{4\pi} \int\int |\nabla_\alpha \mu(\alpha')^T, \nabla_\alpha \mathbf{z}(\alpha')^T| \times \frac{\mathbf{z}(\alpha) - \mathbf{z}(\alpha')}{|\mathbf{z}(\alpha) - \mathbf{z}(\alpha')|^3} d\alpha' \ ,$$

and

$$u^{mod}(\alpha) = -\frac{1}{4\pi}\int\int |\nabla_\alpha \mu(\alpha')^T, \nabla_\alpha \mathbf{z}(\alpha')^T| \times \frac{\mathbf{z}_{\alpha_1}(\alpha')(\alpha_1 - \alpha_1') + \mathbf{z}_{\alpha_2}(\alpha')(\alpha_2 - \alpha_2')}{|\mathbf{z}_{\alpha_1}(\alpha')(\alpha_1 - \alpha_1') + \mathbf{z}_{\alpha_2}(\alpha')(\alpha_2 - \alpha_2')|^3} d\alpha' ,$$

where

$$|\nabla_\alpha \mu(\alpha')^T, \nabla_\alpha \mathbf{z}(\alpha')^T| = \frac{\partial \mu}{\partial \alpha_1}\mathbf{z}_{\alpha_2} - \frac{\partial \mu}{\partial \alpha_2}\mathbf{z}_{\alpha_1} .$$

The difference is

$$Dif(\alpha) = (u^f - u^{mod})(\alpha) = -\frac{1}{4\pi}\int\int |\nabla_\alpha \mu(\alpha')^T, \nabla_\alpha \mathbf{z}(\alpha')^T| \times K(\alpha, \alpha') d\alpha' ,$$

where

$$K(\alpha, \alpha) = \frac{\mathbf{z}(\alpha) - \mathbf{z}(\alpha')}{|\mathbf{z}(\alpha) - \mathbf{z}(\alpha')|^3} - \frac{\mathbf{z}_{\alpha_1}(\alpha')(\alpha_1 - \alpha_1') + \mathbf{z}_{\alpha_2}(\alpha')(\alpha_2 - \alpha_2')}{|\mathbf{z}_{\alpha_1}(\alpha')(\alpha_1 - \alpha_1') + \mathbf{z}_{\alpha_2}(\alpha')(\alpha_2 - \alpha_2')|^3} .$$

It follows from the smoothness of $\mathbf{z}$ that (similar to the proof in the chapter of existence proof)

$$\lim_{\alpha' \to \alpha} K(\alpha, \alpha') \leq \frac{A}{|\alpha - \alpha'|} \tag{5.15}$$

if S_1, S_2, and S_3 are sufficiently small, which is guaranteed by our assumption at time $t = 0$.

Consequently, for each $\mathbf{z} \in S$, $Dif(\mathbf{z}(\alpha))$ is a regular integral. This means that the integral is continuous with respect to α. Thus, there will be no jump on the integral when moving from one side of the real α_2-axis to the other side of the real α_2-axis.

Furthermore, since

$$\omega^{mod} = \omega^f - Dif \ ,$$

where ω^{mod} is the velocity evaluated from the model equation, from equations (5.12) and (5.13), it can be shown that

$$\omega^{mod}(\alpha) = -\omega_{loc}(\alpha) + \omega_1(\alpha) - Dif(\alpha) \ , \tag{5.16}$$

$$= \omega_{loc}(\alpha) + \omega_2(\alpha) - Dif(\alpha) \ . \tag{5.17}$$

Since $Dif(\alpha)$ is continuous across the real α axes, this means that we have derived the same local terms as that of the full equation.

In summary, we have shown that our model equation generates the same tangential velocity jump as that generated by the full equation. As a result, these two equations develop the same type of singularities at almost identical location up to the leading order term.

5.1.3 Local Form of the Curvature Singularity

In this subsection, we show that our three-dimensional model equation preserves the local form of the curvature singularity near physical singularity time.

Following the analysis in Section 3.5 of Chapter 3, it is sufficient to show that we can derive the asymptotic system (3.72) – (3.74) from the model equation. It leads to the asymptotic approximation of the local sheet form straightforwardly, as we have seen in Chapter 3.

In fact, following the derivation by Hou & Zhang [17], as long as the perturbations

are small in magnitude, we can show that the difference between our model equation and the full equation only contributes to the smoother terms. As a result, we claim that the leading order system from our model equation has the same leading order terms as (3.72) – (3.74). Consequently, following the same derivations as in the Section 3.5 of Chapter 3, we can show that by a similar transformation on the interface variable functions, our model equation preserves the local form of the curvature singularity near physical singularity time.

5.2 Two-dimensional Model Equation

5.2.1 Formulation

The motivation of deriving a two-dimensional model equation for the Birkhoff-Rott equation is mainly for computational purposes, and more importantly, as a special case for the three-dimensional model equation. In fact, we provide more detailed analysis to show that our model equations does capture the singularity type and the local physical singularity structure of the full equation.

In the two-dimensional problem, the model equation is derived by approximating

$$z(\xi) - z(\xi') \ ,$$

by its first order Taylor expansion at $z(\xi')$ as

$$z_\xi(\xi')(\xi - \xi') \ ,$$

where z_ξ stands for the space derivative of $z(\xi, t)$ [16].

Therefore, the two-dimensional model equation is defined as:

$$\overline{\frac{\partial z}{\partial t}}(\xi,t) = \frac{1}{2\pi i}\int_{-\infty}^{\infty} \frac{\Gamma_\xi(\xi')d\xi'}{z_\xi(\xi',t)(\xi-\xi')} , \tag{5.18}$$

where the over bar denotes the complex conjugation.

In this section, we assume that the perturbation of the sheet and the vortex sheet strength are 2π periodic, i.e. , that $z(\xi+2\pi,t) = 2\pi + z(\xi,t)$, $\Gamma_\xi(\xi+2\pi) = \Gamma_\xi$. If we normalize the flow so that the average jump in the tangential velocity across the vortex sheet is unity, it implies that $\Gamma(\xi+2\pi) = 2\pi + \Gamma(\xi)$. Given the periodicity, (5.18) can be written as

$$\overline{\frac{\partial z(\xi,t)}{\partial t}} = \frac{1}{4\pi i}\int_0^{2\pi} \frac{\Gamma_\xi(\xi')}{z_\xi(\xi',t)} \cot(\frac{1}{2}(\xi-\xi'))d\xi' . \tag{5.19}$$

Now, we extend ξ' into complex domain, and consider $z(\xi)$ as a complex function defined on complex domain. We write the Cauchy principal value as a contour integral:

$$\int_{-\infty}^{\infty} \frac{\Gamma_\xi(\xi')}{z_\xi(\xi',t)} \cot(\frac{1}{2}(\xi-\xi'))d\xi' = \int_{\mathcal{C}} \frac{\Gamma_\xi(\xi')}{z_\xi(\xi',t)} \cot(\frac{1}{2}(\xi-\xi'))d\xi' + \frac{2\pi i\Gamma(\xi)}{z_\xi(\xi,t)} , \tag{5.20}$$

where the contour $\mathcal{C}$ runs from $\xi' = 0$ to $\xi' = 2\pi$, and is assumed to be deformed beneath a simple pole at $\xi' = \xi$. From the periodicity assumption, it is reasonable to assume that z and Γ have the forms of

$$z(\xi,t) = \xi + s(\xi,t) , \quad \Gamma(\xi) = \xi + \sigma(\xi) . \tag{5.21}$$

Following [9], we complexify s as follows:

$$s^*(\xi,t) = \overline{s(\bar{\xi},t)} \ . \tag{5.22}$$

Equation (5.19) can be analytically continued to the upper half complex ξ domain as:

$$\frac{\partial s^*(\xi,t)}{\partial t} = \frac{1}{4\pi i}\int_C \frac{1+\sigma_\xi(\xi')}{1+s_\xi(\xi',t)}\cot(\frac{1}{2}V(\xi,\xi',t))d\xi' + \frac{1+\sigma_\xi(\xi)}{2(1+s_\xi(\xi,t))} \ , \tag{5.23}$$

where

$$V(\xi,\xi',t) = \xi - \xi' \ . \tag{5.24}$$

Furthermore, we can write the equation as follows:

$$\frac{\partial s^*(\xi,t)}{\partial t} = \frac{\sigma_\xi(\xi) - s_\xi(\xi)}{2(1+s_\xi(\xi,t))} + G(\xi,t) \ , \tag{5.25}$$

where

$$G(\xi,t) = \frac{1}{4\pi i}\int_C (1+\sigma_\xi(\xi'))(i + \frac{\cot(\frac{1}{2}(\xi-\xi'))}{1+s_\xi(\xi',t)})d\xi' \ . \tag{5.26}$$

To derive an evolution equation for $s(\xi,t)$, we take complex conjugate on both side of equation (5.19) and deform the integration contour so that

$$\begin{aligned}
\frac{\partial s}{\partial t}(\xi,t) &= -\frac{1}{4\pi i}\int_0^{2\pi} \frac{\Gamma_\xi(\xi')}{\bar{z}_\xi(\xi',t)}\cot(\frac{1}{2}(\xi-\xi'))d\xi' \\
&= -\frac{1}{4\pi i}\int_C \frac{\Gamma_\xi(\xi')}{\bar{z}_\xi(\xi',t)}\cot(\frac{1}{2}(\xi-\xi'))d\xi' + 2\pi i\frac{\Gamma_\xi(\xi')}{\bar{z}_\xi(\xi',t)} \\
&= -\frac{1+\sigma(\xi)}{2(1+\bar{s}_\xi(\xi,t))} - \frac{1}{4\pi i}\int_C \frac{\Gamma_\xi(\xi')}{\bar{z}_\xi(\xi',t)}\cot(\frac{1}{2}(\xi-\xi'))d\xi' \ .
\end{aligned}$$

Finally, we extend ξ into the upper complex domain to get

$$\frac{\partial s(\xi,t)}{\partial t} = -\frac{\sigma(\xi) - s^*_\xi(\xi,t)}{2(1+s^*_\xi(\xi,t))} + G^*(\xi,t) \ . \tag{5.27}$$

where

$$G^*(\xi,t) = -\frac{1}{4\pi i}\int_{\mathcal{C}} (1+\sigma_\xi(\xi'))(i + \frac{\cot(\frac{1}{2}(\xi-\xi'))}{1+s_\xi(\xi',t)})d\xi' \ . \tag{5.28}$$

From the derivation, $\mathcal{C}$ runs from $\xi' = 0$ to $\xi' = 2\pi$, and is assumed to be deformed beneath a simple pole at $\xi' = \xi$. However, following the idea used by Cowley, Baker & Tanveer [12], we take the contour to run from $\xi' = 0$ to $\xi' = 2\pi$ along the real ξ' axis for the simplicity of the later analysis. The result is going to be confirmed by numerical calculations *a posteriori*.

Assume we start with an almost flat interface, i.e. , $s_\xi(\xi) = O(\varepsilon)$ for $\xi \in \Re$, it can be shown from the Taylor expansion that

$$i + \frac{\cot(\frac{1}{2}(\xi-\xi'))}{1+s_\xi(\xi',t)} = i + \cot(\frac{1}{2}(\xi-\xi')) + O(\varepsilon) \ .$$

On the other hand, it follows from straightforward calculation that

$$|i + \cot(\frac{1}{2}(\xi-\xi'))| \sim 2\exp(-Im(\xi)) \ll 1 \ ,$$

when ξ is far above the real axis. By combining the above two inequalities, we obtain the

inequality that bounds the integral terms in (5.25) and (5.27) that

$$\left| i + \frac{\cot(\frac{1}{2}(\xi - \xi'))}{1 + s_\xi(\xi', t)} \right| = O(\varepsilon) ,$$

for $Im(\xi) \gg 1$.

Under the above estimation, equations (5.25) and (5.27) can be re-written as:

$$\frac{\partial s^*(\xi,t)}{\partial t} = \frac{\sigma(\xi) - s_\xi(\xi)}{2(1 + s_\xi(\xi,t))} , \tag{5.29}$$

$$\frac{\partial s(\xi,t)}{\partial t} = -\frac{\sigma(\xi) - s^*_\xi(\xi,t)}{2(1 + s^*_\xi(\xi,t))} . \tag{5.30}$$

In summary, we have derived the same simplified model system as system (2.13) in [12].

5.2.2 The MBO Initial Condition

In the rest of this section, we concentrate on the singularity formation of model equation. By considering several different classes of initial conditions, we show that our model equation develops the same kind of singularities spontaneously at time $t = 0+$ as the full Birkhoff-Rott equation.

We start with the initial condition given by

$$s(\xi, 0) = 0, \quad \sigma_\xi(\xi) = \varepsilon \cos(\xi) . \tag{5.31}$$

This initial condition was first used and analyzed by Meiron, Baker & Orszag in [22]. Thereafter, we refer to this condition as the MBO initial condition.

Consider the following expansion of $z(\xi, t)$ with respect to t,

$$z = z_0(\xi) + tz_1(\xi) + t^2 z_2(\xi) + \cdots \ . \tag{5.32}$$

Substituting the MBO initial condition into the expansion, we get

$$z_0(\xi) = \xi \ . \tag{5.33}$$

Other terms will have to be derived from the model equation. Substituting the expansion into equation (5.18), and expand it in powers of t, we get:

$$\begin{aligned} & z_1^*(\xi) + 2tz_2^*(\xi) + \cdots = \\ & \quad \frac{1}{4\pi i} \int_0^{2\pi} (1 + \varepsilon \cos \xi') \cot(\frac{1}{2}(\xi - \xi'))[1 - tz_1'(\xi') + \cdots] d\xi' \end{aligned} \tag{5.34}$$

In particular, since $z_0 = \xi$, we can derive the formulation of $z_1(\xi)$ as:

$$z_1^*(\xi) = \frac{\partial z^*}{\partial t}(\xi, t = 0) = \frac{1}{4\pi i} \int_0^{2\pi} (1 + \varepsilon \cos \xi') \cot(\frac{1}{2}(\xi - \xi')) d\xi' \tag{5.35}$$

$$= -\frac{1}{2} i\varepsilon \sin \xi \ . \tag{5.36}$$

Since $\sin^*(\xi) = \sin(\xi)$, it implies

$$z_1(\xi) = \frac{1}{2} i\varepsilon \sin \xi \ . \tag{5.37}$$

Furthermore, we can derive z_2 as

$$\begin{aligned}
2z_2^* &= \frac{1}{4\pi i}\int_0^{2\pi}(1+\varepsilon\cos\xi')\cot(\frac{1}{2}(\xi-\xi'))(-z_1'(\xi'))d\xi' \\
&= \frac{1}{4\pi i}\int_0^{2\pi}(1+\varepsilon\cos\xi')(-\frac{1}{2}i\varepsilon\cos\xi'\cot(\frac{1}{2}(\xi-\xi'))d\xi' \\
&= \frac{1}{4\pi i}\int_0^{2\pi}-(\frac{1}{2}i\varepsilon\cos\xi'+\frac{1}{2}i\varepsilon^2\cos^2\xi')\cot(\frac{1}{2}(\xi-\xi'))d\xi' \\
&= \frac{1}{4\pi i}\int_0^{2\pi}-(\frac{1}{2}i\varepsilon\cos\xi'+\frac{1}{2}i\varepsilon^2\cos 2\xi')\cot(\frac{1}{2}(\xi-\xi'))d\xi' \\
&= -\frac{1}{4}\varepsilon\sin\xi-\frac{1}{8}\varepsilon\sin 2\xi \\
&= -\frac{1}{4}\varepsilon\sin\xi(1+\varepsilon\cos\xi)\ .
\end{aligned}$$

Combining the first two terms, s has the expansion

$$s=\frac{1}{2}i\varepsilon t\sin\xi-\frac{1}{8}\varepsilon t^2\sin\xi(1+\varepsilon\cos\xi)+\cdots\ . \tag{5.38}$$

However, no matter how small the time t is, the power series does not converge far from the real ξ-axis. In particular, it follows from (5.38) that the expansion becomes disordered when

$$\exp(-i\xi)\sim\varepsilon^{-1}t^{-1}\ ,$$

which suggests that for small times, and far from the real ξ-axis, a similarity solution should be sought of the form

$$\eta=\varepsilon t\exp(-i\xi)\ ,\quad s=s_0(\eta)+O(t)\ ,\quad s^*=s_0^*(\eta)+O(t)\ . \tag{5.39}$$

It follows from the transform that

$$\frac{\partial}{\partial t} = \frac{\partial}{\partial \eta}\frac{\partial \eta}{\partial t} = \varepsilon \exp(-i\xi)\frac{\partial}{\partial \eta} , \tag{5.40}$$

$$\frac{\partial}{\partial \xi} = \frac{\partial}{\partial \eta}\frac{\partial \eta}{\partial \xi} = -i\varepsilon t \exp(-i\xi)\frac{\partial}{\partial \eta} = -i\eta\frac{\partial}{\partial \eta} . \tag{5.41}$$

Combining (5.29), (5.30), (5.40) and (5.41), we find that to leading order

$$s_{0\eta} = -\frac{1}{4(1 - i\eta s^*_{0\eta})} , \quad s^*_{0\eta} = \frac{1}{4(1 - i\eta s_{0\eta})} . \tag{5.42}$$

Cowley, Baker & Tanveer [12] has derived the same system from the full equation for the MBO initial condition. This is to be expected since the full equation and the model equation have the same leading order systems (5.29) (5.30) for the MBO initial condition.

From here, we can just follow all the analysis performed in [12]. In particular, their analysis showed that s and s^* have 3/2 power singularities at

$$\xi \sim i \ln(\frac{2}{\varepsilon t}) , \tag{5.43}$$

when $t = 0+$. This shows that the solution of the model equation develops 3/2 power singularities at $\xi \sim i \ln(\frac{2}{\varepsilon t})$ spontaneously at $t = 0+$.

5.2.3 Other Initial Conditions

In this subsection, we study the solution in which, initially, there exists at least one point ξ_0, such that $(1 + s_{0\xi})$ or $(1 + s^*_{0\xi})$ vanishes. In particular, around those points, the right-hand side of equation (5.25) and (5.27) are dominated by the leading order terms.

Since the leading order terms blow up at some position ξ_0, it is very possible that some

singularity emerges from the analytical initial data. In the next two subsubsections, we consider two cases. First, we study the solution around one point $\xi = \xi_0$, where $(1+s_{0\xi}) = 0$ but $(1 + s^*_{0\xi}) \neq 0$. Then, we study the solution around a point $\xi = \xi_0$, where $(1 + s_{0\xi})$ and $(1 + s^*_{0\xi})$ vanishes simultaneously. We show that our model equation generates the same type of singularity as the full equation does under the above initial conditions.

The case $(1 + s_{0\xi}(\xi_0)) = 0$ but $(1 + s^*_{0\xi}(\xi_0)) \neq 0$

Apparently, it is infeasible to expand the solution in powers of t alone, since the expansion would break down around ξ_0. This suggests that we expand the solution as a power series in both $\zeta = \xi - \xi_0$ and time t. We seek a solution in the following form:

$$s = s_{00} - \zeta + \frac{1}{2}s_{02}\zeta^2 + \ldots + (\frac{s^*_{01} - \sigma_{01}}{2(1 + s^*_{01})} + G^*_{00} + \ldots)t + \ldots \ , \tag{5.44}$$

$$s^* = s^*_{00} - s^*_{01}\zeta + \frac{1}{2}s^*_{02}\zeta^2 + \ldots + (\frac{1 + \sigma_{01}}{2s_{02}\zeta} + \ldots)t + \ldots \ , \tag{5.45}$$

$$\tag{5.46}$$

where

$$s_{0n} = \frac{\partial^n s_0}{\partial \xi^n}(\xi_0) \ , \quad \sigma_{01} = \sigma_\xi(\xi_0) \ , \quad \text{and } G^*_{00} = G^*(\xi_0, 0) \ . \tag{5.47}$$

The non-uniformity arises from the leading coefficient of $O(t)$ terms in the expansion. We need to match ζ with t. From the simplified model equation (5.29) and (5.30), we see that the leading coefficient of $O(t)$ terms in (5.44) and (5.59) should play a deterministic role. These two terms should be matched with the s_{02} and s_{01} terms respectively. This suggests that $\zeta = O(t^{\frac{1}{2}})$ be a good match [12].

For $t \ll 1$, let

$$\zeta = \eta\omega t^{\frac{1}{2}}, \qquad \text{where} \qquad \omega = (\frac{2(1+\sigma_{01})}{s_{02}(1+s^*_{01})})^{\frac{1}{2}} , \tag{5.48}$$

and expand s and s^* in the form of

$$s = s_{00} - \eta\omega t^{\frac{1}{2}} + (\frac{1}{2} + G^*_{00} + \frac{1+\sigma_{01}}{1+s^*_{01}}A(\eta))t + \dots , \tag{5.49}$$

$$s^* = s^*_{00} + ((1+s^*_{01})B(\eta) - \eta)\omega t^{\frac{1}{2}} + \dots . \tag{5.50}$$

so that by substituting into the evolution equation, $A(\eta)$ and $B(\eta)$ can be solved. Since we have changed variables from (ξ, t) to (η, t), where $\xi = \xi_0 + \eta\omega t^{\frac{1}{2}}$, the following equalities can be verified:

$$\frac{\partial}{\partial\xi} = \frac{\partial}{\partial\eta}\frac{\partial\eta}{\partial\xi} + \frac{\partial}{\partial t}\frac{\partial t}{\partial\xi} = (\omega^{-1}t^{-\frac{1}{2}})\frac{\partial}{\partial\eta} , \tag{5.51}$$

$$\frac{\partial}{\partial t} = \frac{\partial}{\partial\eta}\frac{\partial\eta}{\partial t} + \frac{\partial}{\partial t}\frac{\partial t}{\partial t} = -\frac{1}{2}\eta t^{-1}\frac{\partial}{\partial\eta} + \frac{\partial}{\partial t} . \tag{5.52}$$

Substituting (5.52) into (5.49), we get:

$$\frac{\partial s}{\partial t} = -\frac{1}{2}\eta\omega t^{-\frac{1}{2}} + \frac{1}{2}\eta\omega t^{-\frac{1}{2}} + (\frac{1}{2} + G^*_{00} + \frac{1+\sigma_{01}}{1+s^*_{01}}A(\eta)) - \frac{1+\sigma_{01}}{2(1+s^*_{01})}\eta A_\eta . \tag{5.53}$$

Substituting (5.51) into (5.50), we have

$$s^*_\xi = ((1+s^*_{01})B_\eta - 1)\omega^{-1} + \dots , \tag{5.54}$$

which implies

$$\frac{s^*_\xi}{2(1+s^*_\xi)} = \frac{1}{2} - \frac{1}{2(1+s^*_{01})B_\eta} + O(t^{\frac{1}{2}}) \ . \tag{5.55}$$

Moreover, substituting (5.53) and (5.55), into (5.27), we extract the leading order terms as

$$\frac{1+\sigma_{01}}{1+s^*_{01}}A(\eta) - \frac{1+\sigma_{01}}{2(1+s^*_{01})}\eta A_\eta + G^*_{00} = -\frac{1}{2(1+s^*_{01})B_\eta} + G^*_{00} \tag{5.56}$$

which can be further simplified to

$$2A - \eta A_\eta = -\frac{1}{B_\eta} \ . \tag{5.57}$$

Similarly, from equation (5.25), it can be shown that

$$B - \eta B_\eta = \frac{1}{A_\eta} \ . \tag{5.58}$$

The system that consists of equation (5.57) and equation (5.58) coincides with system (2.28) in [12]. Therefore, following the analysis presented by Cowley, Baker & Tanveer, we can show that in this case, our model equation develops the same type of singularity as that of the full equation. Furthermore, it follows naturally that the singularity appears at almost the same location up to order $O(t^{\frac{1}{2}})$ when $t \ll 1$ as that of the Birkhoff-Rott equation.

The case $(1 + s_{0\xi}(\xi_0)) = 0$ and $(1 + s^*_{0\xi}(\xi_0)) = 0$

The above analysis is not valid when $(1 + s_{0\xi}(\xi_0))$ and $(1 + s_{0\xi}(\xi_0))$ vanish simultaneously. However, following the idea presented above, we still can expand the solution as a power

series in both $\zeta = \xi - \xi_0$ and time t:

$$s = s_{00} - \zeta + \frac{1}{2}s_{02}\zeta^2 + \ldots + (\frac{-1-\sigma_{01}}{2s^*_{02}\zeta} + G^*_{00} + \ldots)t + \ldots \ , \tag{5.59}$$

$$s^* = s^*_{00} - \zeta + \frac{1}{2}s^*_{02}\zeta^2 + \ldots + (\frac{1+\sigma_{01}}{2s_{02}\zeta} + G_{00} + \ldots)t + \ldots \ , \tag{5.60}$$

where

$$s_{0n} = \frac{\partial^n s_0}{\partial \xi^n}(\xi_0) \ , \quad \sigma_{01} = \sigma_\xi(\xi_0) \ , \quad \text{and } G^*_{00} = G^*(\xi_0, 0) \ . \tag{5.61}$$

Again we need to match ζ with t. From the simplified model equation, we see that the leading coefficient of the $O(t)$ term should play a deterministic role. These two terms should be matched with the s_{02} and s^*_{02} terms respectively. This suggests that $\zeta = O(t^{\frac{1}{3}})$ would be a good match.

Let

$$\zeta = \eta\Omega t^{\frac{1}{3}}, \qquad \text{where} \qquad \Omega = (\frac{4(1+\sigma_{01})}{s_{02}s^*_{02}})^{\frac{1}{3}} \ . \tag{5.62}$$

Therefore, the expansions (5.59) and (5.60) need to be replaced by

$$s = s_{00} - \eta\Omega t^{\frac{1}{3}} + \frac{1}{2}s_{02}\Omega^2 A(\eta)t^{\frac{2}{3}} + \ldots \ , \tag{5.63}$$

$$s^* = s^*_{00} - \eta\Omega t^{\frac{1}{3}} + \frac{1}{2}s^*_{02}\Omega^2 B(\eta)t^{\frac{2}{3}} + \ldots \ . \tag{5.64}$$

Change variable from (ξ, t) to (η, t), where $\xi = \xi_0 + \eta\Omega t^{\frac{1}{3}}$. We find

$$\frac{\partial}{\partial \xi} = \frac{\partial}{\partial \eta}\frac{\partial \eta}{\partial \xi} + \frac{\partial}{\partial t}\frac{\partial t}{\partial \xi} = (\Omega^{-1}t^{-\frac{1}{3}})\frac{\partial}{\partial \eta} , \tag{5.65}$$

$$\frac{\partial}{\partial t} = \frac{\partial}{\partial \eta}\frac{\partial \eta}{\partial t} + \frac{\partial}{\partial t}\frac{\partial t}{\partial t} = -\frac{1}{3}\eta t^{-1}\frac{\partial}{\partial \eta} + \frac{\partial}{\partial t} . \tag{5.66}$$

It follows from substituting (5.66) into (5.63) that

$$\begin{aligned}\frac{\partial s}{\partial t} &= -\frac{1}{3}\eta\Omega t^{-\frac{2}{3}} + \frac{1}{3}\eta\Omega t^{-\frac{2}{3}} + \frac{1}{3}s_{02}\Omega^2 A(\eta)t^{-\frac{1}{3}} - \frac{1}{6}s_{02}\Omega^2\eta A_\eta t^{-\frac{1}{3}} + \dots \\ &= \frac{1}{6}s_{02}\Omega^2 t^{-\frac{1}{3}}(2A(\eta) - \eta A_\eta) + \dots .\end{aligned} \tag{5.67}$$

Similarly, substituting (5.65) into (5.64) yields

$$s^*_\xi = -1 + \frac{1}{2}s^*_{02}\Omega^{-1}t^{\frac{1}{3}}B_\eta + \dots , \tag{5.68}$$

which implies that

$$\frac{-s^*_\xi}{2(1+s^*_\xi)} = \frac{1}{s^*_{02}\Omega B_\eta}t^{-\frac{1}{3}} + O(1) . \tag{5.69}$$

By substituting (5.67) and (5.69) into (5.27), we extract the leading order terms as

$$\frac{1}{6}s^*_{02}s_{02}\Omega^3(2A - \eta A_\eta) = -\frac{1}{4B_\eta}s^*_{02}s_{02}\Omega^3 , \tag{5.70}$$

which can be further simplified to

$$2A - \eta A_\eta = -\frac{3}{2B_\eta} . \tag{5.71}$$

Similarly, we can derive from (5.27) that

$$2B - \eta B_\eta = \frac{3}{2A_\eta} \,. \tag{5.72}$$

System (5.71) and (5.72) coincides with system (2.38) in [12]. Therefore, we can follow the analysis by Cowley, Baker & Tanveer from now on. In particular, we can show that in this case, our model equation also develops the same type of singularity (of power 3/2) as that of the full equation. Further, as in the previous case, we can also show that the singularity appears at almost the same location up to order $O(t^{\frac{1}{3}})$ when $t \ll 1$ as that of the full Birkhoff-Rott equation.

5.2.4 Motion of the Singularity

In the previous two subsections, we have shown that our model equation develops the same type of singularity as the full equation spontaneously in the complex domain at $t = 0+$. In the subsubsection, we show that at time $t = O(1)$, singularities can continue to propagate in the extended complex domain. In particular, we derive an ODE which governs the motion of the singularity, and thus, we show that the singularity type does not change along the trajectory.

Suppose that at time t a singularity is at $\xi = \xi_s(t)$. Close to the singularity we seek an asymptotic expansion of the form:

$$s = S_0(t) + S_1(t)\eta + S_p(t)\eta^p + \dots \,, \tag{5.73}$$

$$s^* = S_0^*(t) + S_1^*(t)\eta + S_p^*(t)\eta^p + \dots \,, \tag{5.74}$$

where $\eta = \xi - \xi_s(t)$.

Substituting the above expansion into (5.25) and (5.27), and equating like powers of η, we derive the equations for the functions in the expansion as:

$$\dot{S}_0 - \dot{\xi}_s S_1 = -\frac{Q_s - S_1^*(t)}{2(1+S_1^*)} + G^*(\xi_s, t) \ , \tag{5.75}$$

$$\dot{S}_0^* - \dot{\xi}_s S_1^* = -\frac{Q_s - S_1(t)}{2(1+S_1)} + G(\xi_s, t) \ , \tag{5.76}$$

$$\dot{\xi}_s^2(t) = -(\frac{1+Q_s}{2(1+S_1)(1+S_1^*)})^2 \ , \tag{5.77}$$

$$S_p(t) = -\frac{2(1+S_1)^2 S_p^*}{2(1+Q_s)}\dot{\xi}_s \ . \tag{5.78}$$

Although we have obtained similar system as (2.43) in [12], the forcing term is different. It shows that although in both equations, the singularity type does not change when they propagate along the complex domain, the actual trajectories can be different. Therefore, the physical singularity time would be different, which has been verified by our numerical calculations.

In summary, we conclude that in our model equation, 3/2 power singularities are generated spontaneously at $t = 0+$, as in the full Birkhoff-Rott equation. The singularities can move around the complex domain at later time but keep the same power. Therefore, the physical singularity should also be of 3/2 power in our model equation for the initial condition we studied. However, the trajectory along which the singularities propagate in our model equation might be different from that in the full equation and the times at which

the physical singularities occur might also be different.

In our next subsection, we study the interface shape in the neighborhood of a singularity near the physical singularity time in our model equation. We also show that our model equation preserves the local singularity structure of the full equation near the physical singularity time. All results will be verified by our numerical calculation in the next chapter.

5.2.5 The Local Form of the Curvature Singularity

In this subsection, we study the local form of the curvature singularity. We hope to obtain the interface shape in the neighborhood of the singularity. Without loss of generality, we consider the case where $\sigma(\xi) = 0$ in (5.21). Moreover, we assume that the singularity forms at $t = 0$, $\xi = 0$, $z = 0$, and that the surface is moving with a velocity $\dot{z}_0$. We also assume that at the time of singularity formation, the surface is locally flat in the neighborhood of the singularity, with $z \sim \lambda\xi$, where λ is a complex number. The assumption is reasonable when the singularity is of power 3/2.

We seek an asymptotic expansion of the solution to our model equation (5.18) in the power series of both t and ξ. We split the integral region into two subregions: a local region with $\xi \sim O(t)$ and an outer region covers the rest of the integration domain. We also split the integral into three parts according to the regions.

$$\int_{-\infty}^{\infty} \frac{d\xi'}{z_\xi(\xi', t)(\xi - \xi')} = \left\{ \int_{-\infty}^{-\delta} + \int_{-\delta}^{\delta} + \int_{\delta}^{\infty} \right\} \frac{d\xi'}{z_\xi(\xi', t)(\xi - \xi')} , \tag{5.79}$$

where $|\xi| \ll \delta \ll 1$.

Under the above assumptions, the first and third integral contribute to $O(t^0)$ and $O(t^1)$ terms, whereas the shape of vortex sheet in the neighborhood of the singularity is determined

by the second integral. In order to approximate this integral, we re-scale it by using:

$$z = \dot{z}_0|\lambda|^2\tau + \lambda(\xi + s(\xi,\tau)), \quad t = |\lambda|^2\tau \ , \tag{5.80}$$

where s here is slightly different from the s defined before in 5.21.

The second integral then becomes:

$$\begin{aligned}
\int_{-\delta}^{\delta} \frac{d\xi'}{z_\xi(\xi',t)(\xi-\xi')} &= \frac{1}{\lambda}\int_{-\delta}^{\delta} \frac{d\xi'}{(1+s_\xi(\xi',t))(\xi-\xi')} \\
&= \frac{1}{\lambda}\int_{-\delta-\xi}^{\delta-\xi} \frac{d\xi'}{(1+s_\xi(\xi+\zeta,t))(-\zeta)} \\
&= \frac{1}{\lambda}\int_{-\delta-\xi}^{\delta-\xi} \frac{-s_\xi(\xi+\zeta,t)\zeta}{(1+s_\xi(\xi+\zeta,t))(-\zeta)}\cdot\frac{d\zeta}{\zeta} - \frac{1}{\lambda}\int_{-\delta-\xi}^{\delta-\xi}\frac{d\zeta}{\zeta} \\
&= \frac{1}{\lambda}\int_{-\delta-\xi}^{\delta-\xi} \frac{s_\xi(\xi+\zeta,t)}{(1+s_\xi(\xi+\zeta,t))}\cdot\frac{d\zeta}{\zeta} - \frac{1}{\lambda}\ln\left(\frac{\delta-\xi}{\delta+\xi}\right) \\
&= \frac{1}{\lambda}\int_{-\delta-\xi}^{\delta-\xi} \frac{s_\xi(\xi+\zeta,t)}{(1+s_\xi(\xi+\zeta,t))}\cdot\frac{d\zeta}{\zeta} + O(\xi) \ .
\end{aligned} \tag{5.81}$$

Again, we take $|\xi| \sim t$ when $|\xi|, t \ll 1$. We see, by splitting the integral, the first and the third integrals must balance the $\dot{z}_0$ term in the expansion, and the next term of $\xi^{\frac{1}{2}}$ matches with the second integral.

Let

$$\xi = (-\tau)\chi \ , \tag{5.82}$$

and seek a similarity solution:

$$s = (-\tau)^q F(\chi) \ , \tag{5.83}$$

where $1 < q < 2$. For the initial conditions we studied in the early subsections,we know

that $q = \frac{3}{2}$.

The change of variable implies

$$\frac{\partial}{\partial \xi} = (-\tau)^{-1}\frac{\partial}{\partial \chi}\,, \tag{5.84}$$

$$\frac{\partial}{\partial t} = \frac{\chi}{\tau|\lambda|^2}\frac{\partial}{\partial \chi} + |\lambda|^{-2}\frac{\partial}{\partial \tau}\,. \tag{5.85}$$

Therefore, by substituting the change of variables into the similarity solution, we get

$$\frac{\partial \bar{z}}{\partial t} = \bar{\lambda}\left(\frac{(-\tau)^{q-1}}{|\lambda|^2}(\chi \bar{F}_\chi - q\bar{F})\right) + o(\tau^{q-1})\,. \tag{5.86}$$

On the other hand, further manipulations on (5.81) implies

$$\int_{-\delta}^{\delta} \frac{d\xi'}{z_\xi(\xi',t)(\xi-\xi')} = \frac{1}{\bar{\lambda}}\int_{-\delta-\xi}^{\delta-\xi} \frac{s_\xi(\xi+\zeta,t)}{(1+s_\xi(\xi+\zeta,t))}\cdot\frac{d\zeta}{\zeta} + O(\xi) \tag{5.87}$$

$$= \frac{1}{\bar{\lambda}}\int_{-\infty}^{\infty} \frac{(-\tau)^{q-1}F_\chi(\chi+\eta)}{\eta(-\tau)}(-\tau)d\eta + O(\tau) \tag{5.88}$$

$$= \frac{1}{\bar{\lambda}}\int_{-\infty}^{\infty} \frac{(-\tau)^{q-1}F_\chi(\chi+\eta)}{\eta}d\eta + O(\tau)\,. \tag{5.89}$$

By matching the $O((-\tau)^{q-1})$ terms, we obtain

$$\chi\bar{F}_\chi - q\bar{F} = \frac{1}{2\pi i}\int_{-\infty}^{\infty}\frac{F_\chi(\chi+\eta)}{\eta}d\eta\,. \tag{5.90}$$

In order to fit the 'outer region' where $\xi = O(1)$, we claim that $F \sim F_\pm|\chi|^q$ as $\chi \to \pm\infty$, where $F_\pm$ are constants and satisfy $F_+ = -F_-$. Under this condition, we perform the integration by part in equation (5.90). The result is:

$$\chi\bar{F}_\chi - q\bar{F} = \frac{1}{2\pi i}\int_{-\infty}^{\infty}\frac{F(\chi+\eta)-F(\chi)}{\eta^2}d\eta\,. \tag{5.91}$$

Note that equation (5.91) is the same as equation (5.7) in [12], which shows that our model preserves the shape of vortex sheet where a physical singularity appears. Here, we just briefly restate the main results in [12] which were derived from equation (5.91). Our numerical calculations have confirmed these results.

By solving equation (5.91), we can show that

$$F = \gamma(1-i)(4\chi^2+1)^{q/2}\sin(q\arctan(2\chi)) \ , \tag{5.92}$$

where γ is a real constant.

For the initial conditions that we considered here, $q = \frac{3}{2}$. Thus the vortex sheet has the local form

$$z_\xi \sim \lambda + 3\gamma(1-i)\lambda(-\tau)^{1/2}\cos(\frac{1}{2}\arctan(2\chi)) \ , \tag{5.93}$$

$$z_{\xi\xi} = \lambda s_{\xi\xi} \sim 3\sqrt{2}\gamma\lambda\exp(-i\pi/4)(-\tau)^{1/2}(4\chi^2+1)^{-1/4}\sin(\frac{1}{2}\arctan(2\chi)) \ . \tag{5.94}$$

Based on (5.94), we would like to mention one special case of our analysis. Note that if we take $\arg\lambda = \pi/4$, the leading order branch-cut singularity is only evident in x, and not in y. It provides an explanation of Shelley's [28] observation that when $\varepsilon = 0.5$ in the MBO initial condition, the nature of singularity in the real variable seems to be different from the imaginary variable in the full vortex sheet equation. From the analysis presented above, we have shown that a similar phenomenon should happen to our model equation as well. This rather surprising result has also been verified by our numerical calculation.

Chapter 6 Numerical Study on the Model Equations

In this chapter, we validate our theoretical analysis by performing numerical computations on both two-dimensional and three-dimensional vortex sheet problems..

The sections in this chapter are arranged as follows. Section 1 presents our numerical results for the two-dimensional problem. While in Section 2, we perform numerical calculations on the three-dimensional problem.

6.1 Two-dimensional Model Equation

6.1.1 Algorithm

The motion of a two-dimensional vortex sheet is governed by the Birkhoff-Rott equation [6].

$$\overline{\frac{\partial z}{\partial t}}(\xi,t) = \frac{1}{4\pi i}\int_{-\pi}^{\pi} \Gamma_\xi(\xi')\cot\left[\frac{1}{2}(z(\xi)-z(\xi'))\right]d\xi' \ , \tag{6.1}$$

where the over-bar denotes the complex conjugate, t is the time, $z(\xi,t) = x(\xi,t) + iy(\xi,t)$ is the complex interface position parametrized by a Lagrangian variable ξ, and $\Gamma(\xi)$ is the circulation in the sheet measured between the point with coordinate z and a reference particle. Most importantly, the integral takes the Cauchy principal value. function $z-\xi$ and function Γ_ξ are assumed to be 2π-periodic.

Following Shelley [28], we use the modified point-vortex approximation (subsequently referred to as MPVA) to study the full vortex sheet equation. Discretizing $z(\xi, t=0)$ and

$\gamma(\xi) = \Gamma_\xi(\xi)$ uniformly in the Lagrangian parameter ξ as

$$z_j(t=0) = z(jh, t=0) \ ,$$

and

$$\gamma_j = \gamma(jh) \ ,$$

with $h = 2\pi/N$ and j ranging from 0 to $N-1$, we can approximate the velocity integral in (6.1) by the alternating trapezoidal rule

$$\frac{d}{dt}\overline{z_j}(t) = \frac{2h}{4\pi i} \sum_{\substack{k=0 \\ j+k \ odd}}^{N-1} \gamma_k \cot \frac{1}{2}[z_j(t) - z_k(t)]. \tag{6.2}$$

Shelley [28] showed that the approximation is of spectral accuracy, which means that the error decreases faster than any algebraic power of h.

Naturally, MPVA can be applied to our model equation as well, since it is described as

$$\overline{\frac{\partial z}{\partial t}}(\xi, t) = \frac{1}{4\pi i} \int_{-\pi}^{\pi} \frac{\Gamma_\xi(\xi')}{z_\xi(\xi')} \cot\left[\frac{1}{2}(\xi - \xi')\right] d\xi'. \tag{6.3}$$

However, since our model equation can be re-written as

$$\overline{\frac{\partial z}{\partial t}}(\xi, t) = \frac{1}{2i} H\left(\frac{\Gamma_\xi}{z_\xi}\right), \tag{6.4}$$

where H stands for the Hilbert transform defined as

$$Hf(\xi) = \frac{1}{2\pi} \int_{-\pi}^{\pi} f(\xi') \cot\left[\frac{1}{2}(\xi - \xi')\right] d\xi' \,. \tag{6.5}$$

The integral can be evaluated by means of FFT.

One common technique needed in numerically solving both the full equation and our model equation is the spectral filtering technique introduced by Krasny [19]. Due to Kelvin-Helmholtz instability, the round-off error of the calculation leads to a rapid and spurious growth of the high-wavenumber amplitudes [27], causing a severe departure of the computed solution of the discrete system from the exact solution. For this reason, Krasny employed a Fourier filter that, at each time-step, zeroes any Fourier amplitude whose modulus is less than some preassigned tolerance. Recently, Caflisch, Hou & Lowengrub [8] have proved the convergence of the modified point-vortex approximation with spectral filtering.

6.1.2 Numerical Results

In this subsection, we study the two-dimensional vortex sheet with MBO initial condition. The initial condition is

$$z(\xi, t = 0) = \xi \tag{6.6}$$

$$\gamma(\xi) = -1 + \varepsilon \cos(\xi) \tag{6.7}$$

for $\varepsilon = 0.5$.

For this initial condition, we perform two sets of numerical computations, using the

full equation and our model equation respectively. The calculations of both equations are performed using quadruple precision in order to detect the early time singularity formation. The procedure can be described as follows:

1. Evolve both equations from $t = 0$ up to $t = 1.3$, by taking $N = 256$, $\triangle t = 0.0025$.

2. Double the mesh points N to 512, reduce $\triangle t$ in half to 0.00125, and calculate both equations from $t = 1.3$ up to $t = 1.5$ by taking the final results of the last step as the initial condition.

3. Further double the mesh points N to 1024, reduce $\triangle t$ to 0.000625, and calculate both equations from $t = 1.5$ up to $t = 1.65$.

In our calculations, the filter tolerance level is set at 10^{-23} for both equations. Both the above procedure and the tolerance level are set to follow that of [28], so that we can compare the computational results with those by Shelley in [28].

The purpose of this section is to confirm our theoretical results for the two-dimensional model equation. Therefore, we analyze the numerical computations in four aspects:

1. Interface shapes and their Fourier spectra.

2. Early time singularity formation.

3. Local sheet form at the physical singularity time.

4. Physical singularity time.

1. Interface shapes and their Fourier spectra. In this part of the numerical analysis, we want to show the sheet interfaces and their Fourier spectra for solutions of both equations. As we can see from Figure (6.1) and Figure (6.2), the Fourier spectra of

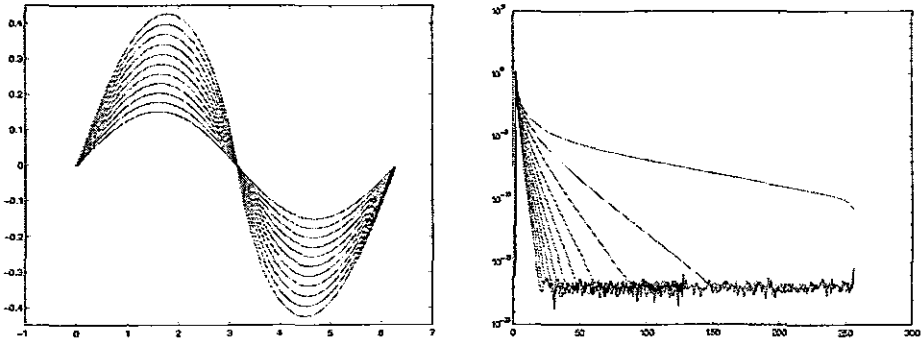

(a) Interface (b) Spectrum

Figure 6.1: The interfaces and Fourier spectrums calculated from the full equation, in which $t = 0.6$ to 1.6 at intervals of 0.1.

the solutions to both equations have grown considerably as time increases, due to Kelvin-Helmholtz instability.

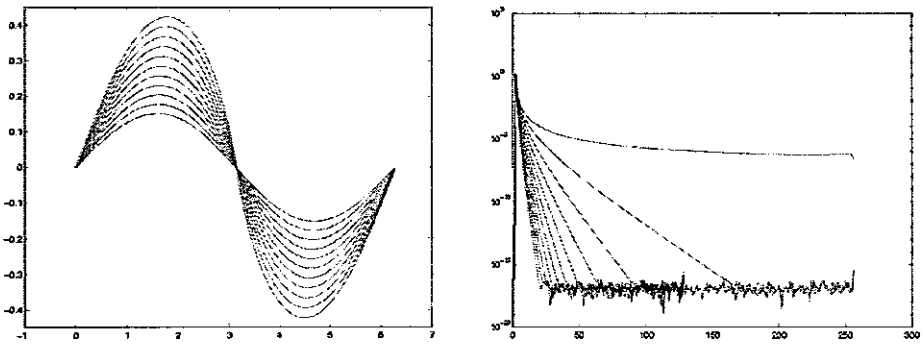

(a) Interface (b) Spectrum

Figure 6.2: The interfaces and Fourier spectrums calculated from the model equation, in which $t = 0.6$ to 1.6 at intervals of 0.1.

2. Early time singularity formation. From the theoretical analysis for both the full equation and the model equation, we know that singularities form spontaneously at $t = 0+$ when complexifying the independent variable. In particular, we showed that the solution to our model equation develops the same type of the singularities at the same position at which the full equation develops a singularity. In order to provide convincing numerical evidence to support our analysis, we form-fit the Fourier spectrum of the data with:

$$|\widehat{X_k}(t)| = C_X k^{-\beta_X} \exp(-\alpha_X k) \ , \tag{6.8}$$

$$|\widehat{Y_k}(t)| = C_Y k^{-\beta_Y} \exp(-\alpha_Y k) \ , \tag{6.9}$$

where $\widehat{X_k}$ is the kth Fourier coefficient of $x(\xi, t) - \xi$ and $\widehat{Y_k}$ is the kth Fourier coefficient of $y(\xi, t)$. This form-fitting idea follows the previous work by Krasny [19], Pugh [26], Shelley [28], and Baker, Caflisch & Siegel [3]. In the form-fitting, α_X measures the distance of the x-direction singularity from the real ξ axis, while $(\beta_X - 1)$ measures the power of singularity

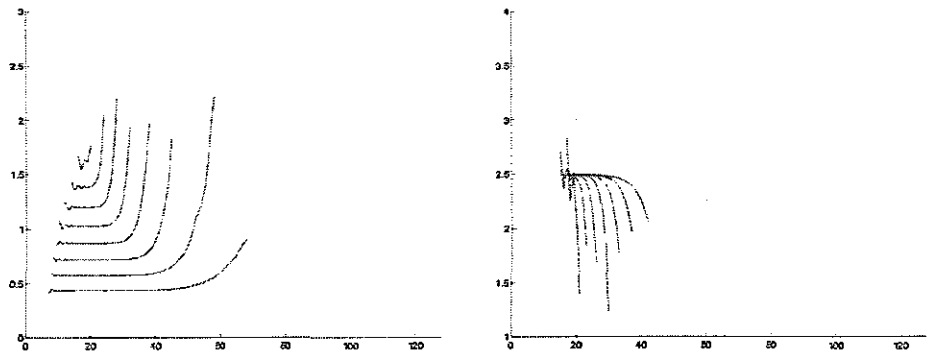

(a) α_X (b) β_X

Figure 6.3: The form-fitted α_X and β_X calculated from the full equation, in which $t = 0.6$ to 1.3 at intervals of 0.1.

in the x-direction and similarly for α_Y and β_Y.

As we can see from Figure (6.3), Figure (6.4), Figure (6.5), and Figure (6.6), β_X and β_Y are around 2.5 for both equations. This shows that at early time, both equations generate 3/2 singularities at x and y directions. Moreover, we notice that form-fitted α's is slightly different between the full equation and our model equations. This indicates the disparity between the trajectories along which singularity propagates in the two equations.

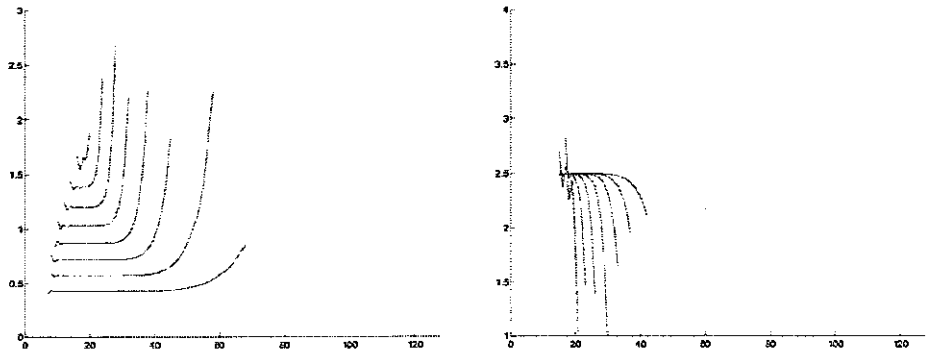

(a) α_X (b) β_X

Figure 6.4: The form-fitted α_X and β_X calculated from the model equation, in which $t =$ 0.6 to 1.3 at intervals of 0.1.

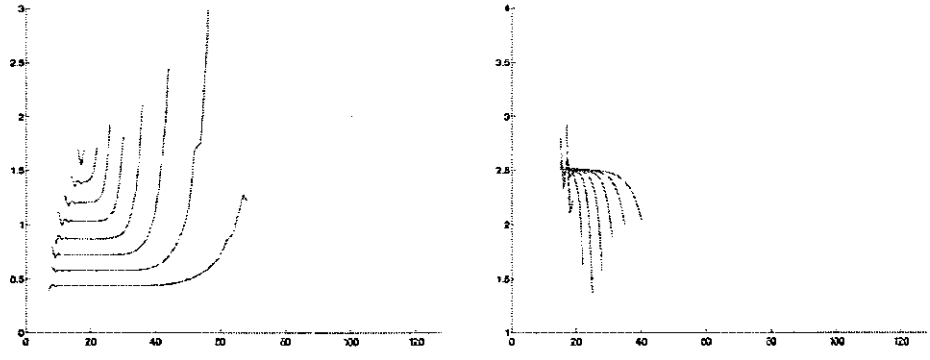

(a) α_X (b) β_X

Figure 6.5: The form-fitted α_Y and β_Y calculated from the full equation, in which $t = 0.6$ to 1.3 at intervals of 0.1.

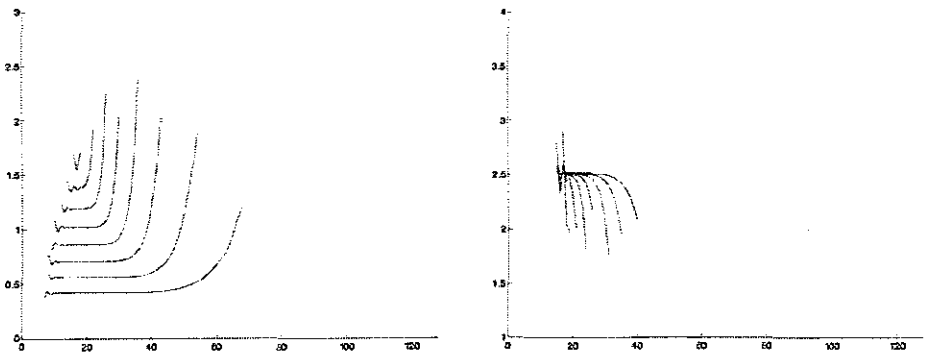

(a) α_Y (b) β_Y

Figure 6.6: The form-fitted α_Y and β_Y calculated from the model equation, in which $t = 0.6$ to 1.3 at intervals of 0.1.

3. Local sheet form at the physical singularity time. In the numerical study by Shelley [28], he observed that the singularity type in the x direction is different from that in the y direction. In later work, Cowley, Baker & Tanveer [12] explained this disparity by asymptotic expansions around the neighborhood of the physical singularity near the singularity time. Further, our analysis predicts that even in this case, our model equation should still capture the local form of the vortex sheet shape at the physical singularity time.

By comparing Figure (6.7) and Figure (6.8), we see that for both equations, the second order space derivative in the x variable becomes singular, while that in the y variable stays regular. To provide a more precise measurement, we form-fit the Fourier spectra of the interfaces. As can be seen in Figure (6.9), Figure (6.10), Figure (6.11), and Figure (6.12), by comparing the β part of the figures, we conclude that the singularity's power is about 3/2 in the x variable, while the singularity's power is about 2 in the y variable. This subtle feature is also captured by our model equation.

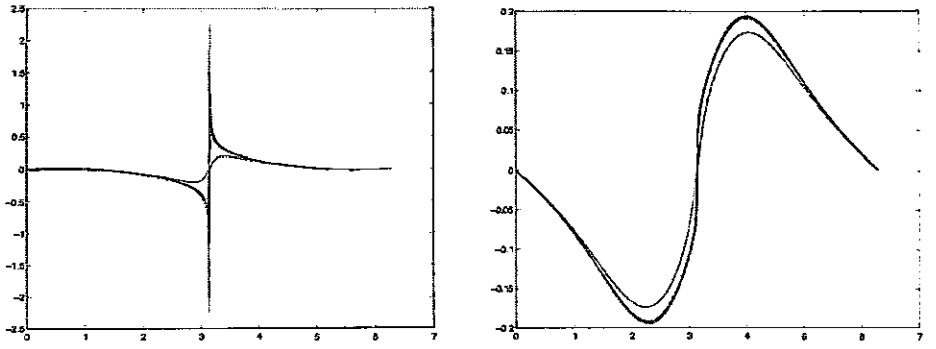

(a) x-direction (b) y-direction

Figure 6.7: The second order differentiation on x and y direction calculated from the full equation, in which $t = 1.5$, 1.525 and 1.6 to 1.625 at intervals of 0.0025.

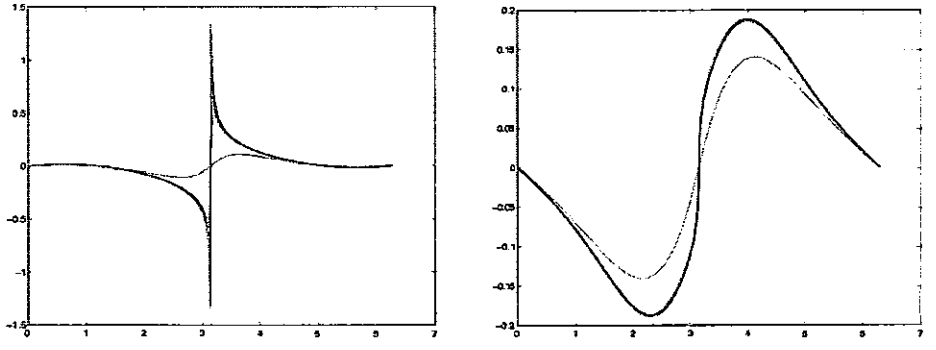

(a) x-direction (b) y-direction

Figure 6.8: The second order differentiation on x and y direction calculated from the model equation, in which $t = 1.3$ and 1.5775 to 1.5925 at intervals of 0.0025.

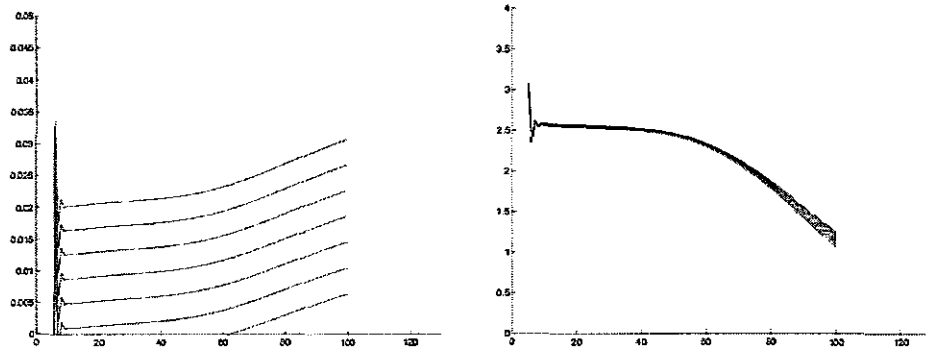

(a) α_X (b) β_X

Figure 6.9: The form-fitted α_X and β_X calculated from the full equation, in which $t = 1.6$ to 1.615 at intervals of 0.0025.

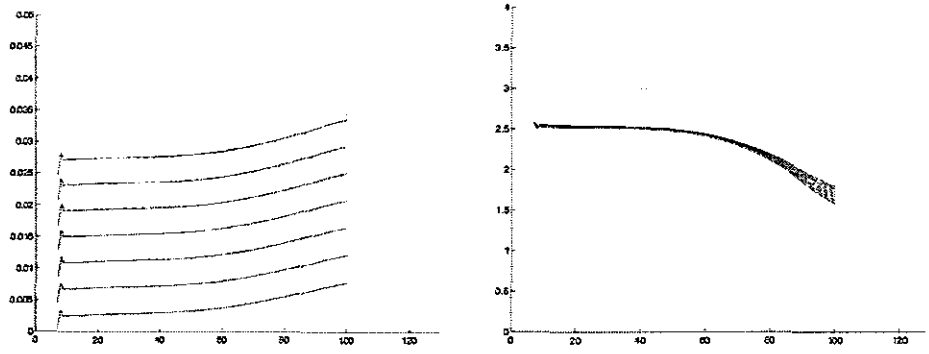

(a) α_X (b) β_X

Figure 6.10: The form-fitted α_X and β_X calculated from the model equation, in which $t = 1.5775$ to 1.5925 at intervals of 0.0025.

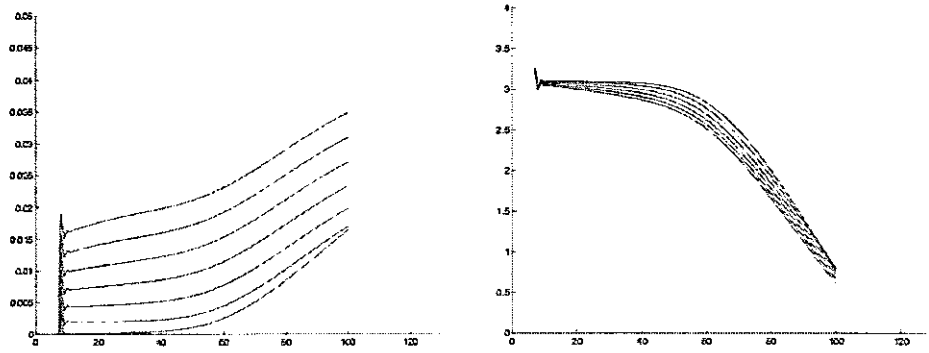

(a) α_Y (b) β_Y

Figure 6.11: The form-fitted α_Y and β_Y calculated from the full equation, in which $t = 1.6$ to 1.615 at intervals of 0.0025.

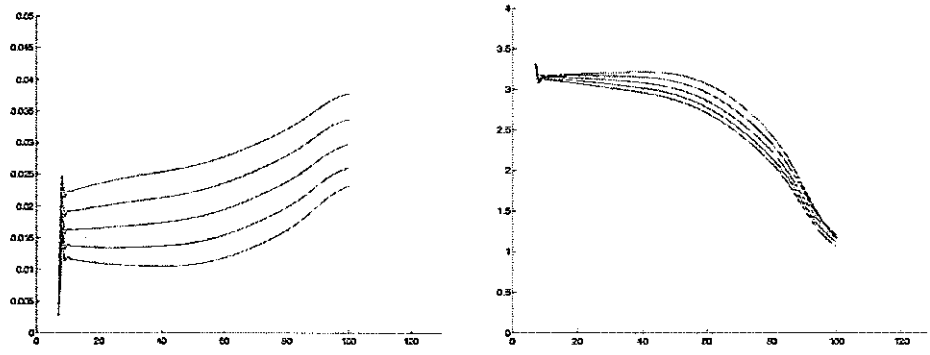

(a) α_Y (b) β_Y

Figure 6.12: The form-fitted α_Y and β_Y calculated from the model equation, in which $t = 1.5775$ to 1.5875 at intervals of 0.0025.

4. Physical singularity time. One of the major differences between the two equations is the singularity time. To have a definite measure on this issue, we check the α form-fitting near the singularity time. As we can see from the α fitting curves in Figure (6.9), Figure (6.10), Figure (6.11), and Figure (6.12), the singularity time is about 1.5925 for our model equation, while it is around 1.6125 to 1.615 for the full equation.

6.2 Three-dimensional Model Equation

6.2.1 Formulation

As we stated in the previous section, our three-dimensional model equation is:

$$\begin{aligned}\frac{\partial \mathbf{z}}{\partial t} &= -\frac{1}{4\pi}\int\int \frac{(\mu'_{\alpha_1}\mathbf{z}'_{\alpha_2} - \mu'_{\alpha_2}\mathbf{z}'_{\alpha_1}) \times (\mathbf{z}'_{\alpha_1}(\alpha_1-\alpha'_1) + \mathbf{z}'_{\alpha_2}(\alpha_2-\alpha'_2))}{|\mathbf{z}'_{\alpha_1}(\alpha_1-\alpha'_1) + \mathbf{z}'_{\alpha_2}(\alpha_2-\alpha'_2)|^3} d\alpha'_1 d\alpha'_2 \\ &= \frac{1}{4\pi}\int\int \frac{(\mu'_{\alpha_1}(\alpha_1-\alpha'_1) + \mu'_{\alpha_2}(\alpha_2-\alpha'_2))|\mathbf{z}'_{\alpha_1}||\mathbf{z}'_{\alpha_2}|\mathbf{N}(\alpha')}{|\mathbf{z}'_{\alpha_1}(\alpha_1-\alpha'_1) + \mathbf{z}'_{\alpha_2}(\alpha_2-\alpha'_2)|^3} d\alpha'_1 d\alpha'_2 \,, \end{aligned} \tag{6.10}$$

where $\mathbf{N}$ stands for the normal direction of the interface.

However, the model equation is not a convolution operator in its present form. If we use direct summation in our evaluation of the velocity integral, it would take $O(N^4)$ computational complexity in each time step, where N is the number of mesh points in each direction. The numerical calculation becomes prohibitively expensive even when N reaches the level of $O(100)$. We will introduce a special coordinate system (α_1, α_2) to reduce the integral operator in (6.10) to a convolution operator. Then the velocity can be evaluated efficiently by FFT.

The special coordinate system is chosen so that the following properties are satisfied

[16]

$$\mathbf{z}_{\alpha_1} \cdot \mathbf{z}_{\alpha_2} = C_1 \mathbf{z}_{\alpha_2} \cdot \mathbf{z}_{\alpha_2} , \tag{6.11}$$

$$\mathbf{z}_{\alpha_1} \cdot \mathbf{z}_{\alpha_1} = C_2 \mathbf{z}_{\alpha_2} \cdot \mathbf{z}_{\alpha_2} , \tag{6.12}$$

where C_1 and C_2 are independent of α_1 and α_2. With this set of coordinates, the integral on the right-hand side of equation (6.10) becomes a convolution operator with kernel

$$\frac{\alpha_i}{2\pi(C_2\alpha_1^2 + 2C_1\alpha_1\alpha_2 + \alpha_2^2)^{3/2}} , \tag{6.13}$$

where $i = 1, 2$. In particular, when $C_1 = 0$ as in the case of our computation, the spectral representation of the operator is:

$$\frac{-i\xi_1}{C_2(\xi_1^2 + C_2\xi_2^2)^{1/2}} , \tag{6.14}$$

and

$$\frac{-i\xi_2}{(\xi_1^2 + C_2\xi_2^2)^{1/2}} . \tag{6.15}$$

In general, even if $C_1 \neq 0$, the spectral representation of the kernels are still known as [16]:

$$\frac{-i(\xi_1 - C_1\xi_2)}{(C_2 - C_1^2)(\xi_1^2 - 2C_1\xi_1\xi_2 + C_2\xi_2^2)^{\frac{1}{2}}} , \tag{6.16}$$

and

$$\frac{-i(C_2\xi_2 - C_1\xi_1)}{(C_2 - C_1^2)(\xi_1^2 - 2C_1\xi_1\xi_2 + C_2\xi_2^2)^{\frac{1}{2}}} . \tag{6.17}$$

For interface near equilibrium, it is possible to prove the existence of a set of coordinates satisfying (6.11) and (6.12) [16]. From our numerical experiences, we find that such coordinates exist even for large initial data.

6.2.2 Some Implementation Issues

In this subsection, we discuss several implementation issues for our computations. These issues have been addressed by Si in [29]. For simplicity, we just present a brief introduction here without going into too much details. Interested readers should refer to [29] (Page 71–75).

In order to construct a coordinate system so that equations (6.11) and (6.12) are satisfied at all time, we need to consider the following details:

1. Initially, we need to find a system of (α_1, α_2) such that equation (6.11) and (6.12) are satisfied. We can derive a system of PDEs for these coordinates which can be solved by an iteration method.

2. During the evolution, it is possible that the coordinates from the last time-step do not satisfy equation (6.11) and (6.12) in the current time-step. To avoid re-adjusting the coordinates every time, we add two tangential velocities f_1 and f_2 to the evolution equation. These two added tangential velocities f_1 and f_2 are determined by a set of linear elliptic PDE's to guarantee that (6.11) and (6.12) are satisfied at all time.

   We point out that adding f_1 and f_2 does not change the singularity structure. It is

because that the only factor that affects the interface shape in the full equation is the normal velocity. The change of tangential velocities only results in a re-arrangements of the Lagrangian fluid particles. It does not change the tangential velocity jump. Thus our analysis comparing the model equation with the full equation still applies to this case.

However, the modification of the tangential velocity changes the evolution equation of the velocity jump potential μ, i.e. μ is not conserved with time any more. Therefore, we need to derive the evolution equation of μ under the new added tangential velocities. In particular, the equation can be written as:

$$\begin{aligned} \frac{d\mu}{dt}(x,y,z,t) &= \frac{\partial \mu}{\partial t} + \nabla_{\mathbf{z}}\mu \cdot \mathbf{z}_t \\ &= \frac{\partial \mu}{\partial t} + \nabla_{\mathbf{z}}\mu \cdot (f_1\mathbf{T}_1 + f_2\mathbf{T}_2 + f_3\mathbf{N}) \,, \end{aligned} \tag{6.18}$$

where $\mathbf{T}_1$, $\mathbf{T}_2$, and $\mathbf{N}$ are the local tangential directions and the normal direction. Note that if the interface evolves with the tangential velocities from the vortex sheet equation, then

$$\begin{aligned} \frac{d\tilde{\mu}}{dt}(x,y,z,t) &= \frac{\partial \tilde{\mu}}{\partial t} + \nabla_{\mathbf{z}}\tilde{\mu} \cdot \mathbf{z}_t \\ &= \frac{\partial \mu}{\partial t} + \nabla_{\mathbf{z}}\tilde{\mu} \cdot (\tilde{f}_1\mathbf{T}_1 + \tilde{f}_2\mathbf{T}_2 + f_3\mathbf{N}) \\ &= 0 \,, \end{aligned} \tag{6.19}$$

where $\tilde{f}_1$ and $\tilde{f}_2$ stand for the tangential velocities derived from the vortex sheet

equation. Therefore, it follows from combining (6.18) and (6.19) that

$$\begin{aligned}\frac{d\mu}{dt}(x,y,z,t) &= \nabla_{\mathbf{z}}\mu\cdot((f_1-\tilde{f}_1)\mathbf{T}_1+(f_2-\tilde{f}_2)\mathbf{T}_2)\\ &= \nabla_{\mathbf{z}}\mu\cdot((f_1-\tilde{f}_1)\frac{\mathbf{z}_{\alpha_1}}{|\mathbf{z}_{\alpha_1}|}+(f_2-\tilde{f}_2)\frac{\mathbf{z}_{\alpha_2}}{|\mathbf{z}_{\alpha_2}|})\\ &= \frac{f_1-\tilde{f}_1}{|\mathbf{z}_{\alpha_1}|}\mu_{\alpha_1}+\frac{f_2-\tilde{f}_2}{|\mathbf{z}_{\alpha_2}|}\mu_{\alpha_2}\ . \end{aligned} \tag{6.20}$$

3. After each small time-step evolution, even though we evolve the interface with the added tangential velocities, (6.11) and (6.12) might not be completely satisfied at the discrete level due to the numerical error. Therefore, we need to reconstruct the surface based on the computed surface. Details in this part of the computation are given in [29].

6.2.3 Algorithm

In this subsection, we briefly describe our Algorithm:

1. Given the initial interface $\mathbf{z}$, construct (α_1, α_2) that satisfies (6.11) and (6.12).

2. For each Lagrangian particle, evaluate the integral on the right-hand side of equation (6.10) using FFT. Compute the normal velocity by projecting the velocity to the normal direction and write it as f_3.

3. Compute the tangential velocities on α_1 and α_2 direction respectively as f_1 and f_2 using f_3.

4. Evolve the interface and the vorticity strength according to a Fourth-order Adams-Bashforth Method.

5. Reconstruct the fluid interface based on the computed interface to satisfy (6.11) and (6.12).

6. Compute the solution at the next time step from Step 2.

6.2.4 Numerical Results

In this section, we will perform an extensive numerical study of the 3-D vortex sheet model equation to confirm our theoretical results obtained in the previous chapters. In particular, we will investigate three aspects of singularity formation in 3-D vortex sheets in our numerical study:

1. Interface shape and the curvature.

2. Singularity formation.

3. Local singularity structure.

In our three-dimensional computations, we take the following initial data:

$$\mathbf{z}(t=0) = (\alpha_1, \alpha_2, \varepsilon_1 \sin(\alpha_1 - \varepsilon_2 \sin(\alpha_2))) \tag{6.21}$$

where $\varepsilon_1 = 0.1$, and $\varepsilon_2 = 0.5$, with

$$\mu(\alpha_1, \alpha_2) = 2\alpha_1 \ . \tag{6.22}$$

For this initial condition, we solve the model equation with $N = 64$, $N = 128$, $N = 256$, $N = 512$, and $N = 1024$ respectively to ensure the convergence of our computation. Every time we double the mesh points, we reduce the time-step Δt by half. As a result, Δt ranges from 0.01 to 0.000625. The filter tolerance level is set to 10^{-12} in our computation, since

we are using the standard double precision for the calculations of the three-dimensional problem due to the computational resource constraint. The procedure can be described as follows:

1. Evolve the interface using $N = 256$, $\Delta t = 0.0025$ up to $t = 1.00$.

2. Double the mesh size, reduce the time step in half, and continue the computation up to $t = 1.65$ with $N = 512$ and $\Delta t = 0.00125$.

3. At time $t = 1.45$, further double the mesh size, reduce the time step in half and compute up to $t = 1.60$ with $N = 1024$ and $\Delta t = 0.000625$.

We summarize our numerical results below.

1. Interface shape and the Curvature Plot. In this part of the study, we illustrate the dynamical evolution of the sheet interface and its mean curvature. We can see from Figure (6.14) – Figure (6.20) that the mean curvature develops a rapid growth in time and a curvature singularity may develop in finite time. It is important to point out that the initially smooth curvature function is pushed to form a sharp gradient along a certain direction (like the β_2 direction in our analysis) while it remains relatively smooth perpendicular to this direction (like the β_1 direction in our analysis). This confirms our analytical prediction that singularity formation for 3-D vortex sheets can be essentially reduced to a 2-D vortex sheet along certain space curve.

In Chapter 3, our analysis predicts that for each fixed β_1, 3/2 singularities form in the extended complex β_2 domain spontaneously at $t = 0+$. Since the speeds at which the singularities propagate depend on β_1, we expect that the physical singularities would generically appear at some isolated points first, and then spread into a one-dimensional manifold. In Figure (6.21), we present the contour plot of the curvature. We can see clearly

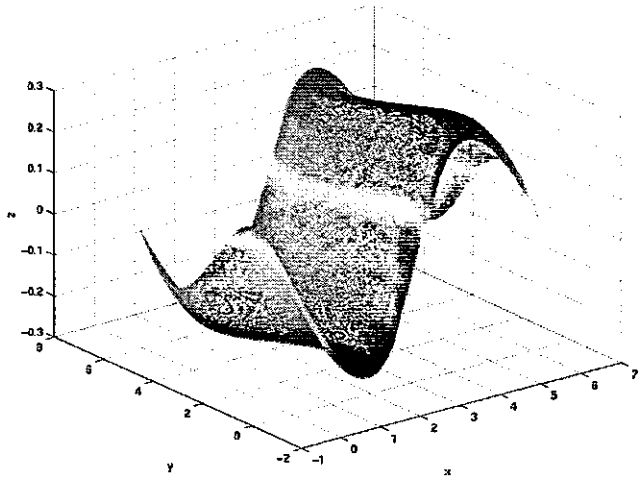

Figure 6.13: Interface calculated from three-dimensional model equation at $t = 1.64$.

that the singular region of curvature is indeed concentrated along a one-dimensional curve which is parametrized by β_1. The curvature achieves its maximum value at isolated points along these one-dimensional curves. Note that in this particular example, we have $\beta_1 = \alpha_1$ and $\beta_2 = \alpha_2$.

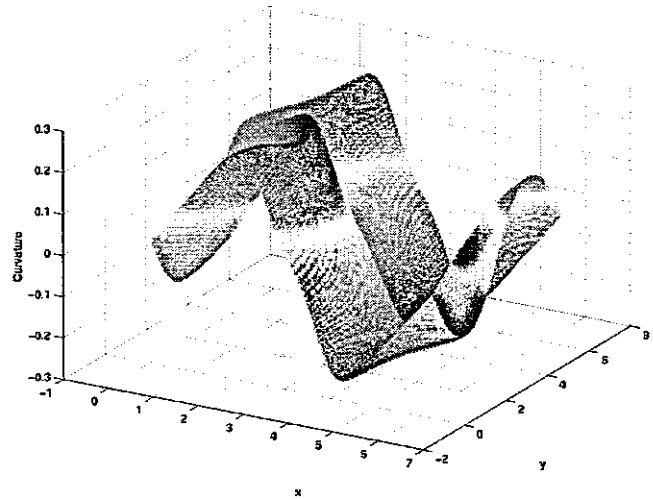

Figure 6.14: Curvature calculated from three-dimensional model equation at $t = 1.20$.

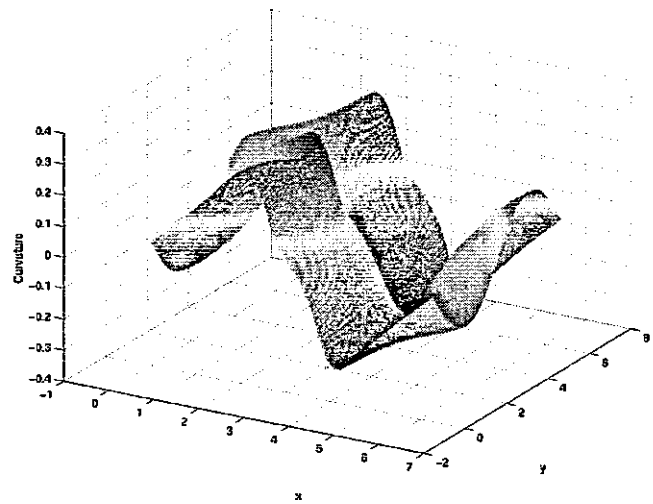

Figure 6.15: Curvature calculated from three-dimensional model equation at $t = 1.30$.

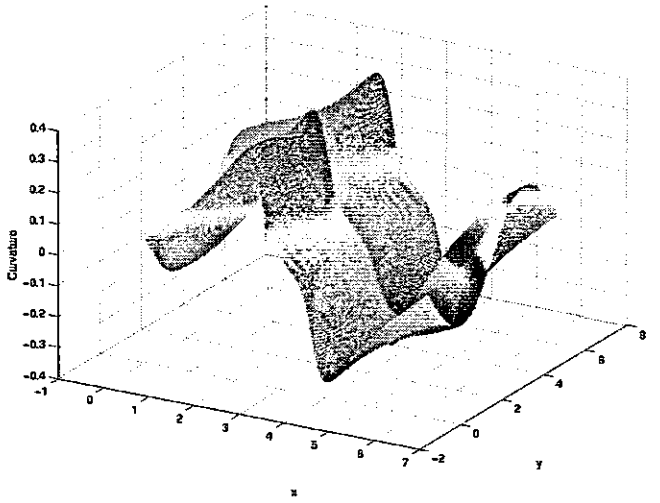

Figure 6.16: Curvature calculated from three-dimensional model equation at $t = 1.400$.

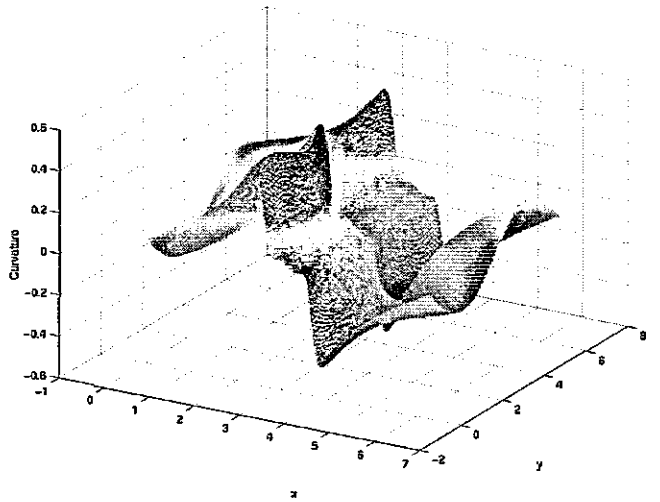

Figure 6.17: Curvature calculated from three-dimensional model equation at $t = 1.50$.

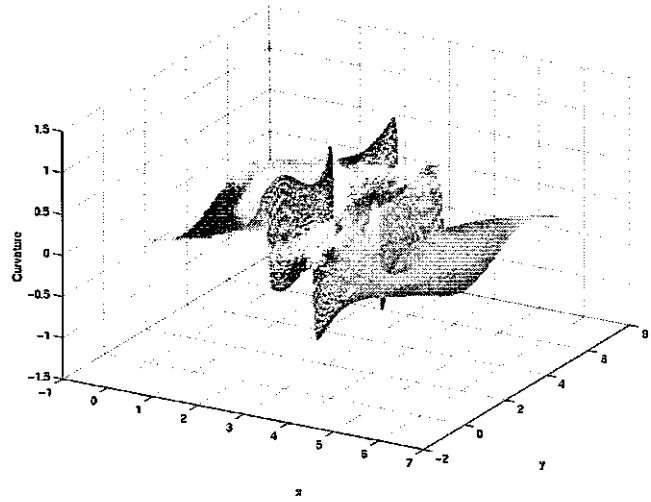

Figure 6.18: Curvature calculated from three-dimensional model equation at $t = 1.60$.

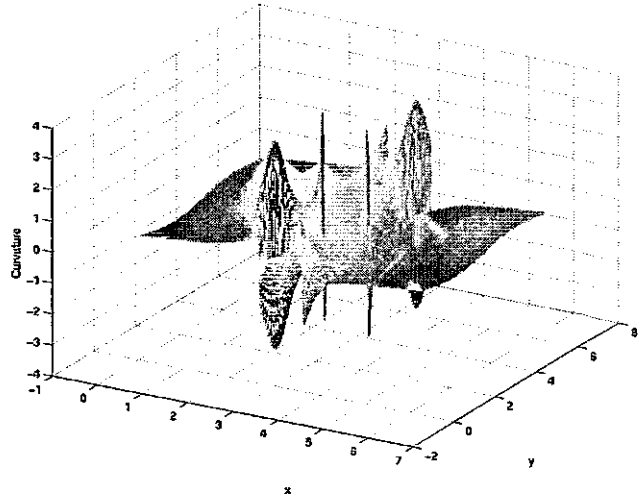

Figure 6.19: Curvature calculated from three-dimensional model equation at $t = 1.64$.

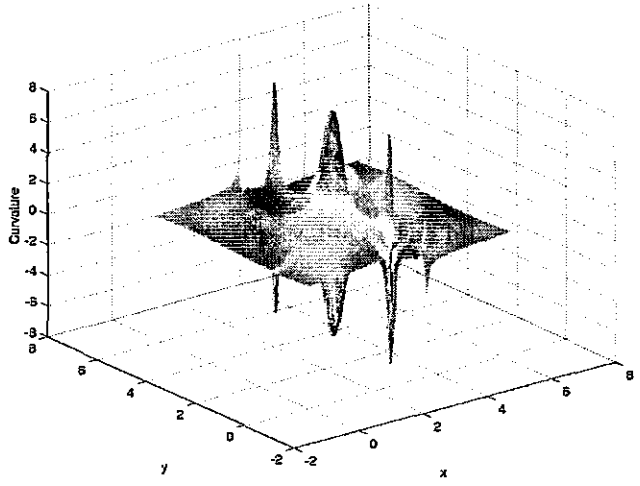

Figure 6.20: Curvature calculated from three-dimensional model equation at $t = 1.646$.

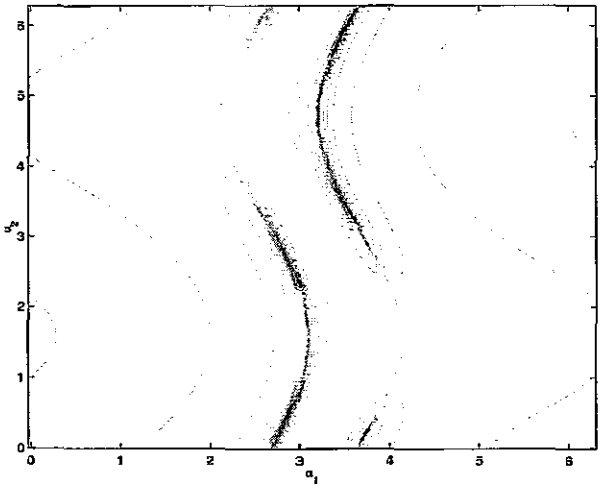

Figure 6.21: Curvature contours calculated from three-dimensional model equation at $t = 1.646$.

Singularity Formation: We study the singularity type in this part of the numerical analysis. The purpose is to further confirm our theoretical result, which has predicted that the singularity is of type 3/2 for a wide range of initial conditions along a certain critical direction. Following the work of Krasny [19], we use the log-log plot of the Fourier coefficients of the x-component of the intersection along the β_2 direction with a fixed β_1 which give rise to the maximum curvature value at the intersection of these two directions. If the interface forms a 3/2 singularity at t_c as predicted by our analysis, the slope of the logarithm of the Fourier modes would approach -2.5 asymptotically. In fact, from Figure (6.23), Figure (6.24), and Figure (6.25), we see that the Fourier modes are approaching the -2.5 slope as time increases. In particular, the four curves in Figure (6.23), Figure (6.24), and Figure (6.25) represent the Fourier modes at four different times. As the singularity time is approached, we can see that the Fourier modes corresponding to the lower to intermediate wave numbers converge to the -2.5 slope, while the higher wave number modes also move towards this slope as the singularity time is approached. In addition, we find that the x, y, and z components form a 3/2 singularity simultaneously. This indicates that the interface may form a singularity of type 3/2 in finite time.

To provide further evidence of singularity formation of type 3/2, we have performed a resolution study. In Figure (6.26), Figure (6.28), and Figure (6.30), we present the numerical results using $N = 1024$. In each of the three figures, two sets of the computational results are presented, using 512 by 512 mesh points and 1024 by 1024 mesh points respectively. In addition, Figure (6.27), Figure (6.29), and Figure (6.31) show the close-up of these three figures in the high frequency region. From the close-up plot, we observe that as soon as the logarithms of the Fourier modes deviate from the -2.5 slope, the curves representing the logarithms in the 512 by 512 computations also deviate from those in the 1024 by

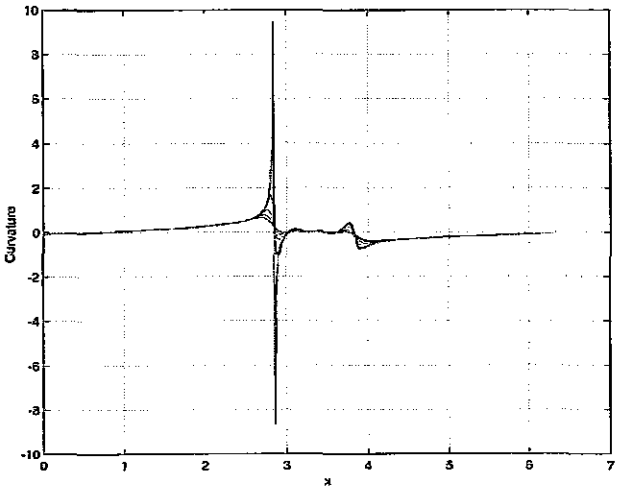

Figure 6.22: Cross section of curvature plot along $y = \pi$, at t = 1.2, 1.3 1.4, 1.5, 1.641 to 1.647 at the interval of 0.001 respectively.

1024 computation. Therefore, we conclude that the decaying behavior of the higher wave number modes in these figures is due to the lack of numerical resolution and the filtering effect. Moreover, we observe that at the same high wave number, the coefficients computed from higher resolution ($N = 1024$) are closer to the -2.5 slope. This indicates that the higher wave number modes will eventually converge to the -2.5 slope as more and more mesh points are used. This resolution study gives convincing evidences that a 3/2 singularity is indeed formed at the singularity time.

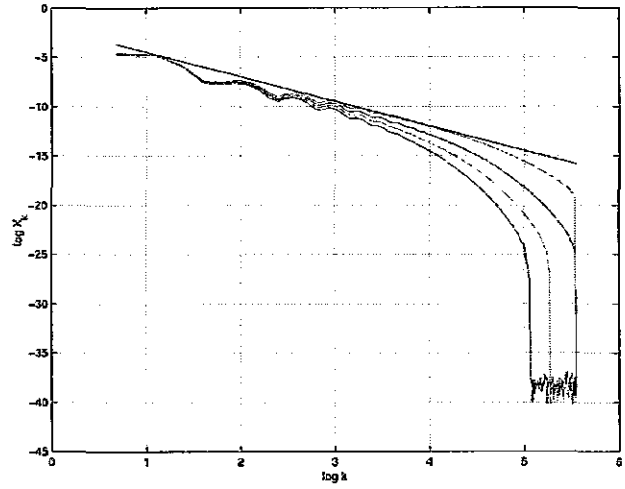

Figure 6.23: Log-log plot of the X variable Fourier coefficients of the α_1-direction intersection passing the maximum curvature position at time $t = 1.61, 1.62, 1.63, 1.64$. The Fourier coefficients plot increases as time increases. The straight line shows the -2.5 slope.

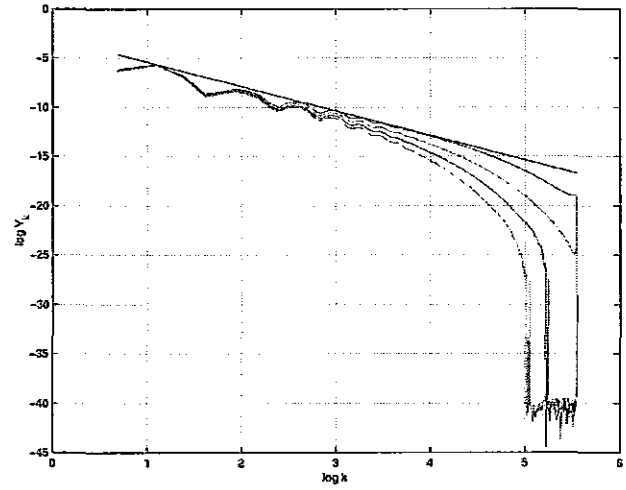

Figure 6.24: Log-log plot of the Y variable Fourier coefficients of the α_1-direction intersection passing the maximum curvature position at time $t = 1.61, 1.62, 1.63, 1.64$. The Fourier coefficients plot increases as time increases. The straight line shows the -2.5 slope.

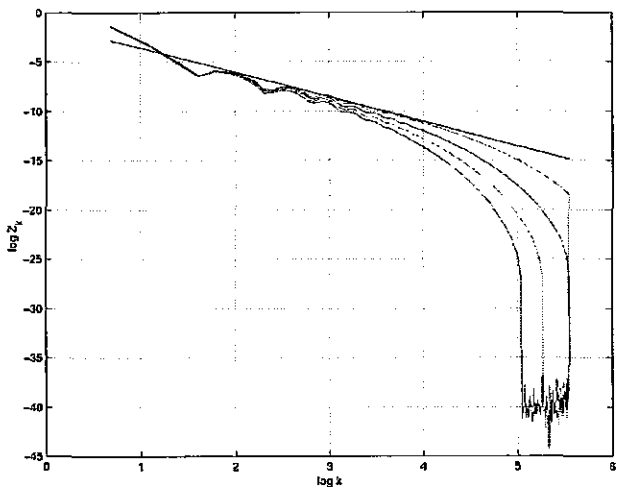

Figure 6.25: Log-log plot of the Z variable Fourier coefficients of the α_1-direction intersection passing the maximum curvature position at time $t = 1.61, 1.62, 1.63, 1.64$. The Fourier coefficients plot increases as time increases. The straight line shows the -2.5 slope.

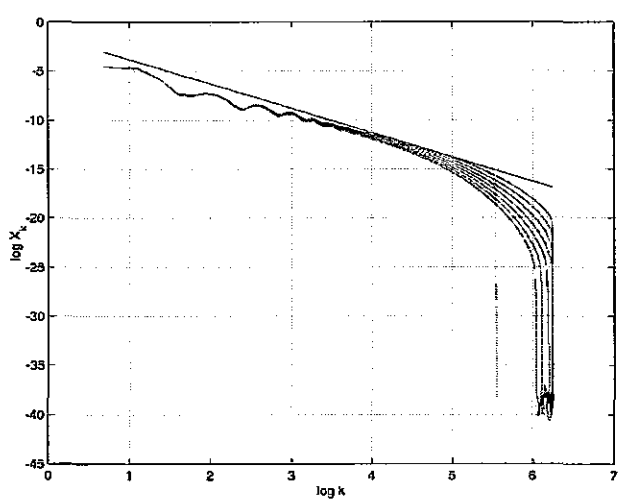

Figure 6.26: Log-log plot of the X variable Fourier coefficients of the α_1-direction intersection passing the maximum curvature position at time $t = 1.641$, to 1.647 at the interval of 0.001. The Fourier coefficients plot increases as time increases. The straight line shows the -2.5 slope. The two sets of curves stand for the computation results for 512 mesh points and 1024 mesh points.

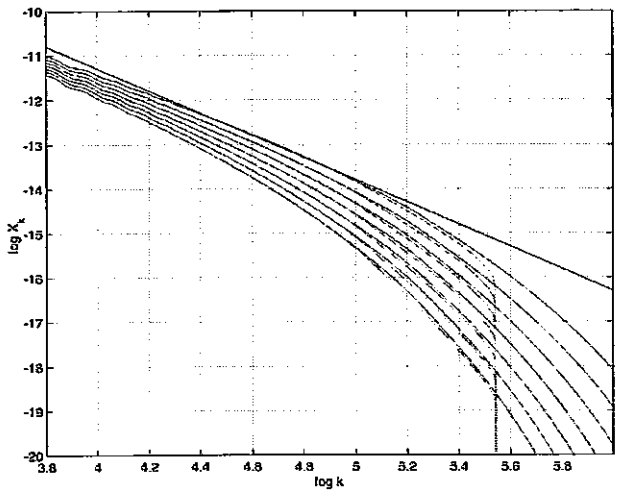

Figure 6.27: Zoomed plot of Figure 6.26. Log-log plot of the X variable Fourier coefficients of the α_1-direction intersection passing the maximum curvature position at time $t = 1.641$, to 1.647 at the interval of 0.001. The Fourier coefficients plot increases as time increases. The straight line shows the -2.5 slope. The two sets of curves stand for the computation results for 512 mesh points and 1024 mesh points.

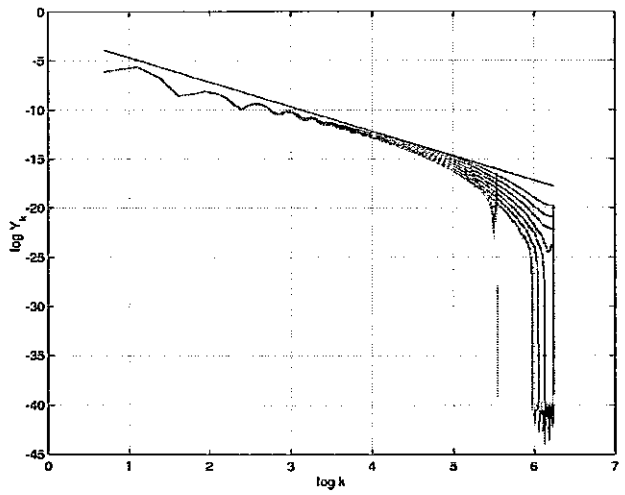

Figure 6.28: Log-log plot of the Y variable Fourier coefficients of the α_1-direction intersection passing the maximum curvature position at time $t = 1.641$, to 1.647 at the interval of 0.001. The Fourier coefficients plot increases as time increases. The straight line shows the -2.5 slope. The two sets of curves stand for the computation results for 512 mesh points and 1024 mesh points.

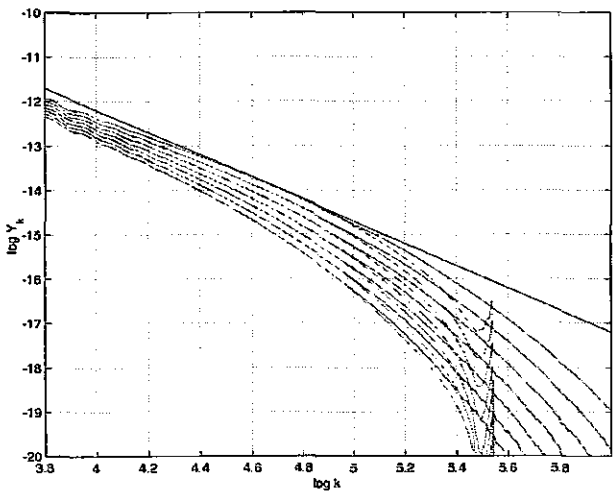

Figure 6.29: Zoomed plot of Figure 6.28. Log-log plot of the Y variable Fourier coefficients of the α_1-direction intersection passing the maximum curvature position at time $t = 1.641$, to 1.647 at the interval of 0.001. The Fourier coefficients plot increases as time increases. The straight line shows the -2.5 slope. The two sets of curves stand for the computation results for 512 mesh points and 1024 mesh points.

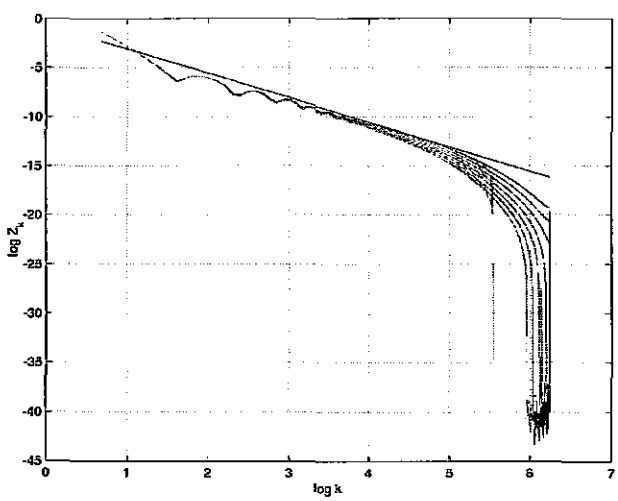

Figure 6.30: Log-log plot of the Z variable Fourier coefficients of the α_1-direction intersection passing the maximum curvature position at time $t = 1.641$, to 1.647 at the interval of 0.001. The Fourier coefficients plot increases as time increases. The straight line shows the -2.5 slope. The two sets of curves stand for the computation results for 512 mesh points and 1024 mesh points.

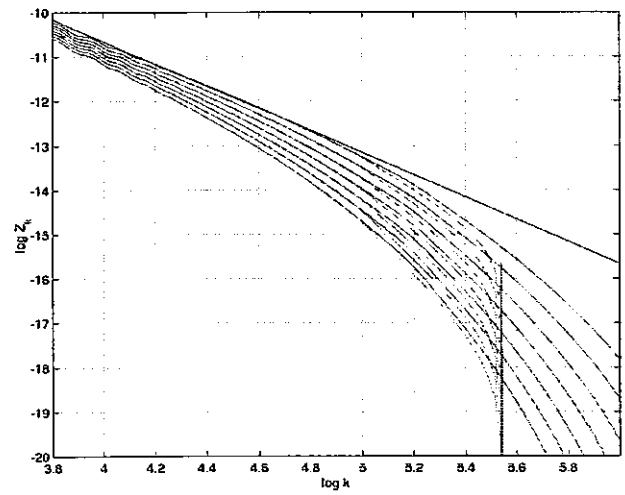

Figure 6.31: Zoomed plot of Figure 6.30. Log-log plot of the Z variable Fourier coefficients of the α_1-direction intersection passing the maximum curvature position at time $t = 1.641$, to 1.647 at the interval of 0.001. The Fourier coefficients plot increases as time increases. The straight line shows the -2.5 slope. The two sets of curves stand for the computation results for 512 mesh points and 1024 mesh points.

4. Local singularity structure. In the last section of Chapter 3, in order to study the local singularity structure, we introduce two new variables ϕ_1 and ϕ_2. We show that to the leading order ϕ_2 and z form 3/2 singularities but there is no 3/2th order singularity in the ϕ_1 variable. Since our analysis is based on formal asymptotic analysis, we would like to validate this result numerically. From the log-log plot of the Fourier coefficients of the ϕ_1 and ϕ_2 variables along the β_2 direction in Figure (6.32) and Figure (6.33), we see that the Fourier modes of the ϕ_1 variable approaches the -3.1 slope, while the Fourier modes of the ϕ_2 variable approaches the -2.5 slope. This confirms that ϕ_1 is smoother than ϕ_2 near the singularity time.

Throughout our analysis, we argue that under the special set of coordinates, one direction is the essential singularity direction (the β_2 direction) In the case we study here, even with the added tangential velocities and the re-adjusted vorticity, the β_2 direction

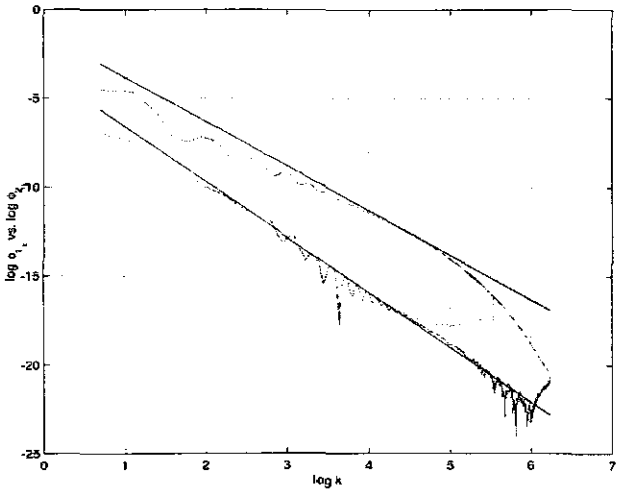

Figure 6.32: Comparison of the log-log plot of the ϕ_1 variable Fourier coefficients to that of the ϕ_2 variable. Both intersections pass the maximum curvature position at time $t = 1.646$. The upper line is the Fourier coefficients of the ϕ_2 variable, the straight line has the slope of -2.5. The lower line stands for the Fourier coefficients of the ϕ_1 variable, the straight line has the slope of -3.1. Similar resolution test is involved.

corresponds to the α_1-direction. So the α_1-direction should be the essential direction to the leading order. To confirm this idea, we compare the Fourier coefficients of the intersection along the α_1-direction to the Fourier coefficients of the intersection along the α_2-direction. As we can see from Figure (6.34), Figure (6.35), and Figure (6.36), even though our $\varepsilon_1 = 0.1$ is not particularly small, there are still disparities in the tails of the Fourier coefficients in all x, y, and z variables. This shows that the β_2 direction, which coincides with the α_1-direction in this case, is indeed the essential direction driving the singularity formation of the 3-D vortex sheet problem. Further evidence is provided in Figure (6.37), Figure (6.38), and Figure (6.39) to confirm this property.

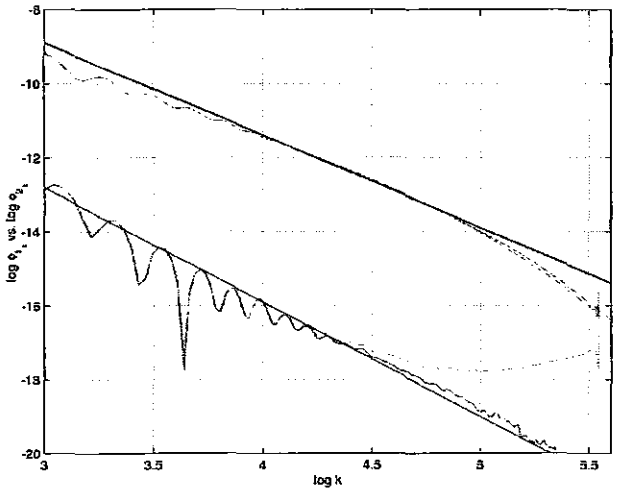

Figure 6.33: Zoomed plot of Figure (6.32). Comparison of the log-log plot of the ϕ_1 variable Fourier coefficients to that of the ϕ_2 variable. Both intersections pass the maximum curvature position at time $t = 1.646$. The upper line is the Fourier coefficients of the ϕ_2 variable, the straight line has the slope of -2.5. The lower line stands for the Fourier coefficients of the ϕ_1 variable, the straight line has the slope of -3.1. Similar resolution test is involved.

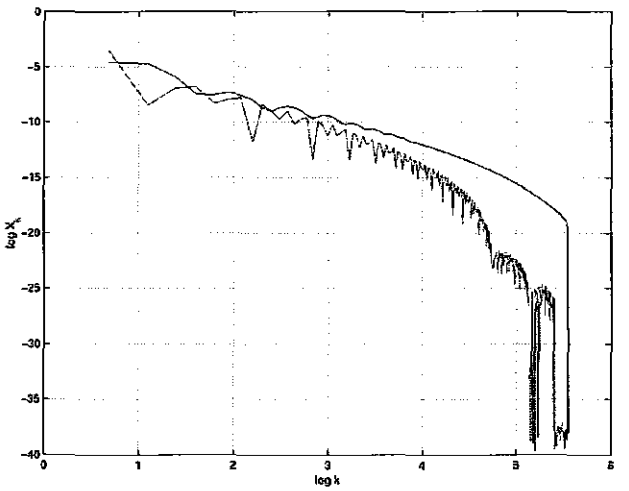

Figure 6.34: Comparison of the log-log plot of the X variable Fourier coefficients of the α_1-direction intersection with the α_2-direction intersection both passing the maximum curvature position at time $t = 1.64$. Upper line is the Fourier coefficients of the α_1-direction intersection. Lower line is the Fourier coefficients of the α_2-direction intersection.

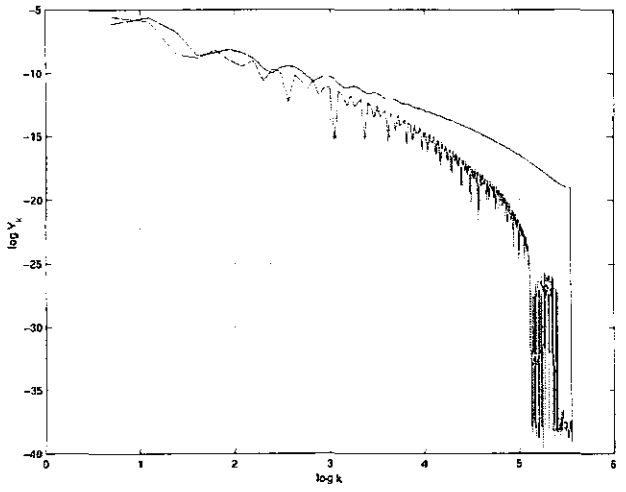

Figure 6.35: Comparison of the log-log plot of the Y variable Fourier coefficients of the α_1-direction intersection with the α_2-direction intersection both passing the maximum curvature position at time $t = 1.64$. Upper line is the Fourier coefficients of the α_1-direction intersection. Lower line is the Fourier coefficients of the α_2-direction intersection.

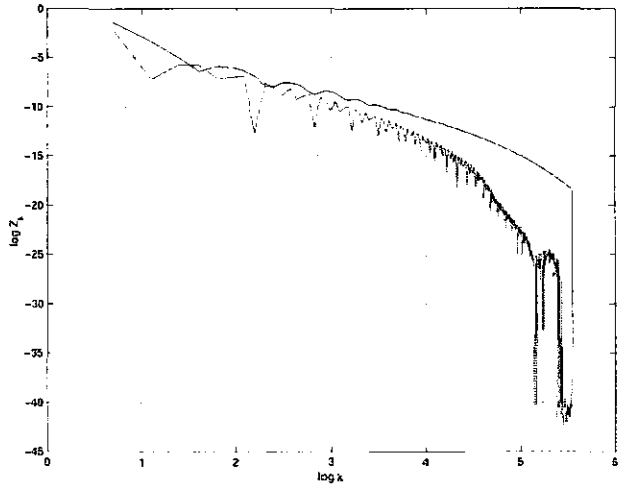

Figure 6.36: Comparison of the log-log plot of the Z variable Fourier coefficients of the α_1-direction intersection with the α_2-direction intersection both passing the maximum curvature position at time $t = 1.64$. Upper line is the Fourier coefficients of the α_1-direction intersection. Lower line is the Fourier coefficients of the α_2-direction intersection.

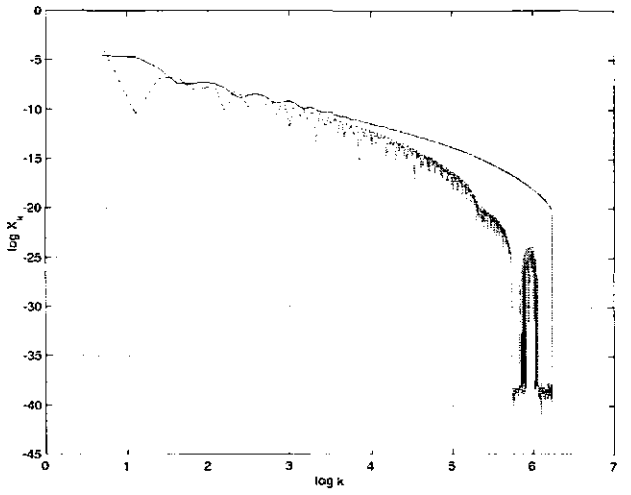

Figure 6.37: Comparison of the log-log plot of the X variable Fourier coefficients of the α_1-direction intersection with the α_2-direction intersection both passing the maximum curvature position at time $t = 1.647$. Upper line is the Fourier coefficients of the α_1-direction intersection. Lower line is the Fourier coefficients of the α_2-direction intersection.

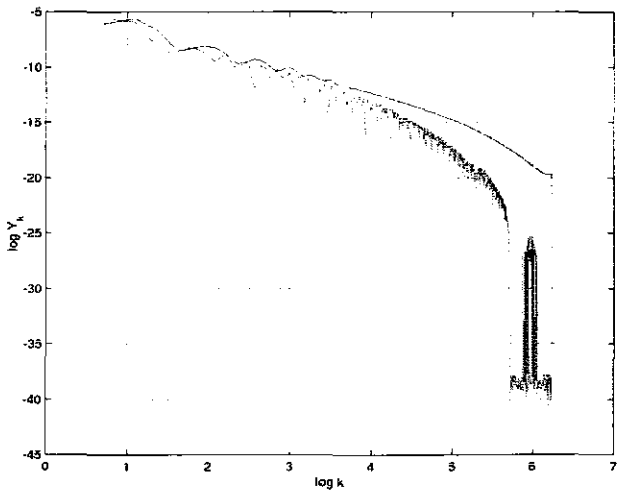

Figure 6.38: Comparison of the log-log plot of the Y variable Fourier coefficients of the α_1-direction intersection with the α_2-direction intersection both passing the maximum curvature position at time $t = 1.647$. Upper line is the Fourier coefficients of the α_1-direction intersection. Lower line is the Fourier coefficients of the α_2-direction intersection.

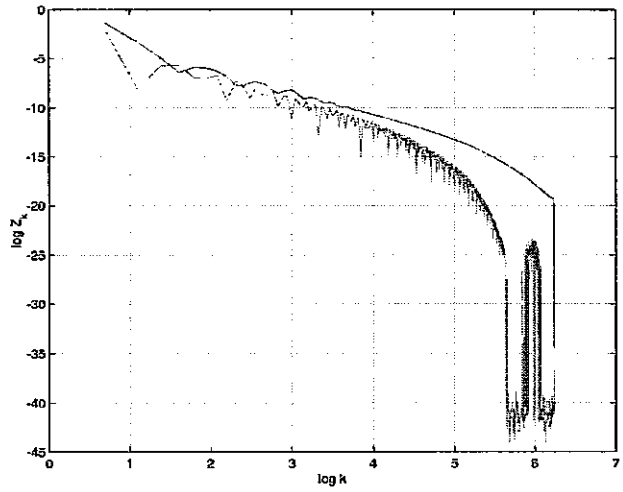

Figure 6.39: Comparison of the log-log plot of the Z variable Fourier coefficients of the α_1-direction intersection with the α_2-direction intersection both passing the maximum curvature position at time $t = 1.647$. Upper line is the Fourier coefficients of the α_1-direction intersection. Lower line is the Fourier coefficients of the α_2-direction intersection.

Chapter 7 Conclusions

In this thesis, we have studied the three-dimensional vortex sheet problem theoretically and numerically. We found that the three-dimensional vortex sheet problem can be reduced to a two-dimensional vortex sheet problem to the leading order along certain space curve and with appropriate change of variables. With this key observation, we have derived the early time singularity formation and the local form of the curvature singularity near the physical singularity time. The results are found to be qualitatively the same as those of the two-dimensional vortex problem. Moreover, we have proved the long time existence theorem for the three-dimensional vortex sheet equation for analytic initial conditions near equilibrium. The existence time is almost optimal if the initial perturbation to equilibrium is sufficiently small. Further, by introducing simplified model equations, we have performed careful numerical computations which confirm some of our theoretical results.

One area worth further research is how to best use our simplified model equations in study of interfacial flows in three space dimensions. The fact that the model equations capture correctly the singular behavior of the interface at small scales and can be evaluated efficiently may find useful applications in other contexts. In fact, from our analysis, we show that the difference between the full equation and the model equation is a smoothing operator. Therefore, it is possible that we can develop an efficient multi-resolution method to represent the large scale regular behavior. This will offer an alternative fast method to study three-dimensional interfacial flows which can capture the singular behavior at small scales.

It is generally believed that vortex stretching is an important mechanism for three-dimensional incompressible Euler equations. It is a long open question whether the 3-D Euler equations can develop a finite time singularity from smooth initial data. In this sense, it is quite surprising that the 3-D vortex sheet is essentially like the 2-D vortex sheet. It would be interesting to investigate whether this has any implication to the 3-D Euler equations with smooth but nearly singular shear layered initial data. For example, what is the limiting behavior of the regularized vortex layer solution as the thickness of the shear layer tends to zero. This may shed some useful light into the singularity formation in 3-D Euler equations with smooth initial data.

Bibliography

[1] Lars V. Ahlfors. *Complex Analysis.* McGraw-Hill, Inc., 1966.

[2] G. R. Baker. Generalized vortex methods for free-surface flows. *In Waves on Fluid Interfaces, R. E. Meyer ed., Academic Press*, pages 53–81, 1983.

[3] G. R. Baker, R. E. Caflisch, and M. Siegel. Singularity formation during Rayleigh-Taylor instability. *J. Fluid Mech.*, 252:51–78, 1993.

[4] G. K. Batchelor. *An Introduction to Fluid Dynamics.* Cambridge University Press, 1970.

[5] C. L. Berman and L. Greengard. A renormalization method for the evaluation of lattice sums. *J. Math. Phys.*, 35:6036–6048, 1994.

[6] G. Birkhoff. Helmholtz and Taylor instability. *Proc. Symp. Appl. Math. Am. Math. Soc.*, 13:55–76, 1962.

[7] M. Brady and D. I. Pullin. On singularity formation in three-dimensional vortex sheet evolution. *Phys. Fluids*, 11(11):3198–3200, Nov. 1999.

[8] R. E. Caflisch, T. Y. Hou, and J. Lowengrub. Almost optimal convergence of the point vortex method for vortex sheets using numerical filtering. *Math. Comput.*, 68(228):1465–1496, Oct. 1999.

[9] R. E. Caflisch and O. F. Orellana. Long time existence for a slightly perturbed vortex sheet. *Comm. Pure. Appl. Math.*, 39:1–18, 1986.

[10] R. E. Caflisch and S. Semmes. A nonlinear approximation for vortex sheet evolution and singularity formation. *Physica D.*, 41(2):197–207, Mar. 1990.

[11] A. P. Calderón and A. Zygmund. Singular integrals and periodic functions. *Studia Math.*, 14:249–271, 1954.

[12] S. J. Cowley, G. R. Baker, and S. Tanveer. On the formation of Moore curvature singularities in vortex sheets. *J. Fluid Mech.*, 378:233–267, Jan. 10, 1999.

[13] L. F. Greengard and V. Rokhlin. A fast algorithm for particle summations. *J. Comp. Phys.*, 73:325–348, 1987.

[14] D. J. Haroldsen and D. I. Meiron. Numerical calculation of three-dimensional interfacial potential flows using the point vortex method. *SIAM J. Sci. Comput.*, 20(2):648–683, Sep. 11, 1998.

[15] Thomas Y. Hou, Zhen-huan Teng, and Pingwen Zhang. Well-posedness of linearized motion for 3-d water waves far from equilibrium. *Commun. in Partial Differential Equations*, 21(9,10):1551–1585, 1996.

[16] Thomas Y. Hou and Pingwen Zhang. An effective model equation for fluid interface problems in two and three dimensions, in preparation.

[17] Thomas Y. Hou and Pingwen Zhang. Growth rates for the linearized motion of 3-d fluid interfaces with surface tension far from equilibrium. *Asian J. Math.*, 2(2):263–288, June 1998.

[18] T. Ishihara and Y. Kaneda. Singularity formation in three-dimensional motion of a vortex sheet. *J. Fluid Mech.*, 300:339–366, 1994.

[19] R. Krasny. A study of singularity formation in a vortex sheet by the point vortex method. *J. Fluid Mech.*, 167:65–93, 1986.

[20] P. D. Lax. Development of singularities of solutions of nonlinear hyperbolic partial differential equations. *J. Math. Phys.*, 5:611–613, 1964.

[21] T. S. Lundgren. Strained spiral vortex model for turbulent fine structure. *Phys. Fluids*, 25:2193, 1982.

[22] D. I. Meiron, G. R. Baker, and S. A. Orzsag. Analytic structure of vortex-sheet dynamics. part 1. Kelvin-Helmholtz instability. *J. Fluid Mech.*, 114:283–298, 1982.

[23] D. W. Moore. The spontaneous appearance of a singularity in the shape of an evolving vortex sheet. *Proc. R. Soc. Lond.*, A365:105–119, 1979.

[24] D. W. Moore. Numerical and analytical aspects of Helmholtz instability in theoretical and applied mechanics. *Proc. XVI ICTAM, eds. Niordson and Olhoff, North-Holland*, pages 263–274, 1984.

[25] T. Nishida. A note on a theorem of nirenberg. *J. Diff. Geom.*, 12:629–633, 1977.

[26] D. A. Pugh. *Development of vortex sheets in Boussinesq flows - formation of singularities. Ph.D. Thesis.* University of London, 1989.

[27] P. G. Saffman and G. R. Baker. Vortex interactions. *Ann. Rev. Fluid Mech.*, 11:95–122, 1979.

[28] M. J. Shelley. A study of singularity formation in vortex-sheet motion by a spectrally accurate vortex method. *J. Fluid Mech.*, 244:493–526, 1992.

[29] H. Si. *Numerical study of interfacial flow with surface tension in two and three dimensions, Ph.D. Thesis.* California Institute of Technology, 2000.

[30] Elias M. Stein. *Singular Integrals and Differentiability Properties of Functions.* Princeton University Press, 1970.

[31] M. H. Taibleson. The preservation of Lipschitz spaces under singular integral operators. *Studia Math.*, 24:105–111, 1963.